

OCEAN THERMAL EXTRACTABLE ENERGY VISUALIZATION

Award #
DE-EE0002664

October 28, 2012

Final Technical Report

Prepared by
Lockheed Martin Mission Systems & Sensors (MS2)

Project Title: Ocean Thermal Extractable Energy Visualization

Recipient: Lockheed Martin Corporation

Award #: DE-0002664

Working Partners

Project Lead: Matthew Ascari – Lockheed Martin Corporation, matthew.b.ascari@lmco.com

Howard P. Hanson, Ph.D. – Florida Atlantic University, hphanson@fau.edu

Lynn Rauchenstein – Florida Atlantic University, lrauchen@my.fau.edu

James Van Zwieten Ph.D. - Florida Atlantic University, jvanzwi@fau.edu

Desikan Bharathan PhD. - National Renewable Energy Labs, desikan.bharathan@nrel.gov

Donna Heimiller- National Renewable Energy Labs, donna.heimiller@nrel.gov

Nicholas Langle- National Renewable Energy Labs, nicholas.langle@nrel.gov

George N. Scott- National Renewable Energy Labs, george.scott@nrel.gov

James Potemra Ph.D. - University of Hawai'i, jimp@hawaii.edu

Eugene Jansen- Lockheed Martin Corporation, eugene.jansen@lmco.com

N. John Nagurny- Lockheed Martin Corporation, john.nagurny@lmco.com

Acknowledgements

Contributions to this report were funded by the Wind & Water Power Program, Office of Energy Efficiency and Renewable Energy of the U.S. Department of Energy under Contract No. DE-EE0002664.

This report was prepared as an account of work sponsored by an agency of the United States Government. Neither the United States Government nor any agency thereof, nor any of their employees, makes any warranty, express or implied, or assumes any legal liability or responsibility for the accuracy, completeness, or usefulness of any information, apparatus, product, or process disclosed, or represents that its use would not infringe privately owned rights. Reference herein to any specific commercial product, process, or service by trade name, trademark, manufacturer, or otherwise does not necessarily constitute or imply its endorsement, recommendation, or favoring by the United States Government or any agency thereof. The views and opinions of authors expressed herein do not necessarily state or reflect those of the United States Government or any agency thereof.

The authors would like to thank the following people and organizations whose contributions, either direct or indirect, have helped ensure the success of this project;

Department of Energy's Hoyt Battey, Nick Johnson, Tim Ramsey, Samantha Quinn and Caitlin Frame

University of Hawai'i's Gerard Nihous Ph.D., Luis Vega Ph.D.

Makai Ocean Engineering's Steven Rizea and Patrick Grandelli

National Renewable Energy Laboratory's Pamela Gray-Hann,

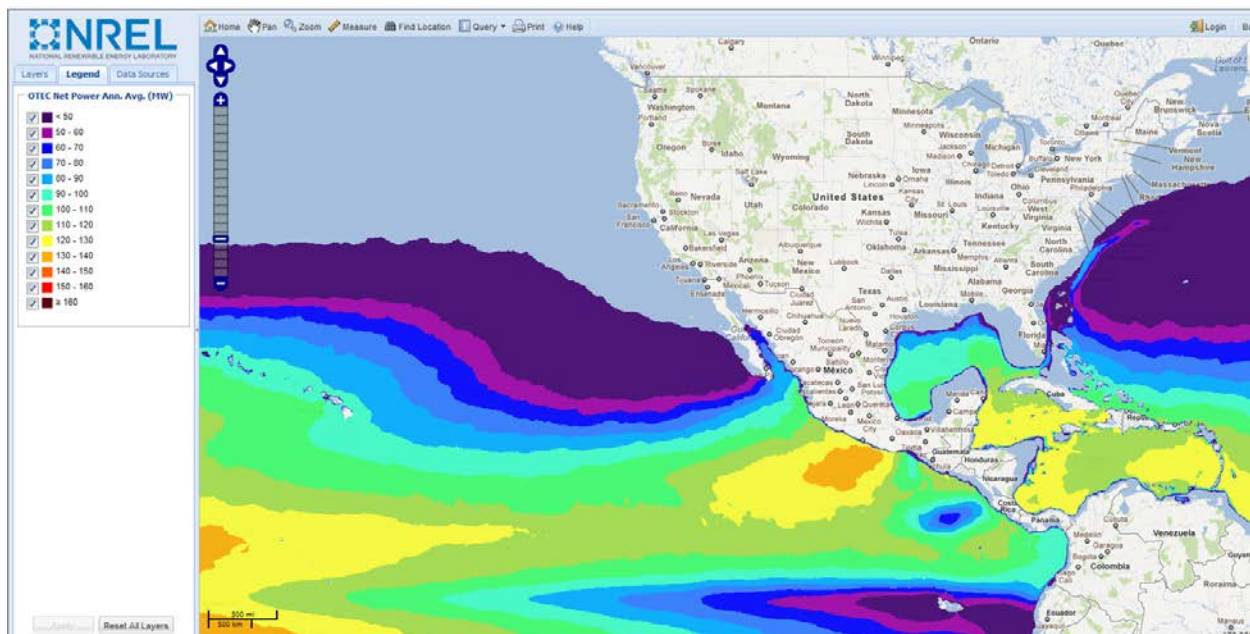
Lockheed Martin Corporation's Laura Martel, Robert Varley

Frederick Driscoll Ph.D., Robert J Howard, Andrew Plumb

Abstract

The Ocean Thermal Extractable Energy Visualization (OTEEV) project focuses on assessing the Maximum Practically Extractable Energy (MPEE) from the world's ocean thermal resources. MPEE is defined as being sustainable and technically feasible, given today's state-of-the-art ocean energy technology. Under this project the OTEEV team developed a comprehensive Geospatial Information System (GIS) dataset and software tool, and used the tool to provide a meaningful assessment of MPEE from the global and domestic U.S. ocean thermal resources.

The OTEEV project leverages existing NREL renewable energy GIS technologies and integrates extractable energy estimated from quality-controlled data and projected optimal achievable energy conversion rates. Input data are synthesized from a broad range of existing in-situ measurements and ground-truthed numerical models with temporal and spatial resolutions sufficient to reflect the local resource. Energy production rates are calculated for regions based on conversion rates estimated for current technology, local energy density of the resource, and sustainable resource extraction. Plant spacing and maximum production rates are then estimated based on a default plant size and transmission mechanisms. The resulting data are organized, displayed, and accessed using a multi-layered GIS mapping tool, http://maps.nrel.gov/mhk_atlas with a user-friendly graphical user interface, as seen in the image below.



NREL's MHK_Atlas application displaying the Annual Average Extractable Net Power Capacity from Ocean Thermal Energy Conversion

Executive Summary

As the sun warms the earth each day much of that heat is captured and stored in the surface layers of the oceans, while the depths of the oceans remain frigid. For over a century scientists have envisioned ways of extracting this thermal energy resource and converting it into useful forms to power and cool cities. This report documents the modeling efforts and results of a resource assessment focused on Ocean Thermal Energy funded by the Department of Energy under grant number DE-EE0002664. The project team, comprising members from industry, government and academia, collaborated to assess the thermal characteristics available in the layers of the world's oceans and, through advanced modeling techniques, define the extractable resource in terms of the total net electrical capacity that could be produced using an established conversion process. The OTEEV Project takes the available oceanographic data to another level by providing regionally adjusted results in an interactive format available to the public.

The team of Lockheed Martin (LM), Florida Atlantic University (FAU), University of Hawai'i (UH) and National Renewable Energy Labs (NREL) carefully selected the approach and methods to perform this resource assessment and has clearly documented the group's assumptions, techniques and rationale behind these selections. The result is a new set of information in the form of a visualization tool to map the resources for both Ocean Thermal Energy Conversion (OTEC) and Seawater Cooling (SWC) systems across the globe.

This report describes the ocean thermal resource and the conventional methods for extracting energy from it. It then takes the reader through each step of the project, detailing the data processing, modeling and validation efforts employed. This is followed by a discussion of OTEC plant spacing and sustainability. Finally it delivers the results of this resource assessment and development of the visualization tool to be used in bringing those results to the public in an interactive presentation.

The web-based Geospatial Information System (GIS) application and Energy Extraction model are enhancements of previous assessments and visualizations. They provide a higher spatial resolution, geographically complete, three-dimensional, time-dependent depiction of the oceans and extractable ocean energy. The visualization tool, accessible through http://maps.nrel.gov/mhk_atlas, includes minimum plant spacing recommendations in addition to temperature distributions and predicted net electrical capacity. This visualization also captures cold, shallow reservoirs missing from previous assessments and balances the benefits of colder water with the pumping costs associated with greater depths.

Past ocean thermal resource assessments have established the foundation and basis for this approach, while recent models of the ocean supply pertinent data at a higher resolution than previously available. Results highlight the quality of this resource in all practical locations across the globe as it pertains to extractable energy and provide a visual mapping of the specific factors that determine the classifications. Estimates of the extractable net power are 55,000 Terawatt hours per year globally with 4,600 of that total coming from within U.S. waters. Developers of ocean thermal energy systems can now access this information through an interactive tool to help identify feasible locations to develop ocean thermal energy systems. It is anticipated that the results accomplished under this effort and the prior research on which it is based will provide a solid foundation on which further research and models will be refined to develop an OTEC industry.

Table of Contents

| | | |
|-------|--|----|
| 1 | Technical Approach Summary | 1 |
| 1.1 | OTEC and Seawater Cooling (SWC) Technologies Defined | 1 |
| 1.2 | Theoretical, Technical and Practical Assessments | 3 |
| 1.3 | Methodology for Assessing Net Power | 3 |
| 1.4 | Statement of Project Objectives..... | 4 |
| 2 | Ocean Data..... | 5 |
| 2.1 | Selection Criteria and Available Data Sources | 5 |
| 2.2 | HYCOM+NCODA Data Attributes..... | 8 |
| 2.3 | Processing and Dataset Generation..... | 9 |
| 2.4 | Dataset Validation..... | 11 |
| 3 | Energy Extraction Model..... | 12 |
| 3.1 | Assumptions..... | 12 |
| 3.2 | Gross Power..... | 14 |
| 3.3 | Fixed Loss Factors | 15 |
| 3.3.1 | Cold Water Intake Power Loss | 15 |
| 3.3.2 | Condenser and Distribution Pumping Loss | 16 |
| 3.3.3 | Evaporator and Distribution Pumping Loss..... | 16 |
| 3.3.4 | Ammonia Pumping Loss | 16 |
| 3.4 | Variable Loss Factors | 17 |
| 3.4.1 | Cold Water Head Loss to Pumping Loss Factor..... | 17 |
| 3.4.2 | Cold Water Pipe (CWP) Friction Loss | 18 |
| 3.4.3 | Static Head Loss | 19 |
| 3.5 | Final Equation..... | 20 |
| 3.6 | Model Output..... | 20 |
| 3.7 | Sensitivity Analysis | 21 |
| 4 | Independent Validations | 24 |
| 4.1 | Plant Design..... | 24 |
| 4.2 | Plant Design Validation Methodology..... | 24 |
| 4.3 | Validation Results..... | 27 |
| 5 | Plant Spacing Estimates..... | 30 |
| 5.1 | Cold Water Constraint | 30 |
| 5.2 | Establishing a Practical Plant Spacing Approach | 31 |
| 6 | Resource Assessment Model Results and Analysis..... | 33 |

| | | |
|-----|---|----|
| 6.1 | Data File Output..... | 33 |
| 6.2 | Specific Areas of Interest..... | 34 |
| 6.3 | Obtaining Regional Resource Calculations | 40 |
| 6.4 | Resource within the U.S. EEZ regions | 44 |
| 6.5 | Resource within the United Nations Recognized EEZs..... | 45 |
| 7 | Visualization | 46 |
| 7.1 | Data Processing..... | 46 |
| 7.2 | Tool Functionality..... | 48 |
| 7.3 | Intended Audience | 54 |
| 7.4 | Comparison to other Resource Assessments | 54 |
| 8 | Conclusions and Recommendations | 55 |
| 8.1 | Summary of the OTEEV Project | 55 |
| 8.2 | Suggestions for Future Research | 56 |
| 8.3 | Promise of Ocean Thermal Energy..... | 57 |
| 9 | Products, Presentations and Data Dissemination..... | 58 |
| 10 | References Cited | 61 |
| 11 | Abbreviations and Key Terminology..... | 63 |
| 12 | Appendices..... | 65 |

List of Tables

| | | |
|-----------|--|----|
| Table 3-1 | 100MWe Net/150MWe Gross Power Process Conditions | 12 |
| Table 3-2 | 100MW Net Power Heat Exchanger UA Values | 14 |
| Table 3-3 | OTEC Net Power Equation Parameter Dependence | 21 |
| Table 4-1 | Plant Design Conditions | 24 |
| Table 4-2 | Power Plant Design Constraints | 24 |
| Table 4-3 | Comparison of Predicted Net Power by NREL and the Project Team | 28 |
| Table 5-1 | Plant Spacing as A function of Current Velocity | 32 |
| Table 6-1 | Hawai‘i OTEC Characteristics | 41 |
| Table 6-2 | Miami, Florida OTEC Characteristics | 42 |
| Table 6-3 | Power Within the Exclusive Economic Zones of US Interests | 44 |
| Table 6-4 | Top 10 Nations in Total OTEC Net Power | 45 |
| Table 7-1 | Grouping for Seawater Cooling (SWC) Variables | 46 |
| Table 7-2 | Grouping for OTEC Variables | 47 |

List of Figures

| | |
|---|----|
| Figure 1-1 Diagram of a Closed Rankine Cycle OTEC System | 2 |
| Figure 2-1 Cold Water Depth Based on Energy Extraction Model Output Data..... | 10 |
| Figure 2-2 Ocean Surface to Deep Water Temperature Difference for a) July 2010 and b) January 2011 from HYCOM Data | 10 |
| Figure 3-1 OTEC Closed Cycle Process Diagram..... | 13 |
| Figure 3-2 Gross Power as a Function of ΔT | 14 |
| Figure 3-3 OTEEV Net Power Model Sensitivity | 22 |
| Figure 4-1 Closed-cycle OTEC Power Plant Using Ammonia as the Working Fluid at Chosen Design Conditions..... | 26 |
| Figure 4-2 Variation of Projected Net Power as a Function of the Overall Resource Temperature Difference; Both NREL and LM Predictions are Shown..... | 29 |
| Figure 5-1 Schematic of Cold Water Usage by a Single OTEC Plant..... | 30 |
| Figure 6-1 Annual and Seasonal (Jun-Jul-Aug and Dec-Jan-Feb) Mean Net Power Capacity | 34 |
| Figure 6-2 Hawaiian Islands | 35 |
| Figure 6-3 South America..... | 36 |
| Figure 6-4 Australasia and South Pacific..... | 37 |
| Figure 6-5 Gulf of Mexico, Florida Straits and the Caribbean | 38 |
| Figure 6-6 Prime Seawater Cooling resources (8° cold water found at depths less than 300 m)..... | 39 |
| Figure 6-7 Resource Assessment by Grid Point: Hawai‘i | 41 |
| Figure 6-8 Ocean Data point off of Miami, Florida | 42 |
| Figure 7-1 MHK_Atlas Tool Components | 48 |
| Figure 7-2 Selectable Layers..... | 48 |
| Figure 7-3 MHK_Atlas Tool Bar Selections | 49 |
| Figure 7-4 Base Map Layer Selections | 49 |
| Figure 7-5 Sharing Through Social Media | 50 |
| Figure 7-6 Point Query Result Display..... | 50 |
| Figure 7-7 Query by Selected Region Feature..... | 51 |
| Figure 7-8 Attribute Query Feature List | 51 |
| Figure 7-9 View Selection Capabilities | 52 |
| Figure 7-10 Customizable Color Palettes | 52 |
| Figure 7-11 Example Selection Specific Metadata | 53 |

1 Technical Approach Summary

Ocean thermal energy conversion (OTEC), first envisioned over a century ago, is the process whereby thermal energy associated with oceanic temperature stratification is converted to electricity. Both OTEC's history and discussions of OTEC technologies are reviewed, for example, by Avery, *et al.* (1994) and more recently by Vega (2003). Because the density of seawater varies inversely with its temperature, and because the oceans are stably stratified except in very localized regions of deep convection, temperature decreases with depth. When the surface water is sufficiently warmer than the water at depth, OTEC becomes practical. Various attempts to implement OTEC technology over the decades have been made, but for a variety of reasons, progress toward commercial-scale deployment has been slow.

With the recent emphasis on implementing renewable energy solutions for the future, interest in OTEC has renewed in the U.S. Based on the significant OTEC potential to provide clean, baseload power to U.S. interests, the Department of Energy's (DoE) Wind and Water Power Program commissioned a study of global ocean thermal energy resources. This report is the result of that study.

An important component of ocean thermal resources is availability of cold water (temperature generally $<10^{\circ}\text{C}$), and because water at these temperatures can also be used as the heat sink for air conditioning and other process cooling purposes, a global ocean thermal energy resource study automatically provides information about this resource as well. These energy-saving resources are also discussed in this report.

Wide dissemination of project results is a key objective, therefore the more salient results are included in the Global Marine and Hydrokinetic Energy Resource Atlas, an online, geospatial information system (GIS)- based utility maintained by the DoE's National Renewable Energy Laboratory (NREL). The utility can be found at http://maps.nrel.gov/mhk_atlas.

1.1 OTEC and Seawater Cooling (SWC) Technologies Defined

A variety of OTEC architectures have been analyzed since the process was first envisioned. The most basic is a single-stage closed-Rankine thermodynamic cycle, shown in Figure 1-1. Warm water (near the ocean surface) is directed through a heat exchanger to vaporize a working fluid. The pressurized vapor expands and spins a turbine connected to a generator. Cold water (from deeper in the ocean) is directed through another heat exchanger to condense the vapor back to the working fluid's liquid form. The working fluid is recycled back to the initial heat exchanger to continue the process. A typical working fluid is anhydrous ammonia, although sometimes an ammonia-water mixture is used in hybrid cycles to vaporize and condense at the temperatures of the available seawater streams. Multiple-stage systems use the warm and cold seawater more than once in multiple heat exchangers.

Open-cycle OTEC systems, which have been prototyped to about 200 kW (and may have trouble scaling beyond a few megawatts (MW)), inject warm seawater into a vacuum-pressure vessel, causing water to flash evaporate. The very low-pressure steam expands to spin a turbine. Because the steam is distilled water vapor, these systems produce fresh water as a byproduct when the steam is condensed using the cold water stream. Hybrid systems combine the features of the open and closed cycle in a 2 stage process to maximize the utility of the pumped seawater.

Both closed-cycle and open-cycle OTEC technologies can be hosted by shore based or floating infrastructure depending on the most direct and feasible access to the required cold water. While they have both been demonstrated previously on a small scale, commercial-scale deployments have not yet been accomplished or attempted mainly due to high capital costs. This is expected to change due to advances in composite riser technology (cold water pipe) and low-cost heat exchangers, coupled with the petroleum industry's recent decades of experience operating from deepwater floating platforms.

There are a growing number of viable OTEC technologies and alternate cycles, such as the Kalina and Uehara cycles, evolving to harness power from this vast reservoir of thermal energy. The OTEEV project employs a conventional single-stage closed Rankine cycle, much like the process depicted in Figure 1-1, for the purposes of consistent OTEC plant modeling to generate comparative power extraction estimates.

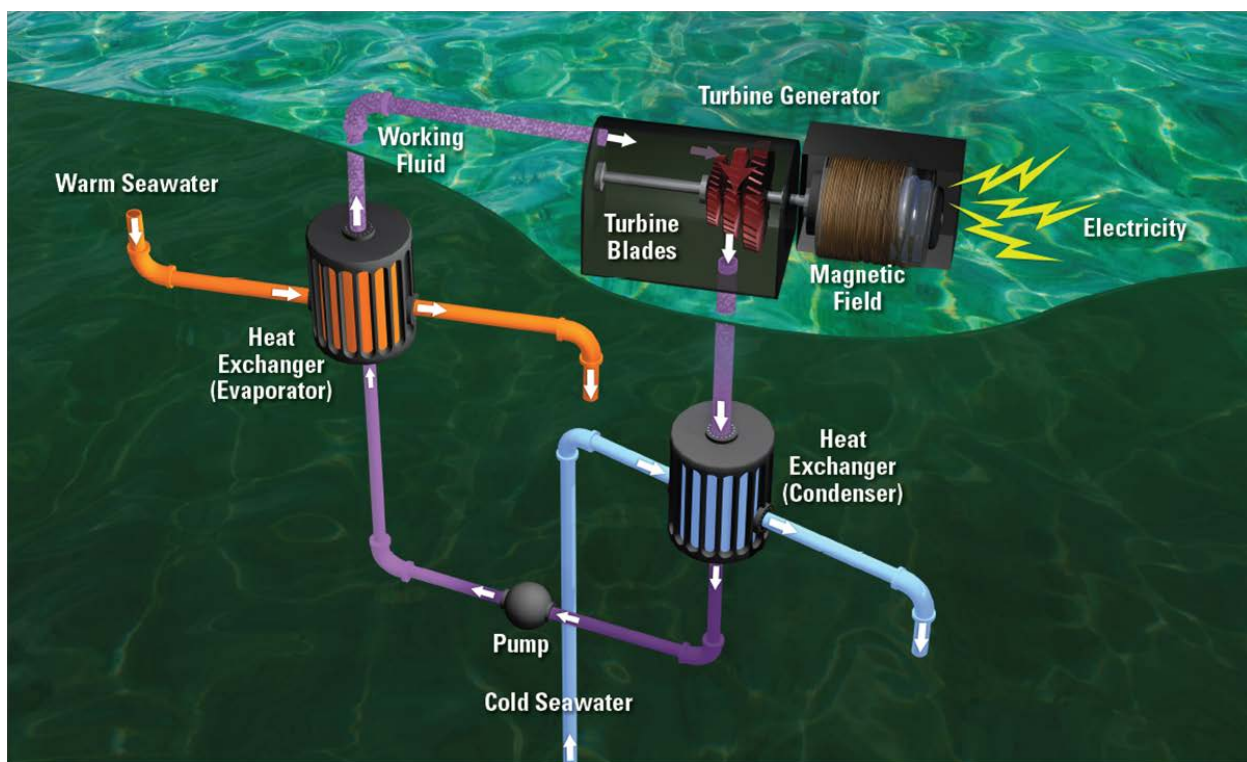


Figure 1-1 Diagram of a Closed Rankine Cycle OTEC System

Seawater cooling (SWC) systems, by comparison, simply use cold seawater rather than a compressor-chilled working fluid as the heat sink for air-conditioning heat exchangers and other refrigeration applications. Since pumping the cold seawater involves significant infrastructure, most applications of SWC are likely to take place in the district cooling context. The shorter the distance required to pump the cold water the more efficient these processes become, and so floating systems with vertical cold water piping are gaining attention. Many industrial processes, including the liquefaction of natural gas, require some form of refrigeration that can be met with SWC. In this age of information technology, large data centers stand to benefit from both the equipment cooling and power generation that can be provided using the available thermal gradients in the ocean.

1.2 Theoretical, Technical and Practical Assessments

Assessment of global and regional ocean thermal energy resources can conveniently be broken down into a hierarchy. At the most basic level, a *theoretical assessment*, oceanic datasets are used to provide the basic geophysical quantities relevant to the process. The most basic of these is the temperature difference ΔT between warm, surface seawater (temperature T_S) and cold, deep seawater (temperature T_D). Present-day heat exchanger technology suggests that regions with $\Delta T \geq 20^\circ\text{C}$ provide a resource of potential interest. Such an assessment has been reported previously (Nihous, 2005; 2007), and the theoretical assessment in this project updates and improves on that work.

A second level, a *technical assessment*, combines the geophysical dataset with additional information about technology capabilities to estimate the potential for power generation. In the case of OTEC technology, this requires additional geophysical information, in particular the depth of the deep water (in order to estimate parasitic power losses from pumping) and the actual water temperatures from the warm and cold sources.

A third level, a *practical assessment*, adds factors such as sustainability, exclusion from protected area, shipping lanes and view-sheds as well as other societal issues that limit deployment. Nihous (2005) reviewed global sustainable OTEC estimates, which range over three orders of magnitude. This study provides localized resource usage estimates based on the available cold water resource calibrated to Nihous' published results, but does not address practical assessment factors. As a global resource assessment, the scope of this project does not include those extremely heterogeneous and complex factors and thereby does not present a full "practical" assessment.

1.3 Methodology for Assessing Net Power

The technical assessment results reported here pertain to the potential for power generation at any given location of a model OTEC plant, which is based on a nominal 100 MWe net power design. To estimate the total power that could potentially be generated in a given region, whether the entire world ocean or a more localized area, it is also necessary to estimate the number of such plants that can be supported by the oceanic resource there. It is at this point in the resource assessment process that the technical assessment approaches a practical one. In effect, the results from the theoretical assessment are used with the OTEC plant model to develop localized baseload power potentials (MW/plant) as a technical assessment, which are combined with the results from the sustainability estimates (plants/area) to produce an estimate of power in a given region (MW/area). This last estimate can be summed over regions of interest to produce net power estimates. The specifics of each of these steps in the overall process are discussed in Sections 2, 3 and 5 of this report.

Throughout this report the discussion of net power generation will be related using two units of measurement. The first one is used to describe power generation capacity of a plant or number of plants and is listed in terms of Megawatts (MW) or Megawatts electric (MWe). The other is used to describe yearly output from these plants in terms of power production and is labeled as Megawatt hours per year or (MWhr/yr). The former can easily be converted into the latter by multiplying average capacity by 8760 (365*24) which is the number of hours in a year.

1.4 Statement of Project Objectives

With this background, it is useful to re-state the original project's scope and objectives.

A. PROJECT OBJECTIVES

The objectives of the Ocean Thermal Extractable Energy Visualization (OTEEV) project are to:

1. Compile necessary and sufficient sets of quality data synthesized from existing (historic) sources (measurement databases and numerical model data) that accurately represent (and provide the basis for) the global ocean thermal energy resource.
2. Establish parametric criteria for determining viability of ocean thermal energy extraction methods based on ocean thermal profile, bathymetry, proximity to power grids and resource energy density.
3. Develop parametric models to calculate the ocean thermal maximum practicably extractable energy (MPEE) based on likely technology performance, sustainable resource extraction, and resource energy density.
4. Extend NREL's existing GIS technologies to include a global ocean thermal component capable of displaying global and U.S. domestic ocean thermal viable extraction mechanisms and MPEE information.
5. Apply the GIS tool to develop and deploy the information layers and data access methods needed to readily access and understand the global and U.S. domestic ocean thermal resource.
6. Publish results and disseminate novel insights into regionally available MPEE to policymakers, the energy industry and the public to help accelerate market penetration and commercialization of ocean thermal energy extraction.

B. PROJECT SCOPE

The Ocean Thermal Extractable Energy Visualization (OTEEV) project focuses on assessing the Maximum Practicably Extractable Energy (MPEE) from the Ocean Thermal resource. MPEE is defined as being sustainable and technically feasible, given today's state-of-the-art ocean energy technology. Under this project the OTEEV team will develop a comprehensive Geospatial Information System (GIS) dataset and software tool, and then use the tool to provide a meaningful assessment of MPEE from the global and domestic U.S. ocean thermal resource.

The OTEEV project leverages existing NREL renewable energy GIS technologies and integrates extractable energy estimated from quality-controlled data and projected optimal achievable energy conversion rates. Input data are synthesized from a global database that includes available observations and physically consistent computations. Energy production rates are calculated for regional areas based on conversion rates estimated for existing technology, local energy density of the resource, and sustainable resource extraction. Plant spacing and maximum production rates, based on these considerations, lead to MPEE estimates in regions of interest. All data is organized, displayed, and accessed using a multi-layered GIS mapping tool with a user-friendly graphical user interface.

Details of the tasks performed under this effort are provided in the Statement of Project Objectives in "Appendix A – Summary of Tasks from the Statement of Project Objectives" of this report.

2 Ocean Data

This section describes the selection and use of the dataset for the hierarchy of resource assessments discussed above. It pertains primarily to Objective 1, Task 1 and its subtasks of the Statement of Project Objectives (SOPO).

This assessment of global OTEC resources is one of several marine renewable energy resource assessment projects supported by the DoE Wind and Water Power Program. During the course of work on the projects, the Principal Investigators (PI) of the various projects met, and an important distinction emerged from their discussions: *resource assessments* are separate from and only precursors to *site characterization* studies. This distinction is particularly important in the case of this global ocean thermal energy resource assessment, for two reasons. First, the resources allocated to the project preclude the detailed focus that would constitute a site characterization. Indeed, a global site characterization study would not be a useful investment of resources in any case. By starting with a resource assessment, it becomes possible to select sites of interest for OTEC development and substantiate the additional attention that would constitute a site characterization. Second, there is simply no universally consistent oceanographic dataset available that would allow the detail of site characterization to be developed globally. Given the results of the present resource assessment, it is possible to select candidate sites for OTEC development. Developers interested in a specific site would need to perform a complete site characterization to determine feasibility, cost drivers and optimum plant placements.

Data used for this resource assessment was assembled with these considerations in mind.

2.1 Selection Criteria and Available Data Sources

Because “necessary and sufficient” data for global-scale site characterization do not exist, the application of those criteria to the resource characterization challenge becomes the issue. There are several factors to consider, each of which is discussed in more detail following:

- Observational data, while preferable, is both sparse and inhomogeneous in space and time in the ocean. While there are long-term climatologies available (such as that used by Nihous 2007), these compilations are limited by their coarse resolution.
- There is some question about the value of long-term climatologies for a contemporaneous resource assessment in an era when the overall trend of global temperatures is upward. (e.g., IPCC, 2007; Xue *et al.*, 2010).
- While the main geophysical data of interest here are global ocean temperature patterns and variations, developing the hierarchy of resource assessments (the practical assessment in particular) requires information about ocean currents, especially at depth. Observational datasets are even less complete for currents than for temperatures.

Fundamentally, an important part of the problem at hand involves translating the natural resource – quantities such as ΔT in the water column – into power potential. Published estimates (Nihous, 2007) used a simplified model for the OTEC process and its interaction with the water column to scale the commonly discussed global value of ~10-20 terawatt (TWe) potential back to a more realistic value of about 5 TWe. The present study uses a completely different approach, discussed in Section 5.1, to estimate local limitations based on cold-water usage rates.

First, however, it is necessary to understand the natural resource itself and to assemble a dataset suitable for translation (OTEEV Objective 1). As noted, one approach is climatology. Nihous used the 1° latitude-longitude dataset of surface and 1000-m temperatures from the National Oceanographic Data Center's (NODC) World Ocean Atlas 2005 (NOAA, 2001) to produce global monthly maps of ΔT values large enough to drive the OTEC process, thus quantifying the oceanic resource itself.

This approach advanced the OTEC resource assessment, but the limitations of that dataset (relatively coarse resolution and the relatively conventional use of 1000-m temperatures for the cold source, T_D , which eliminated possible resources in shallower water) suggest that more can be done. In a later paper, Nihous (2010) recognized this and turned to numerical model results; his localized daily resource maps (around Hawai‘i) based on high-resolution simulations for two months are also available online.¹

Numerical model results offer the advantages of consistent gridding, availability of all state variables, and global coverage. Of course, because they are results from numerical model integrations, they suffer the limitations of the model fidelity itself. These limitations, however, can be mitigated by the use of results from numerical integrations that include *data assimilation*; that is, results from simulations in which global observational data is incorporated in real (model) time to ensure that the results are as consistent as possible with the real ocean. Such datasets as the NODC WOA05 compilation used by Nihous employ modeling in the form of interpolation to grid the irregular observational data, so even those “observations” have undergone significant computational processing.

Ideally, there would be a global climatology of ΔT and other quantities suitable for integration into the overall DoE resource database at high resolution via the OTEEV Project. However, no such climatology exists, and interpolation to higher resolution of the NODC WOA 2005 dataset is not justifiable. Further, a climatology of ΔT alone would leave open the issue of water-mass movement. Deployment of OTEC plants will, by their nature, deplete both the warm and cold water masses locally unless they are replenished by solar radiation and the ocean circulation respectively. Numerical simulations include this component of the oceans’ climatology, and resource replenishment rates can be estimated.

Following Nihous (2010), therefore, OTEEV is turning to results from data-assimilation-constrained numerical simulation of the oceans. To this end, results from a real-time global nowcast/forecast system² employed at the Naval Research Laboratory (NRL) will be used.

HYCOM, the HYbrid Coordinate Ocean Model (e.g., Chassignet *et al.*, 2003; 2009), is the latest generation of atmosphere/ocean simulation tools in a family of numerical models based on using density (or, in the atmosphere, potential temperature) as the vertical coordinate. These derive from work on isentropic models in the atmosphere (e.g., Bleck, 1978); the HYCOM concept was first discussed by Bleck (2002) following many years of work on a pure isopycnic-coordinate model (MICOM, the Miami Isopycnic Coordinate Model – Bleck and Boudra, 1986; Bleck and Smith, 1990) and simplified approaches to overcoming MICOM’s limitations (Bleck *et al.*, 1989).

The rationale for using this approach to solving the equations of motion in finite-difference form lies in the nature of the deep oceans’ adiabatic flow field. Below the surface photic zone and mixed layer, where mechanical mixing and thermodynamic processes can dominate, the oceans conserve temperature and

¹ See <http://netserver.aip.org/cgi-bin/epaps?ID=E-JRSEBH-2-002004>

² See <http://www7320.nrlssc.navy.mil/GLBhycom1-12/prologue.html>

salinity, and therefore density. The dynamics are well described by potential-vorticity conserving layers – for which density is the “natural” coordinate system. Because thermodynamic processes at the surface, however, can alter the density of upper-ocean seawater, it is necessary to use a more traditional formulation (such as depth or pressure coordinates) there – hence the “hybrid coordinate” designation. Complexities associated with matching the two coordinate systems at their interface have been the subject of intensive research over the past 15 years, and the current formulation of HYCOM conserves appropriate state variables and is numerically stable.

HYCOM has matured into a community effort, and the simulations to be used in OTEEV are those from the NRL using the Navy Coupled Ocean Data Assimilation (NCODA – see Cummings, 2005) multivariate technique. The assimilation includes use of satellite altimetry data (for sea-surface height) and multi-channel sea-surface temperature and salinity as well as all available *in situ* temperature and salinity profiles from bathythermograph profiling floats and sea ice concentrations. The surface data are projected downward using the Navy’s Modular Ocean Data Assimilation System (Fox *et al.*, 2002). Atmospheric forcing is taken from the Navy’s operational Naval Operational Global Atmospheric Prediction System (Hogan and Rosemond, 1991) and includes wind stress and speed, heat fluxes (including evaporation) and precipitation. In this way, both the model’s dynamics and thermodynamics are forced realistically and steered toward the observations as the model steps forward in time.

In essence, for the time period of the integration, the model results include all observations pertinent to OTEEV placed into the context of a physically and dynamically consistent interpolation scheme that produces very-high-resolution results. It thus presents a useful platform from which to assemble the dataset needed to further refine the global assessment of the OTEC resource.

All climatological investigations of this nature involve balancing data coverage and fidelity against dataset homogeneity and climatological stationarity. For example, combining expendable bathythermograph deep temperatures from the 1980s with satellite-derived surface temperatures from the 1990s, for example, would be fraught with potential error. Purely observational datasets such as the WOA (NOAA, 2001) or the Navy’s Generalized Digital Environmental Model (Teague *et al.*, 1990) of both T_s and T_d are neither homogeneous nor, given the present warming trend in ocean surface temperatures, stationary (IPCC, 2007; Xue *et al.*, 2010). Ocean current datasets, required to estimate transport rates for the practical assessment here, are far less homogeneous and stationary.

On the other hand, because they are derived from a global, full-physics circulation model, the HYCOM+NCODA results provide full data coverage. And because they include global data assimilation, their fidelity is also quite good, although some of the early HYCOM+NCODA simulations include a deep-water temperature bias.³ While this is small and generally confined to depths below 1000 m, using results without this bias ensure that the T_d values in the analysis are as accurate as possible. For this reason, the OTEEV analysis will be based on the results from simulations 90.6 and 90.8, which cover the period September 2008 to the present and are continually updated. Thus, the methods developed in this project can easily be applied to maintain a near-real-time OTEEV resource assessment in the future.

³ See <http://www.hycom.org/dataserver/glb-analysis>

2.2 HYCOM+NCODA Data Attributes

As previously noted, HYCOM has evolved from an ocean circulation model developed at the University of Miami to an international effort by a large community of researchers. The community website (<http://www.hycom.org>) includes information about the model and its applications, including detailed documentation and user guides as well as a bibliography. The hybrid approach to the ocean's vertical structure allows the model to calculate optimally the effects of both surface exchange processes and conservative advection in the oceanic interior. Because both of these effects on the oceanic temperature structure are important for OTEC resources, HYCOM is the appropriate vehicle for this resource assessment.

Of the many applications for which HYCOM has been adopted, the one used for the present study is the operational prediction version employed by NRL. As noted previously, the global forecasts produced by NRL include the assimilation of all available data – notably satellite products, but also sub-surface data – in real time. Of interest is the fact that the climatologies referenced above are also implicitly part of the model results, having been used originally for model initialization.

The process used for the forecasts is as follows. Each day [Day N], a ten-day model integration is computed, from Days N-4 to N+5, with Days N+1 to N+5 constituting that day's forecast and the others a daily hindcast. New observational data for Day N are incorporated via the NCODA process. Initial conditions, at the beginning of Day N-4, are taken from the previous day's results for that same day, which include data assimilated during the forecasts made four days previously. Results at 00:00 Greenwich Mean Time (GMT) (a daily snapshot of the model state) are archived for each integration, and Day N-3 of the previous day's forecasts are written over by Day N-4 of the Day N forecast run.

The version of HYCOM used for these forecasts is the global, $1/12^\circ$ latitude-longitude grid (E-W resolution of ~ 8 km at 30° latitude; N-S resolution of ~ 9 km everywhere) with 32 layers in the vertical, depth-coordinate layers near the surface and isopycnic-coordinate layers below the reach of diabatic processes. Although the finite differencing in the model uses a staggered grid, the archived data, for user convenience, is re-mapped onto an un-staggered, depth-coordinate grid and stored in netCDF (Rew and Davis, 1990) files.

Each day's results are composed of four files for temperature, salinity, and the two velocity results (1.93GB each) and a file of sea-surface height results (509 MB). For this resource assessment, two years of such results were obtained (a total of about 6,000 GB of netCDF data), covering the period March 2009–February 2011. Because the boreal winter (Dec-Feb) of 2009–2010 was in an El Niño year and that of 2010–2011 was in a La Niña year, the results reported here include examples of the strongest inter-annual signal in the global climate system. The main results included in the NREL Global MRE Resource Atlas are averages over the extreme seasons of this two-year period; additional results are discussed in this report.

2.3 Processing and Dataset Generation

Given the description of the dataset, processing for the resource assessment for both OTEC and SWC potential is straightforward. However, it is important to note that a purely theoretical assessment is not possible. This is because finding relevant values for ΔT requires a criterion for which to find T_D , and this, in turn, requires information about the technology under consideration. The previous climatology-based work (Nihous, 2007) used temperatures from 1000 m for T_D , but choice of depth is largely arbitrary.

OTEC technology produces power based on the Rankine cycle discussed previously, and, in the process, some energy is needed to power the OTEC plant itself. It is necessary to divert a portion of the power to pump large quantities of cold (heavy) water from some appropriate depth. Because the ocean is stably stratified, the deeper the water, the colder it is. Yet the temperature structure is generally more highly stratified (meaning the vertical temperature gradient is larger) in the upper parts of the water column. Therefore, seeking colder water to produce more power requires more pumping, and is the cost-benefit trade-off between additional pumping and greater power production needs to be considered in the choice of cold-water depth. On top of this power trade-off is the additional cost of long cold water pipes, underscoring the relevance of seeking the T_D source at as shallow a level as possible. To quantify the power trade-off requires a model of the OTEC technology under consideration, which moves the assessment from the theoretical to the technical category. But such a model is needed to predict power levels in any case, so using it to develop the ΔT dataset is appropriate.

For the online atlas and the results presented here for ΔT and the surface temperature T_S , the HYCOM+NCODA data were averaged into seasonal (D-J-F and J-J-A) files for the two years of boreal winter and summer, to represent the seasonal extremes. They were also averaged over the entire two years of the dataset, for annual averages. In order to account for nonlinearities in finding the appropriate depth for the cold water, the daily HYCOM+NCODA output files were processed by examination of each of the 4500 x 3298 grid columns in the main grid.⁴ The OTEC plant model discussed in Section 3 was applied to $\Delta T = T_S - T_D$ for each vertical layer until the maximum power production was found for the two-year average dataset at each grid column; this layer was then used for both D and T_D . The rationale for this approach is that at any location, a plant would be designed to take advantage of the optimum cold-water depth, but once designed that depth would remain fixed (i.e., the cold water pipe would not change its length over time). T_S was taken from the averaged 20 m data. In addition, values of the current speed were extracted from the appropriate netCDF files at the depths corresponding to the results for D for use in the plant spacing calculation discussed in Section 5. Example maps for ΔT and D are shown in Figure 2-1 and Figure 2-2.

⁴ HYCOM uses a Mercator projection grid between 78°S and 47°N, with a displaced bipolar patch for the Arctic Ocean. Only the main Mercator grid is analyzed in this work, as there are no OTEC resources of interest in the Arctic. The minimum water temperature in the model is around 3°C, and the requirement of $\Delta T \sim 20^\circ\text{C}$ restricts areas of interest to the tropics and subtropics.

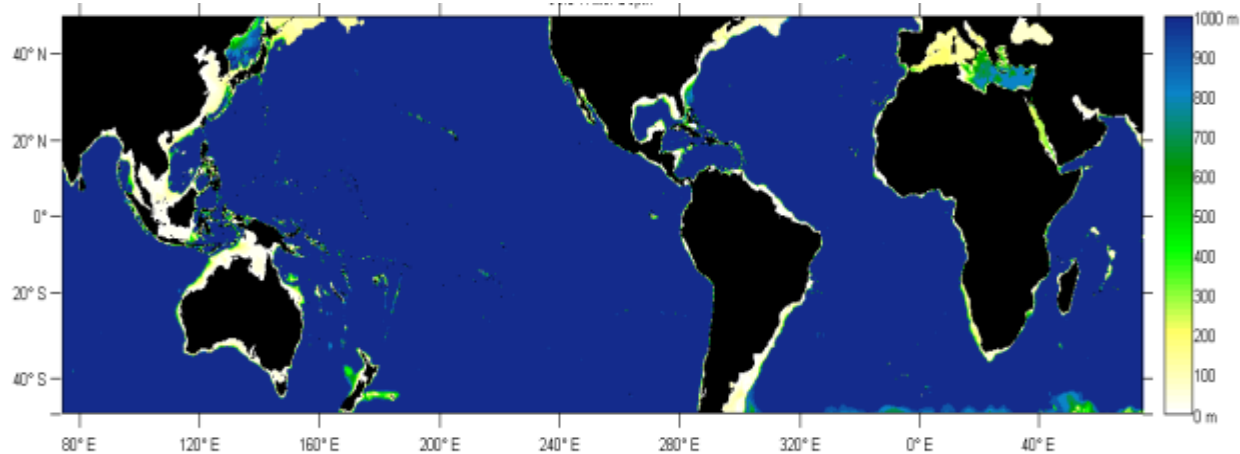


Figure 2-1 Cold Water Depth Based on Energy Extraction Model Output Data

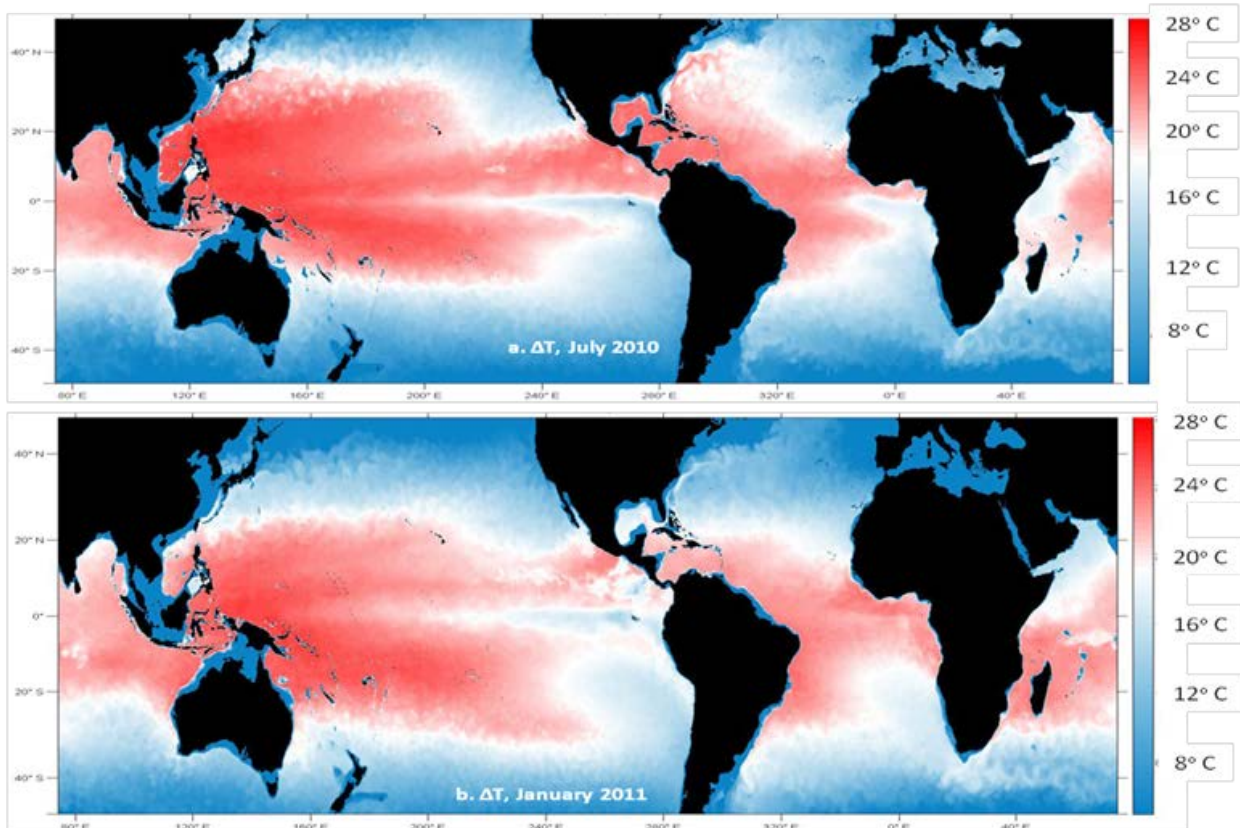


Figure 2-2 Ocean Surface to Deep Water Temperature Difference for a) July 2010 and b) January 2011 from HYCOM Data

In an analogous fashion, each grid column was examined to find the depth of the 8°C, 14°C, and 20°C water using cubic spline interpolation across the model grid. These depths were used to produce the isotherm maps for the SWC assessment.

2.4 Dataset Validation

As a community resource, HYCOM and its applications have been discussed and analyzed in hundreds of publications. The model is continually under development and improvement, with new versions and their documentation available at <http://www.hycom.org>.

A full validation of the HYCOM+NCODA results utilized in this resource assessment is impossible, because the observational data that would be used for such a validation is included in the results themselves via the data assimilation process. Comparing two years of results with climatological atlas results would reveal only the extent to which the time period March, 2009 to February 2011 is climatologically anomalous. As noted, climatological trends underway would bias such a comparison in any case.

Based on many observations the HYCOM model is in good qualitative agreement with the World Ocean Atlas and the Argo-derived temperatures (Potemra, 2011). Spot checks, however, are possible. One such comparison (Nihous, 2010) provides part of the motivation for adopting the HYCOM+NCODA results for this study, as it showed a very close correspondence between ΔT_{1000} values from the model and from observations at long-term monitoring stations in Hawai‘i.

A second such spot check (Rauchenstein *et al.*, 2011; VanZwieten *et al.*, 2011) was somewhat less encouraging, as it showed warm biases in T_D of about 1°C on average in the Straits of Florida, with the larger biases occurring on the Miami Terrace, a relatively shallow (~250 m) bench just offshore Florida. This small-scale feature is represented in the HYCOM bathymetry only crudely, and it may be that the processes responsible for maintaining a cold-water pool on the Miami Terrace are not well represented even by the relatively high resolution of the HYCOM version used here. A near-bottom temperature sensor on the terrace also showed evidence of a strong diurnal tidal signal, which is not present in HYCOM+NCODA results because no tidal forcing is used in the version of the model employed here.

The result of this bias in the Florida Straits is an under-prediction of the OTEC resource there. Because other such localized biases in the results of this study are unknown, the difference between this resource assessment and a complete site characterization is worth re-emphasizing.

3 Energy Extraction Model

There are several key components that have a significant impact on the net power production of an OTEC power plant. As such, an energy extraction model was developed under this project to process the available site specific ocean characteristics that determine a plant's electricity production capacity. The factors included in the model can be categorized into three groups: gross power, cold water pipe (CWP) pumping cost, and all other pumping and transmission power costs. CWP pumping costs are further subdivided into static and dynamic losses. Gross power is calculated using established thermodynamic equations of a Rankine cycle. Pumping and transmission losses are calculated from derivations of pumping loss equations and assumptions associated with the characteristics of an OTEC plant. Section 3 addresses the 2nd and 3rd Objectives as well as Task 2 and its subtasks of the SOPO.

The OTEC plant model predicts the net power production at a specific location, given three inputs: surface temperature (°C), depth (m), and difference between warm surface water temperature and cold deep seawater temperature (ΔT in °C) at the given depth, relative to the surface temperature. The grid size is 1/12° latitude-longitude and the depth can extend to 5500 m, which is well beyond the 1000m limit used for this investigation.

In order to normalize values for the purposes of visualization of the OTEC resource around the world, it is necessary to establish assumed baseline conditions based on a nominal design. The baseline design detailed in Section 3.1 has been optimized for conditions indicative of the Hawai‘i OTEC resource. As such, power output as described by the results of this study is not optimized for local conditions, but does provide guidance for site selection.

3.1 Assumptions

The baseline design chosen has been optimized for roughly 100MWe net power/150MWe gross power based on a 10MWe nominal net power LM/Makai Ocean Engineering design performed for U.S. Naval Facilities Engineering Command (NAVFAC) to be located off Kahe Point in Hawai‘i⁵. Assumed process conditions and efficiencies for the base case are presented in Table 3-1 and Figure 3-1.

Table 3-1 100MWe Net/150MWe Gross Power Process Conditions

| | |
|------------------------------|---------------|
| Warm Water Temperature T_S | 25.7 °C |
| Warm Water Flow Rate | 460000 kg/sec |
| Cold Water Temperature T_D | 4.1 °C |
| Cold Water Flow Rate | 366000 kg/sec |
| Cold Water Pipe Depth | 1000 m |
| Ammonia Mass Flow Rate | 4060 kg/sec |
| Turbine Expander Efficiency | 86 % |
| Ammonia Pump Efficiency | 75 % |
| Seawater Pump Efficiency | 80% |
| Generator Efficiency | 97.5% |

⁵ N62583-09-C-0083 CDRL A003“OTEC System Design Report”

<http://www.dtic.mil/cgi-bin/GetTRDoc?AD=ADA532389&Location=U2&doc=GetTRDoc.pdf>

OTEEV 100MW NOMINAL NET POWER CYCLE DIAGRAM

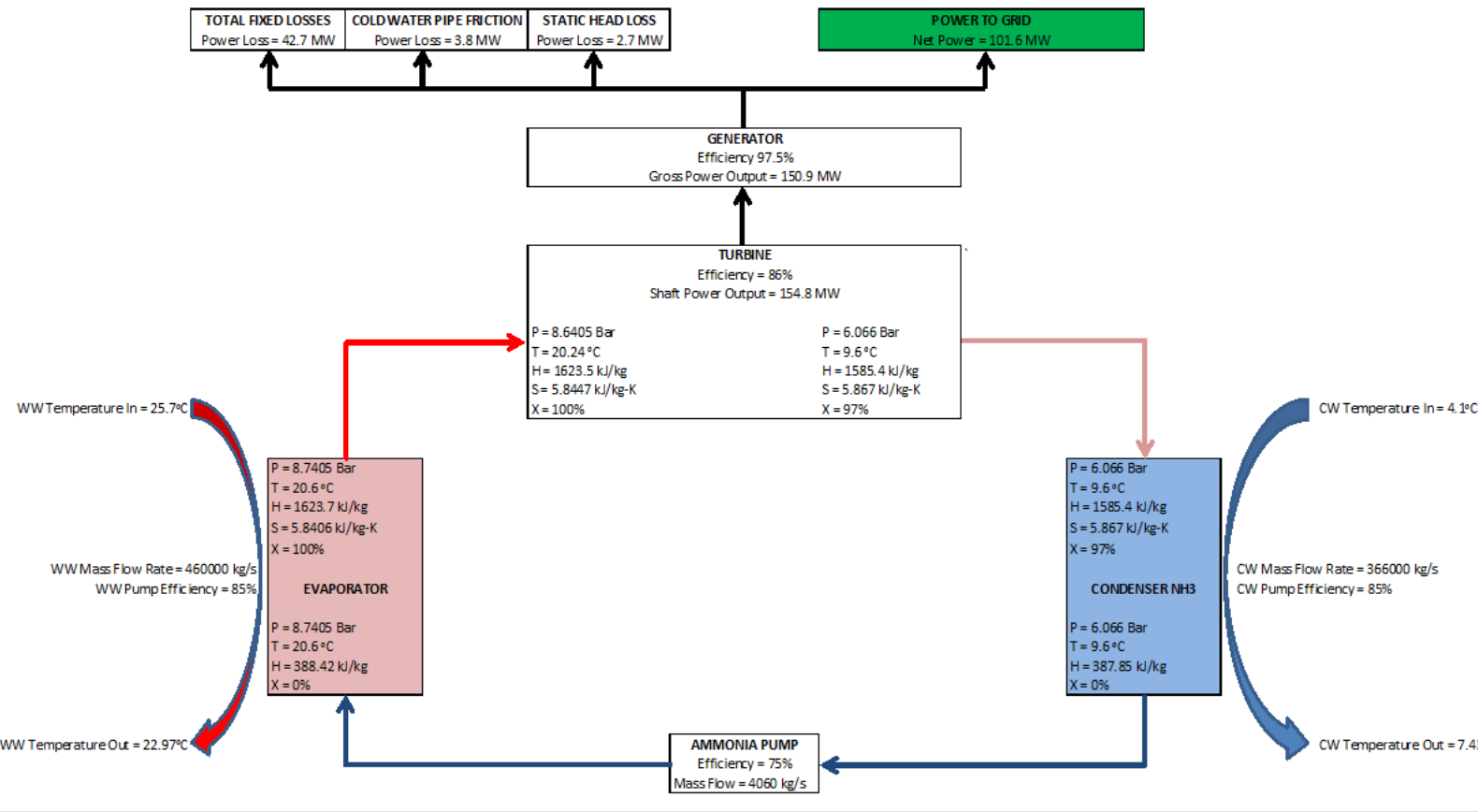


Figure 3-1 OTEC Closed Cycle Process Diagram

The demister has been represented as a pressure loss between the evaporator and turbine and is not shown for clarity in the figure above. In the true system, approximately 1/3 of the ammonia flow is re-circulated from the demister back to the evaporator, but this has a negligible effect on the cycle power calculations and was used to select the UA values used herein.

The term UA is a measure of heat exchanger performance consisting of overall heat transfer coefficient (U-value) and heat exchange area (A). In keeping with the thermodynamic model established for the system by Makai Ocean Engineering, the corresponding UA values are presented in Table 3-2.

Table 3-2 100MW Net Power Heat Exchanger UA Values

| | |
|----------------|------------|
| *Evaporator UA | 1410 MW/°C |
| *Condenser UA | 1350 MW/°C |

* These UA values combine with an OTEC plant design log mean temperature difference (LMTD) between water and ammonia working fluid of about 3.5 °C. The result is a heat exchanger thermal duty close to 5000 MW for the evaporators, and slightly less for the condensers.

3.2 Gross Power

$$\text{Gross Power (MW)} = 13.89\Delta T - 149.71$$

The gross power production has been found to be directly proportional to the temperature difference between the (near) surface and cold deep water, $\Delta T = T_S - T_D$, where T_S and T_D are the surface (warm) and deep (cold) water temperatures (°C), respectively. The above equation for gross power was established by calculating the gross power output of 28 representative points in the ocean and fitting an equation to those points to simplify a multi-variable equation into a single-variable equation. Complete results are provided in Appendix D. The 28 data points were comprised of the highest net power return, a 0 MW net power return (as defined by a simplified OTEEV power formulation presented at OCEANS '11 in Kona, HI⁶) and 26 intermediary points across the net power spectrum. A sample set of calculations for the base case is outlined in Appendix C. Gross power was then graphed against ΔT and the characteristic equation was found to be highly linear (Figure 3-2).

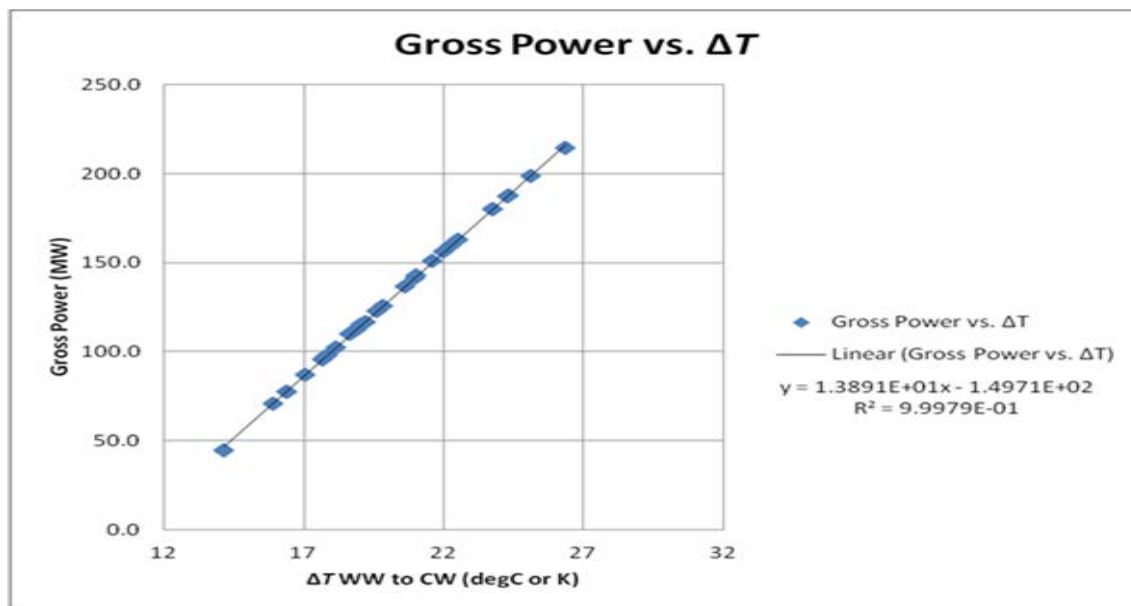


Figure 3-2 Gross Power as a Function of ΔT

⁶ Nagurny et al

3.3 Fixed Loss Factors

$$\text{Fixed Losses}(L_{\text{Fixed}} \text{ in MW}) = 42.7$$

The total fixed loss factor L_{Fixed} is approximated as the sum of the cold water intake power loss, condenser and distribution pumping loss, evaporator and distribution pumping loss, and ammonia pumping loss within the process. These losses are each estimated in Sections 3.3.1 through 3.3.4.

3.3.1 Cold Water Intake Power Loss

$$\text{Cold Water Intake Power Loss} = 3.8\text{MW}$$

This fixed loss is established based on water velocity and a known factor for a protruding pipe entrance, which is assumed for the cold water inlet.

$$^7 \text{ Minor Head Loss } (h) = \frac{CV^2}{2g}, \text{ where } V = \frac{Q}{A} = \frac{4\dot{m}}{\pi\rho D^2}$$

$$^8 \text{ Head Loss Coefficient for Protruding Pipe Entrance } (C) = 0.8$$

$$\text{Nominal Sea Water Density } (\rho) = 1025 \frac{\text{kg}}{\text{m}^3}$$

$$\text{Cold Water Pipe Internal Diameter } (D) = 10\text{m}$$

$$V = \frac{4\dot{m}}{\pi\rho D^2} = \frac{4 \times 366,000 \frac{\text{kg}}{\text{sec}}}{\pi \times 1025 \frac{\text{kg}}{\text{m}^3} \times (10\text{m})^2} = 4.546 \frac{\text{m}}{\text{sec}}$$

$$\text{Intake Head Loss } (h_{\text{Intake}}) = \frac{0.8 \times \left(4.546 \frac{\text{m}}{\text{sec}}\right)^2}{2 \times 9.81 \frac{\text{m}}{\text{sec}^2}} = 0.843\text{m}$$

$$\begin{aligned} \text{Cold Water Intake Power Loss} &= \text{Pump Loss Factor} \times \text{Intake Head Loss} = 4.488 \frac{\text{MW}}{\text{m}} \times 0.843\text{m} \\ &= 3.8\text{MW} \end{aligned}$$

The Cold Water Intake Power Loss has been identified as an opportunity for reduction in power loss. The entrance could be rounded and formed to reduce the losses, which could be verified by model testing or computational fluid dynamics. However, it is unknown what filter elements may be required at the entrance, so the 0.8 coefficient for a typical protruding pipe entrance is used for this investigation.

⁷ NCEES 47

⁸ NCEES 48

3.3.2 Condenser and Distribution Pumping Loss

$$\text{Condenser and Distribution Pumping Loss} = 22.4 \text{ MW}$$

This fixed loss is established based on assumed losses through the condensers and distribution piping. 5m of head was assumed. The 5m of head accounts for bends from the cold water pipe to the heat exchangers, seawater manifolding losses into and out of the heat exchanger, heat exchanger passage entry/exit, losses through the heat exchanger passages and losses from the heat exchangers to the outlet. The total loss becomes 22.4 MW when the Head Loss to Power Loss Factor is applied.

$$\text{Condenser and Distribution Pumping Loss} =$$

$$\text{Pump Loss Factor} \times \text{Assumed Design Head} = 4.488 \frac{\text{MW}}{\text{m}} \times 5\text{m} = 22.4 \text{ MW}$$

3.3.3 Evaporator and Distribution Pumping Loss

$$\text{Evaporator and Distribution Pumping Loss} = 14.1 \text{ MW}$$

This fixed loss is established based on previous modeling and corresponding fixed assumptions for the 150 MW gross (100MWe net power) nominal case. The corresponding head loss would be approximately 2.5m. The 2.5m of head accounts for the loss across intake screens at the inlet, seawater manifolding losses into and out of the heat exchanger, heat exchanger passage entry/exit, losses through the heat exchanger passages and losses from the heat exchangers to the outlet.

$$\text{Evaporator and Distribution Pumping Loss} = \frac{\dot{m}_{\text{warm}} g h_{\text{warm}}}{\eta}$$

$$\text{Warm Water Mass Flow Rate } (\dot{m}_{\text{warm}}) = 460,000 \frac{\text{kg}}{\text{sec}}$$

$$\text{Warm Water Head Loss } (h_{\text{warm}}) = 2.5\text{m}$$

$$\text{Sea Water Pump Efficiency } (\eta) = 80\%$$

$$\text{Evaporator and Distribution Pumping Loss} = \frac{460,000 \frac{\text{kg}}{\text{s}} \times 9.81 \frac{\text{m}}{\text{s}^2} \times 2.5\text{m}}{80\%} = 14.1 \text{ MW}$$

3.3.4 Ammonia Pumping Loss

$$\text{Ammonia Pumping Loss} = 2.4 \text{ MW}$$

This fixed loss is established based on previous modeling and corresponding fixed assumptions for the 150 MW gross (100MWe net power) nominal case. This loss accounts for the circulation of the assumed 4060 kg/s of liquid ammonia flow.

$$\text{Ammonia Pumping Loss} = \frac{Q_{\text{NH}_3} \Delta P_{\text{NH}_3}}{\eta_{\text{NH}_3}}$$

$$\text{Ammonia Volumetric Flow Rate } (\dot{Q}_{NH_3}) = \frac{\dot{m}_{NH_3}}{\rho_{NH_3}} = \frac{\frac{4060}{\text{sec}} \frac{\text{kg}}{\text{sec}}}{\frac{625}{\text{m}^3} \frac{\text{kg}}{\text{m}^3}} = 6.496 \frac{\text{m}^3}{\text{s}}$$

$$\text{Ammonia Pressure Delta } (\Delta P_{NH_3}) = 274 \text{ kPa}$$

$$\begin{aligned}\text{Ammonia Pump Efficiency } (\eta_{NH_3}) \\ &= 83\% \text{ Hydraulic Efficiency} \times 95\% \text{ Gear Box Efficiency} \\ &\quad \times 95\% \text{ Motor Efficiency} = 75\%\end{aligned}$$

$$\text{Ammonia Pumping Loss} = \frac{6.496 \frac{\text{m}^3}{\text{s}} \times 274 \text{ kPa}}{75\%} = 2.4 \text{ MW}$$

3.4 Variable Loss Factors

$$L_{Var}(\text{MW}) = 0.0038d + 4.488d \times (5.234 \times 10^{-10}d^3 - 1.378 \times 10^{-6}d^2 + 1.313 \times 10^{-3}d - 0.6541) \times \left(\frac{-0.00599T_s^2 + 0.031T_s + 1025}{-0.00599(T_s - \Delta T)^2 + 0.031(T_s - \Delta T) + 1025} - 1 \right)$$

The total variable loss factor L_{Var} is the sum of pipe friction and static head losses, where d represents the depth of the cold water in meters.

3.4.1 Cold Water Head Loss to Pumping Loss Factor

$$\text{Pump Loss Factor} = 4.488 \frac{\text{MW}}{\text{m}}$$

Using the pump power equation, it is possible to determine power loss in MW as a function of pump head in meters.

$${}^9 \text{ Pump Power } (\dot{W}) = \frac{Q\gamma h}{\eta} = \frac{Q\Delta P}{\eta} = \frac{\dot{m}gh}{\eta} = \text{Pump Loss Factor} \times h$$

$$\text{Pumping Loss Factor} = \frac{\dot{m}g}{\eta}$$

$$\text{Cold Water Mass Flow Rate } (\dot{m}) = 366,000 \frac{\text{kg}}{\text{sec}}$$

⁹ NCEES 48

$$\text{Gravitational Constant } (g) = 9.81 \frac{m}{sec^2}$$

Sea Water Pump Efficiency (η)
 $= 89\% \text{ Hydraulic Efficiency} \times 95\% \text{ Gear Box Efficiency}$
 $\times 95\% \text{ Motor Efficiency} = 80\%$

Head Loss (h) = Data Input in meters

$$\text{Pump Loss Factor} = \frac{366,000 \frac{kg}{sec} \times 9.81 \frac{m}{sec^2}}{80\%} = 4.488 \frac{MW}{m}$$

3.4.2 Cold Water Pipe (CWP) Friction Loss

$$\text{Pipe Frictional Loss} = 0.0038 \frac{MW}{m}$$

This variable loss is dependent entirely upon the length of the CWP. The factor is established by calculations of pipe wall friction based on the smoothness of the pipe, pipe diameter and water velocity.

$$\text{Head Loss due to Friction } (h_f) = \frac{fLV^2}{2Dg}$$

$$\text{Head Loss due to Friction per Unit Length } \left(\frac{h_f}{L} \right) = \frac{fLV^2}{2DgL} = \frac{fV^2}{2Dg}$$

Hydraulic Pipe Diameter (D) = 10m

$$\text{Velocity in Pipe } (V) = \frac{\dot{m}}{\rho \times A} = \frac{366,000 \frac{kg}{s}}{1025 \frac{kg}{m^3} \times \frac{\pi(10m)^2}{4}} = 4.546 \frac{m}{s}$$

Colebrook Equation for Friction Factor (f): $\frac{1}{\sqrt{f}} = -2 \log_{10} \left(\frac{\epsilon}{3.7D} + \frac{2.51}{Re\sqrt{f}} \right)$

Pipe Roughness Coefficient (ϵ) = .00005

$$\text{Reynold's Number } (Re) = \frac{DV\rho}{\mu}$$

$$\text{Density of Seawater } (\rho) = 1025 \frac{\text{kg}}{\text{m}^3}$$

$$\text{Absolute Viscosity } (\mu) = 1.79 \text{ cP} = .00179 \text{ Pa} \cdot \text{s}$$

$$\text{Reynold's Number } (Re) = \frac{10m \times 4.546 \frac{\text{m}}{\text{s}} \times 1025 \frac{\text{kg}}{\text{m}^3}}{.00179 \text{ Pa} \cdot \text{s}} = 26.032 \times 10^6$$

$$\text{Colebrook Equation for Friction Factor } (f): \frac{1}{\sqrt{f}} = -2 \log_{10} \left(\frac{\frac{.00005}{10m}}{3.7} + \frac{2.51}{26.032 \times 10^6 \sqrt{f}} \right)$$

(Solving Iteratively) $f = .007933$

$$\text{Head Loss due to Friction per Unit Length } \left(\frac{h_f}{L} \right) = \frac{0.007933 \times \left(4.546 \frac{\text{m}}{\text{s}} \right)^2}{2 \times 10m \times 9.81 \frac{\text{m}}{\text{s}^2}} = 0.0008356$$

$$\text{Pipe Frictional Loss} = \frac{h_f}{L} \times \text{Pump Loss Factor} = 0.0008356 \times 4.488 \frac{\text{MW}}{\text{m}} = 0.0038 \frac{\text{MW}}{\text{m}}$$

3.4.3 Static Head Loss

$$\begin{aligned} \text{Static Head} &= (5.234 \times 10^{-10} d^3 - 1.378 \times 10^{-6} d^2 + 1.313 \times 10^{-3} d - 0.6541) \\ &\times \left(\frac{-0.00599 T_s^2 + 0.031 T_s + 1025}{-0.00599 (T_s - \Delta T)^2 + 0.031 (T_s - \Delta T) + 1025} - 1 \right) \times d \end{aligned}$$

Determination of correct static head involves the integration through the CWP depth (d) of density difference between the cold water inside the CWP and the warmer water on the outside of the pipe as a function of depth. However, the detailed information on the density depth profile is not available at each site for use in this assessment. The difference between average density and surface water density can be used instead to provide a very accurate approximation of the more correct integration method. At the most commonly occurring CWP depth of 1000m, the error between static head produced by the integration method and static head produced by the approximation presented here is just 0.05%. Maximum error occurs at the 900m depth at 0.94%. A detailed formulation of the static head loss equation is presented in Appendix B.

3.5 Final Equation

The final equation for net power is a function of gross power and all losses, fixed and variable.

$$\begin{aligned}
 OTEC \text{ Net Power} &= \text{Gross Power} - L_{\text{Fixed}} - L_{\text{Var}} \\
 &= 13.891\Delta T - 149.71 - 42.7 - 0.0038d - 4.488d \cdot (5.234 \cdot 10^{-10}d^3 - 1.378 \cdot 10^{-6}d^2 \\
 &\quad + 1.313 \cdot 10^{-3}d - 0.6541) \cdot \left(\frac{-0.00599T_s^2 + 0.031T_s + 1025}{-0.00599(T_s - \Delta T)^2 + 0.031(T_s - \Delta T) + 1025} - 1 \right)
 \end{aligned}$$

3.6 Model Output

More than 14 million data points assimilated in HYCOM+NCODA were post-processed using an energy extraction model in MATLAB. Output from the model retains the 1/12th degree resolution of gridded data points. The results of this model were provided to the NREL for independent validation and for incorporation into a GIS database for renewable energy resources. This visualization of quantifiable power output with high resolution is a significant achievement over past work, which relied on low resolution data and only visually reported the difference between sea surface temperature and temperature at 1000 m (Nihous, 2007). The result serves as the first step to providing the “technical” resource assessment and thus establishes the ability to assign power extraction estimates regionally.

3.7 Sensitivity Analysis

To better understand the effect of each parameter of this technical study on the overall net power output, each parameter was varied by $\pm 10\%$ and net power was re-evaluated for the base case designed to conditions yielding 101.1 MWe Net. The results of this study are shown in Table 3-3 and Figure 3-3.

Table 3-3 OTEC Net Power Equation Parameter Dependence

| OTEC Net Power Equation Parameter Dependence | | | | | | |
|---|----------------|----------------|-------------|------------|------------------------------|-----------------------------|
| Parameter | Starting Value | 10% Difference | High (+10%) | Low (-10%) | Net Power (MW) at High Value | Net Power (MW) at Low Value |
| Temperature Difference (°C) | 21.6 | 2.16 | 23.76 | 19.44 | 131.1 | 71.2 |
| Surface Temperature (°C) | 25.7 | *2.16 | 27.86 | 23.54 | 100.6 | 101.6 |
| Cold Water Pipe Depth (m) | 1000 | 100 | N/A | 900 | N/A | 102.1 |
| **Warm Water Flow Rate (kg/s) | 460,000 | 46000 | 506,000 | 414,000 | 101.7 | 100 |
| **Cold Water Flow Rate (kg/s) | 366,000 | 36600 | 402,600 | 329,400 | 100.7 | 100.9 |
| **Ammonia Flow Rate (kg/s) | 4060 | 406 | 4,466 | 3,654 | 99.7 | 99.7 |
| Turbine Efficiency (%) | 86% | 8.6% | 94.6% | 77.4% | 116.5 | 86 |
| Ammonia Pump Efficiency (%) | 75% | 7.5% | 82.5% | 67.5% | 101.3 | 100.9 |
| Seawater Pump Efficiency (%) | 80% | 8.0% | 88.0% | 72.0% | 105.4 | 95.9 |
| ***Generator Efficiency (%) | 97.5% | 9.8% | 100.0% | 87.8% | 104.9 | 86.1 |
| Condenser & Piping Head Loss (m) | 5.0 | 0.5 | 5.5 | 4.5 | 103.3 | 98.9 |
| Evaporator & Piping Head Loss (m) | 2.5 | 0.3 | 2.8 | 2.3 | 102.5 | 99.7 |
| * Same difference used for Surface Temperature as Temperature Difference for consistency and relevance. | | | | | | |
| ** Heat Exchanger U-value held constant. | | | | | | |
| *** Maximum efficiency 100%. | | | | | | |

OTEC 100MW System Model Parameter Study

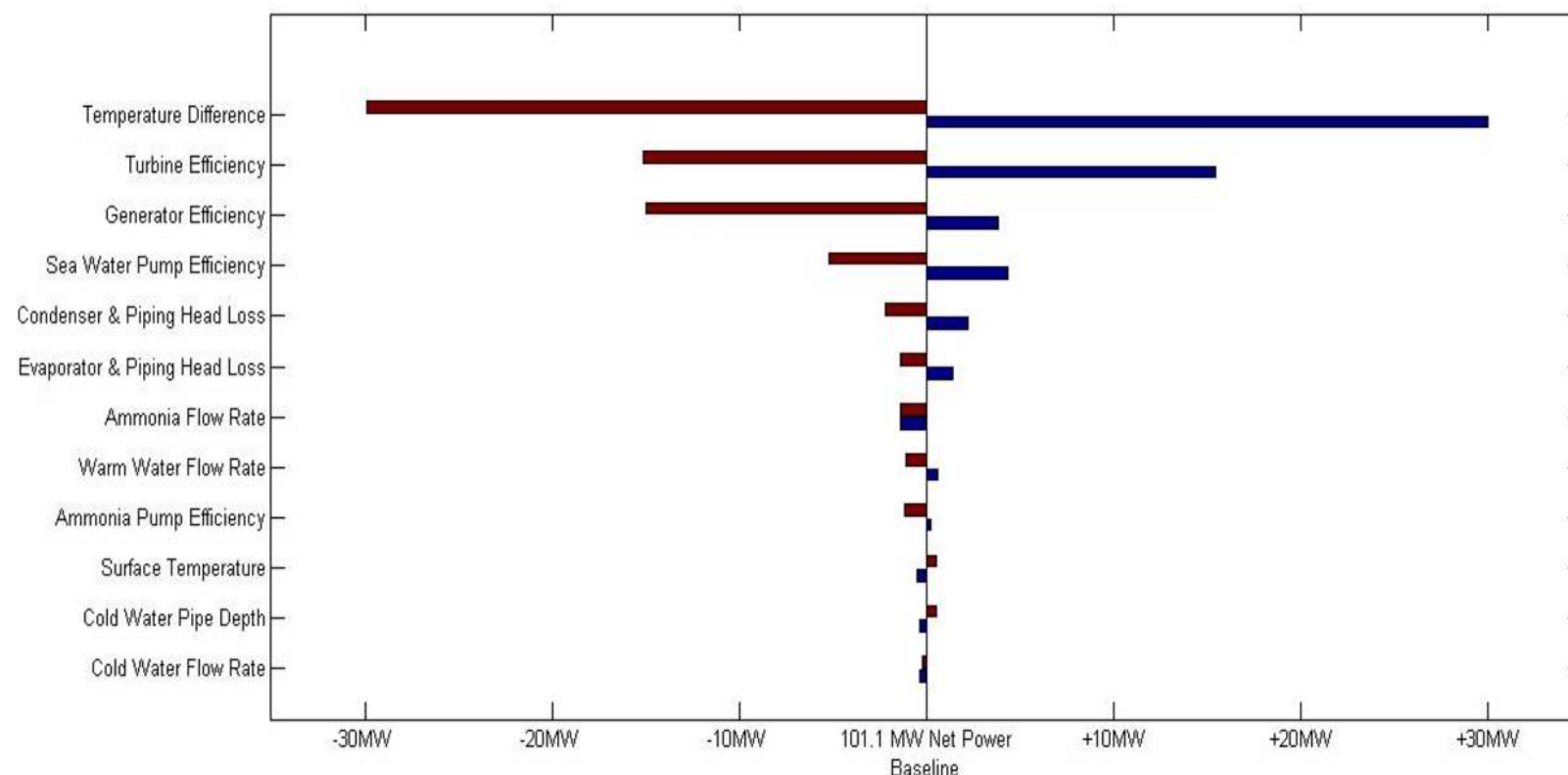


Figure 3-3 OTEEV Net Power Model Sensitivity

The above “tornado” graph arranges the parameters in order of decreasing significance to the net power output. Developers and engineers of an OTEC system would be advised to spend the most time locating and optimizing the conditions that have the most impact to their specific design.

Temperature difference dominates the net power calculation, as can be seen in Figure 3-3. This result emphasizes the importance of site selection in maximizing power output of an OTEC plant. Temperature difference drives gross power output, as discussed in Section 3.2. Gross power dominates the overall net power equation for the baseline case and all cases with reasonable net power output. These constitute the cases of greatest potential and interest.

Close behind temperature difference in importance are turbine and generator efficiencies, which are directly proportional to power output. Turbine and generator efficiencies maximize the use of state-of-the-art technologies for optimal power return. This means that little can be done to further increase net power by tweaking turbine and generator systems with current technology.

Seawater pump efficiency has a large impact to total net power also. Other than proper selection of location to optimize temperature difference, seawater pump efficiency represents the greatest potential for net power increase. In this study, 89% hydraulic, 95% gear box and 95% motor efficiency were used. With detailed design, it is possible to obtain hydraulic efficiency on the order of 92%. It is also possible to eliminate the gear box entirely. In this scenario, water-to-water efficiencies greater than 87% can be realized. This would result in a nearly 4% increase in net power.

Cold water and warm water distribution losses show potential for increasing net power output. However, these passages have been designed to minimize frictional loss while providing adequate heat transfer. Little can be done to further minimize these losses without excessive reduction to heat transfer and subsequent power production.

Ammonia flow rate seems to cause a power reduction when flow is increased or decreased. This appears to confirm that an optimum ammonia flow rate has been selected. However, U-value was held constant for this investigation, even though increase in ammonia flow would cause a subsequent increase in U-value. The relationship is not linear and an increase in ammonia flow would likely show little to no increase in power output. Decreasing ammonia flow while adjusting U-value would show even less power than this investigation.

Increasing warm water flow rate appears to increase net power output. If a corresponding increase in U-value were considered, power would increase even more significantly. This investigation, considering a simplified system model, appears to suggest that increasing seawater flow rate allows for a corresponding increase in net power.

Changes to ammonia pump efficiency have a small effect to overall net power output. With the low overall power consumption and nearly negligible contribution to thermodynamics, this result is expected.

As can be expected, decreasing the length of the cold water pipe, while keeping the temperature difference steady, results in an increase in net power. This results from the cold water pumps having less frictional head to overcome in order to flow an equivalent amount of water.

Increasing the sea surface temperature, while holding temperature difference constant, results in less dense surface water. This change to density negatively impacts the static head that must be overcome by the cold water pumps. As such, it requires more power to pump an equivalent amount of cold seawater.

Changes to cold water flow rate appear to decrease total net power output. Though changes to U-value are not considered, this appears to indicate that cold water flow rate has been properly selected.

4 Independent Validations

As part of the development team, NREL researchers were assigned to validate the projections of potential net power production result supplied by the energy extraction model detailed in Section 3. The independent validation effort described in the following pertains primarily to Objective 3 and Task 4 of the Statement of Project Objectives (SOPD).

4.1 Plant Design

The LM team picked a single 100-MWe Net closed-cycle plant for a baseline design. The resources of the design plant correspond to a location off the island of O‘ahu in Hawai‘i. All plant details were generated by LM. OTEC resources at other locations were then evaluated as if this plant was physically transported to that location and operated with the same resource seawater flow rates.

During this effort a concern arose regarding the ratio of flow rate of warm seawater to cold seawater. This ratio as chosen by the design team was $(460/366) = 1.26$. Prior thermo-economic studies indicate that due to larger costs involved in acquiring large volumes of cold seawater flow, when calculating optimum costs for the plant, the preferred designs used substantially more warm seawater than the cold seawater to push this ratio to about 2. Since cost was only addressed for the baseline design case in this design study, the site specific warm water to cold water flow ratios could be further optimized.

4.2 Plant Design Validation Methodology

For the validation, the plant design resource conditions were set as stated in Table 4-1.

Table 4-1 Plant Design Conditions

| Descriptions | Values | Units |
|------------------------------|---------|--------|
| Warm seawater flow rate | 460,000 | (kg/s) |
| Cold seawater flow rate | 366,000 | (kg/s) |
| Warm seawater temperature | 25.7 | °C |
| Cold seawater temperature | 4.1 | °C |
| Cold seawater resource depth | 1000 | m |

Additional constraints that were imposed on the power plant include stated conditions in Table 4-2. The plant working fluid chosen was pure anhydrous ammonia. A single-stage Rankine cycle is chosen as the energy conversion system of the plant.

Table 4-2 Power Plant Design Constraints

| Descriptions | Value | Units |
|-------------------------------|-------|--------|
| Evaporator UA | 1,410 | MW/K |
| Condenser UA | 1,360 | MW/K |
| Turbine isentropic efficiency | 86 | (%) |
| Generator efficiency | 97.5 | (%) |
| Working fluid pump efficiency | 75 | (%) |
| Warm seawater pump efficiency | 80 | (%) |
| Cold seawater pump efficiency | 80 | (%) |
| Working fluid flow rate | 4060 | (kg/s) |

Considering the large number of resource locations and conditions required for the development of the world map, the validation effort was restricted to a few resource locations and conditions. Only a set of 28 resource locations were chosen for validation purposes. However, these data locations were chosen to represent the full spectrum of expected conditions in the entire database.

The power system was modeled by NREL using ASPEN™ commercially available process modeling software. Figure 4-1 illustrates the model used in the simulation. For lack of detailed seawater properties, only freshwater properties are used for the warm and cold water resource streams. The process model shows the conditions for the plant at design. Pressure losses in the working fluid stream are not included in the simulation. The evaporator and condenser pressures were allowed to float to achieve full vaporization in the evaporator (quality of 1.0) with no superheating and full condensation with no subcooling of the working fluid.

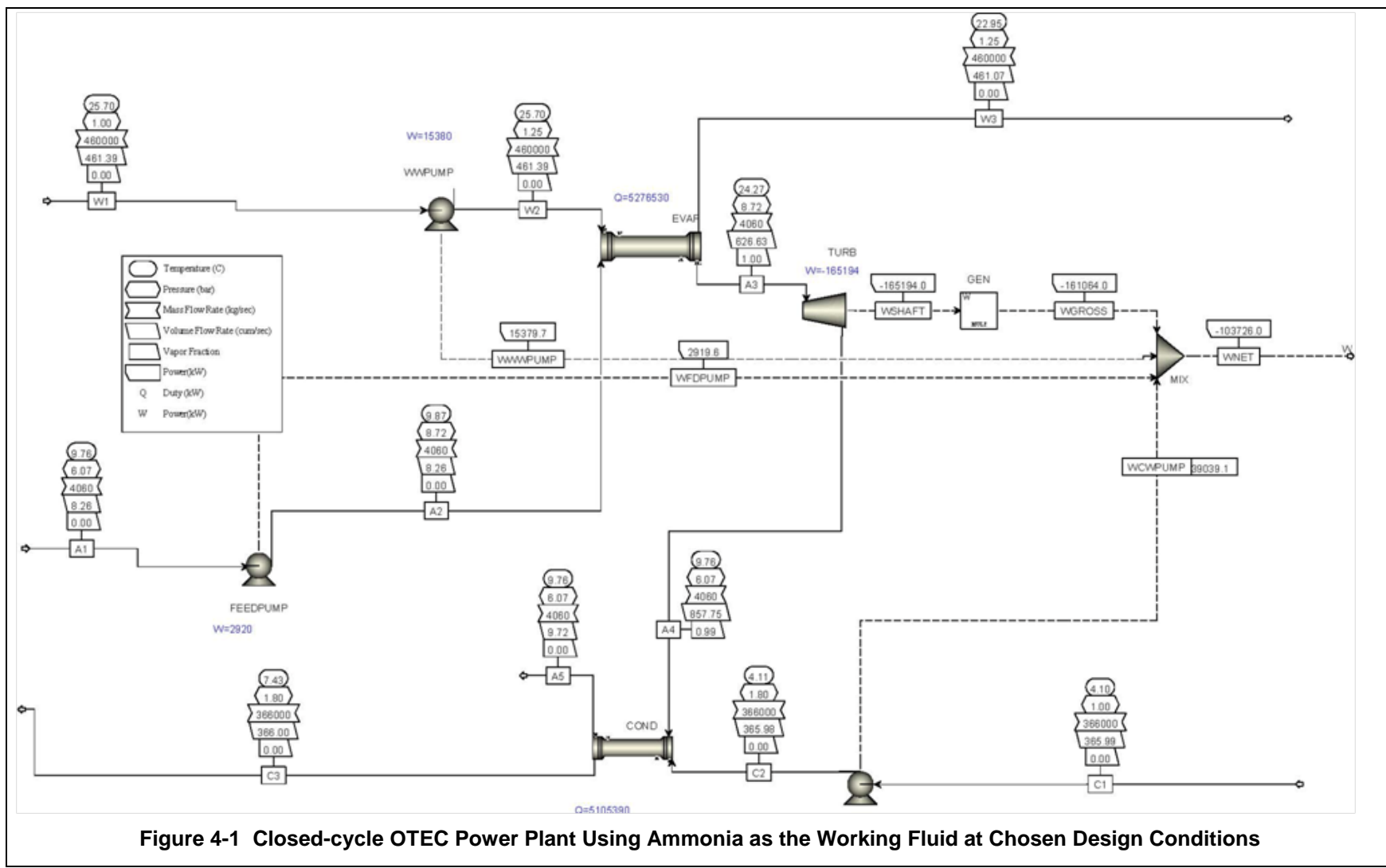


Figure 4-1 Closed-cycle OTEC Power Plant Using Ammonia as the Working Fluid at Chosen Design Conditions

4.3 Validation Results

The net power from the plant as indicated amounts to 107 MWe. This power level is somewhat higher than what would be expected with seawater due to its lower specific heat when compared to freshwater. When applying corrections for this property difference on power, we get a net power of 101 MWe. This compares well with the energy extraction model's design value of 101.1 MWe.

NREL's validation efforts and the results are compared in Table 4-3. Expected resource conditions are listed in the second to fourth columns. Projected powers by NREL and the project team are listed in the sixth and seventh columns. The last column indicates the differences in the predicted net power as a percentage. The differences are generally small, except for a few data points at the lower end of net power capacity where the differences are larger than 10%. However, those cases represent unrealistic deployment where a nominally designed 100-MWe power plant is producing less than 50 MW of electricity. Such deployments are unlikely and would be uneconomical. For all cases where the net power is projected to be over 58 MWe, the differences average out to around 1%.

This table basically confirms the predictions of net power made by the project team from a single-stage closed-cycle OTEC power plant using ammonia as the working fluid. We estimate the overall uncertainty in the net power predictions to be less than 5%.

Table 4-3 Comparison of Predicted Net Power by NREL and the Project Team

| Point # | Temperatures | | Depth | Delta-T | Projected Net Power | | Difference (%) |
|---------|--------------------|--------------------|-------------------|--------------------------|---------------------|----------|----------------|
| | Warm Seawater (°C) | Cold Seawater (°C) | Cold Seawater (m) | Overall (warm-cold) (°C) | NREL (MWe) | LM (MWe) | |
| 1 | 30.53 | 4.19 | 1000 | 26.34 | 164 | 164 | -0.1 |
| 2 | 28.92 | 4.60 | 1000 | 24.32 | 138 | 138 | 0.4 |
| 3 | 28.64 | 4.37 | 1000 | 24.27 | 138 | 137 | 0.7 |
| 4 | 29.08 | 3.98 | 1000 | 25.10 | 149 | 149 | 0.6 |
| 5 | 27.74 | 3.98 | 1000 | 23.76 | 131 | 131 | 0.4 |
| 6 | 28.08 | 4.32 | 1000 | 23.76 | 130 | 130 | -0.4 |
| 7 | 25.95 | 3.96 | 1000 | 21.99 | 109 | 107 | 1.4 |
| 8 | 25.64 | 5.81 | 1000 | 19.83 | 77 | 77 | 0.2 |
| 9 | 27.58 | 6.62 | 1000 | 20.96 | 92 | 92 | 0.9 |
| 10 | 25.41 | 4.39 | 1000 | 21.02 | 94 | 94 | 0.2 |
| 11 | 25.08 | 5.48 | 1000 | 19.60 | 75 | 74 | 0.7 |
| 12 | 20.01 | 3.62 | 1000 | 16.39 | 29 | 30 | -0.3 |
| 13 | 22.21 | 4.39 | 1000 | 17.82 | 50 | 50 | 1.0 |
| 14 | 17.78 | 3.64 | 1000 | 14.14 | -3 | -3 | 1.6 |
| 15 | 24.25 | 5.45 | 1000 | 18.80 | 63 | 63 | 0.3 |
| 16 | 25.77 | 8.11 | 1000 | 17.66 | 47 | 47 | 0.4 |
| 17 | 21.96 | 5.59 | 700 | 16.37 | 29 | 30 | -4.9 |
| 18 | 27.40 | 4.90 | 700 | 22.50 | 114 | 115 | -0.7 |
| 19 | 26.96 | 4.70 | 800 | 22.26 | 111 | 111 | -0.4 |
| 20 | 23.55 | 4.51 | 800 | 19.04 | 66 | 68 | -1.8 |
| 21 | 22.63 | 3.98 | 900 | 18.65 | 61 | 62 | -0.6 |
| 22 | 26.12 | 5.53 | 900 | 20.59 | 88 | 88 | 0.0 |
| 23 | 24.19 | 8.31 | 600 | 15.88 | 22 | 24 | -11.7 |
| 24 | 27.93 | 10.89 | 600 | 17.04 | 36 | 40 | -12.1 |
| 25 | 26.79 | 9.03 | 500 | 17.76 | 46 | 51 | -8.9 |
| 26 | 28.89 | 9.71 | 500 | 19.18 | 69 | 70 | -1.1 |
| 27 | 28.20 | 9.29 | 400 | 18.91 | 63 | 67 | -5.3 |
| 28 | 28.94 | 10.80 | 400 | 18.14 | 51 | 56 | -10.5 |

Further, we find that the overall temperature difference between the warm and cold seawater resource is the major variable that affects the net power. A plot of the net power as a function of this overall ΔT is provided in Figure 4-2.

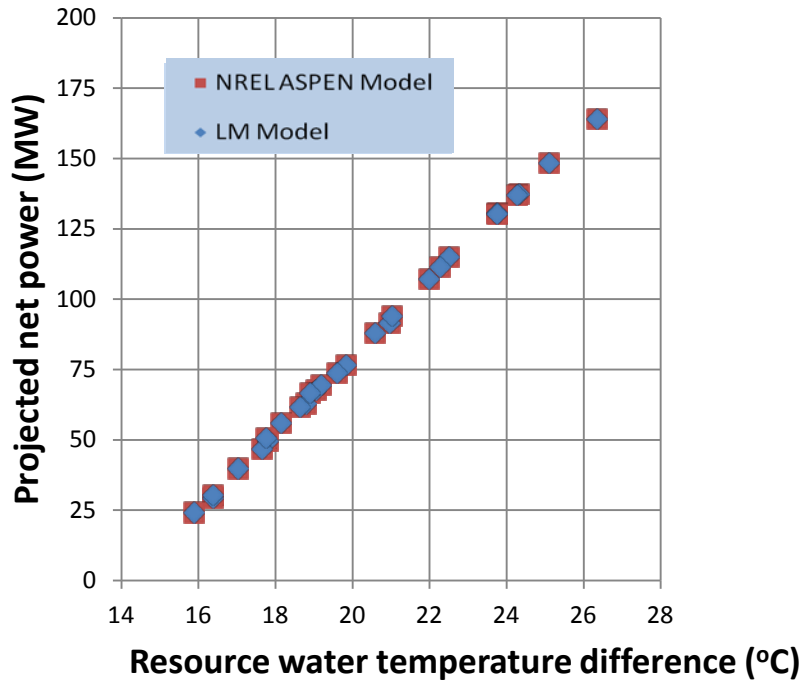


Figure 4-2 Variation of Projected Net Power as a Function of the Overall Resource Temperature Difference; Both NREL and LM Predictions are Shown

The net power varies more or less linearly with this overall temperature difference. With this nominal design, production of net power of more than 150 MWe is possible at a high ΔT of over 26°C.

Average slopes of these variations indicate about 13.6 MWe of net power increase for each one-degree (Celsius) increment in the temperature difference.

Influence of cold seawater pipe length is minimal on the net power. However, it is likely to have substantial influence on the overall cost of the power plant.

Economic evaluations will indicate what minimum ΔT might be acceptable for any given location.

5 Plant Spacing Estimates

Combining the results from the HYCOM+NCODA dataset discussed in Section 2 with the OTEC plant model discussed in Section 3 allows computation of the localized OTEC power potential of a single OTEC plant, wherever it may be deployed. This begs the question of the total potential power that could be produced using OTEC technology in a given region, whether it is one of national interest, such as the U.S. Exclusive Economic Zone or the entire world ocean. To address the question of total potential power, it is necessary to consider limitations on resource usage and translate that into the number of such OTEC plants that can be deployed in a particular region.

5.1 Cold Water Constraint

The approach here builds on a global OTEC potential estimate of 5 TWe (Nihous, 2007) and provides a method for obtaining regional results as called out in subtask 2.2 of the SOPO. Based on earlier work, Nihous hypothesized that global OTEC sustainability would be constrained by the production of cold water in the polar regions and used a simplified one-dimensional model of global usage of cold-water resources by OTEC constrained to produce steady-state maintenance of those resources, albeit at a somewhat reduced level compared to the present. This study retains the cold-water constraint on OTEC potential and utilizes the HYCOM+NCODA results to address the question of depletion of the cold-water resource in the vicinity of an OTEC plant. It does so by introducing the concept of cold-water usage, that is, the amount of cold water an OTEC plant pumps from a particular area relative to the amount being advected into that area by oceanic circulation. This rate can be expressed as an equivalent layer thickness for the cold water being pumped.

Consider an isolated OTEC plant, as depicted in Figure 5-1, which draws cold water at a rate of F_c [$\text{m}^3 \text{s}^{-1}$] from some deep layer of thickness Δz that is moving at a velocity V_{in} . The OTEC plant is assumed to sit in an oceanic area with dimensions $\Delta x \times \Delta x$, and the cold water is drawn from this area. In steady state, the (volume) pumping rate F_c must be equal to the (volume) inflow to that layer, which is $V_{in} \cdot \Delta z \cdot \Delta x$.

Thus, $F_c = (V_{in} \cdot \Delta z \cdot \Delta x)$ from which it can be seen that $\Delta x^2 = [F_c / (V_{in} \cdot \Delta z)]^2$.

Spacing plants so that they do not interfere with each other, then, requires Δx^2 square meters of area for each plant, or one plant for each Δx^2 square meters of ocean.

The free parameter here, Δz , is simply the thickness of the inflow layer required to accommodate the pumping, a *usage layer thickness*.

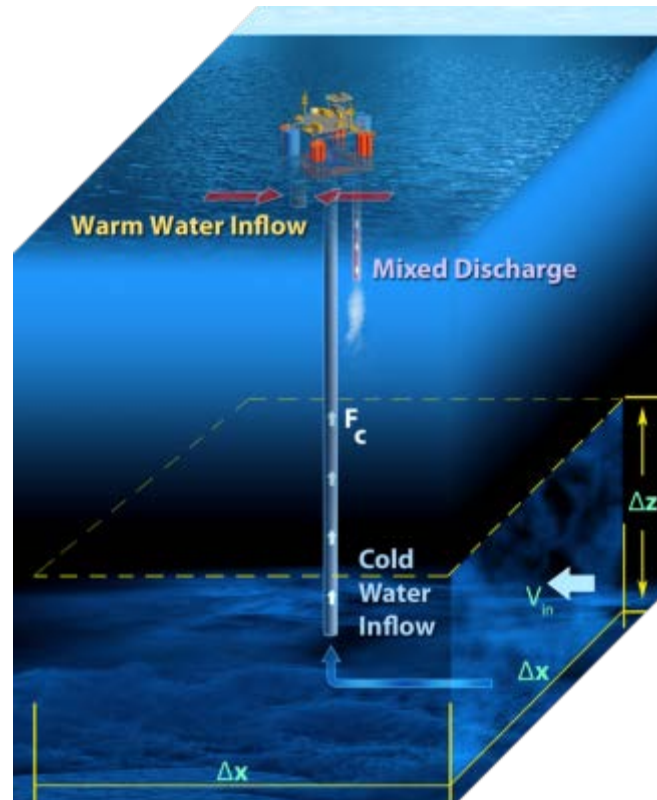


Figure 5-1 Schematic of Cold Water Usage by a Single OTEC Plant

For the OTEC plants considered in this project, $F_c = 357 \text{ m}^3 \text{s}^{-1}$ and V_{in} is available from the HYCOM+NCODA results for the East to West(EW) and North to South(NS) current velocities using the Pythagorean equation, ($V_{in} = \sqrt{EW^2 + NS^2}$). This then allows the calculation of Δx^2 as a function of Δz . As the single adjustable parameter, Δz allows the cold-water usage question to be posed in terms of the power potential in a particular area as a function of the equivalent layer cold-water usage layer thickness.

Thus, given the power potential per OTEC plant calculated from ΔT and other geophysical quantities from HYCOM+NCODA, which is the *technical* OTEC resource assessment, an OTEC plant spacing for this study, which depends on choosing a value for Δz and on the HYCOM-provided V_{in} , allows calculation of power per unit area (*OTEEV Net Power*)/(*OTEEV Plant Spacing*)². Integration over areas then provides an overall OTEC power potential for regions of interest. The result is the *technically sustainable* OTEC resource assessment. It depends, of course, on the free parameter Δz , but the Nihous (2007) result can be used to calibrate this for global sustainability. As the global OTEC estimate is refined or modified over time, this approach is still valid and can be scaled to remain in line with the new values.

$$\text{OTEEV Plant Spacing} = \Delta x = \frac{F_c}{(V_{in} \cdot \Delta z)}$$

It should be pointed out that the 357 cubic meters per second parameter is tied to the cold water flow rate of our chosen 100 MWe OTEC plant design. Systems designed to use more or less of the cold water resource could substitute their flow rate into any of the related equations and determine applicable plant spacing and plant density consistent with this approach.

5.2 Establishing a Practical Plant Spacing Approach

Suppose the 5 TW global OTEC potential discussed by Nihous (2007) is realized by distributing 50,000 of the nominal 100-MW OTEC plants discussed in Section 3 throughout the tropics and subtropics, that is, over some 189 million square kilometers of ocean. This implies an *OTEEV Plant Spacing* of about 60 km. It turns out that the average velocity of the HYCOM+NCODA dataset at the level of T_D is roughly 5 centimeters per second. This, along with the cold-water pumping rate of $F_c = 357 \text{ m}^3 \text{s}^{-1}$ can be used in the equation above to find that $\Delta z \approx 12 \text{ cm}$. This *global* value can then be used along with local values of V_{in} to calculate *local* plant density as $\text{OTEEV Plant Spacing} = 2.975 / V_{in} [\text{km}]$, for V_{in} in [m s^{-1}].

This approach is, of course, highly simplified. In the case of an isolated OTEC plant, it provides a first-order estimate of the area required to supply the plant's cold-water requirements. It does not, however, say anything about the effects of the plant's discharge of the same amount of cool water or about the plant's utilization and discharge of the warm surface water. Nor does it directly address the question of multiple OTEC plants, for example a second plant downstream of the original, isolated one. It can be argued, however, that the very small value for $\Delta z = 12 \text{ cm}$ provides for the possibility of such alignment of multiple plants, because then the first plant will not "use up" all the available cold water in the deep-water flow.

The assumption that global OTEC production is constrained by cold-water availability can now be tested. The annual average solar heating of the tropical and subtropical oceans is known from climatological heat-balance studies to be of the order 250 W m^{-2} , or, integrated over the tropical and subtropical oceanic area, about 47,000 TW. The global OTEC production of 5 TW represents a mere 0.01% of that heating. This validates the use of the cold-water availability for the constraint on production.

Further, there are additional logical and physical limitations that must be considered to the actual placement and spacing of floating OTEC facilities, such as the surface area of the platform itself at the extreme minimum. Maintaining navigable waters and wildlife migration channels are expected to be a primary concern of regulators and developers, not to mention the desire to avoid potential mooring line interference of adjacent platforms.

With respect to the water return from these plants, there is still much to be learned about the impact of situating several commercial-scale OTEC systems in close proximity. Although well out of the scope of the OTEEV project, plume studies are necessary to determine the downstream near and far field effects of a mixed seawater discharge on local nutrient levels and marine ecosystems.

Many of these physical and biological effects would be of most concern near shore where cold water currents are often found to be accelerated. For this reason, the team selected a minimum plant spacing of 3.97 km, thus safely accommodating a typical mooring radius of 2000 meters for a grid-connected floating OTEC platform.

Table 5-1 Plant Spacing as A function of Current Velocity

| OTEEV Plant Spacing | | | | | | | | | | |
|---|--------|------|-------|------|-------|-----|------|-----|------|------|
| Current Velocity (V_{in}) in meters per second | 0.0075 | 0.01 | 0.025 | 0.05 | 0.075 | 0.1 | 0.25 | 0.5 | 0.75 | 0.83 |
| Plant Spacing (Δx) in kilometers | 397 | 298 | 119 | 60 | 40 | 30 | 12 | 6 | 4 | 3.57 |

Although OTEC Systems require significantly larger areas or spacing than other ocean renewable energy devices to support their water usage, this works to their advantage in that the placement of floating plants have considerable latitude. Without the requirement to put in at an exact location for optimal performance, developers can manage or outright avoid several common permitting issues such as competing use, viewshed protections, national security and other socioeconomic filters that will determine the truly “practical” estimates of extractable energy¹⁰.

Ultimately, it will be necessary to perform new simulations using HYCOM or a similar model with the inclusion of something resembling OTEC technology (i.e., artificially introduced removal of deep cold waters and mixing of these with warm surface waters) in the simulation. This assertion echoes that of Nihous in his papers cited here: it is only by examination of the results of fully interactive simulations that a true understanding of OTEC sustainability will be possible. Such simulations are underway on a localized basis in Hawai‘i to examine both cold water usage and the effects on the water column of the discharge streams. Conducting such simulations in a global model, however, is a computing task of daunting proportions.

¹⁰ A comprehensive *practical* assessment requires the assessment of exclusion areas due to other factors such as shipping lanes, protected areas and political agreements which are beyond the scope of this study.

6 Resource Assessment Model Results and Analysis

6.1 Data File Output

The results from the power analysis, seawater cooling, and resource limitation studies of Sections 2 through 4 were output to file in network common data form (netCDF). The netCDF data format is a versatile, open standard format that allows for the storage of data arrays that are self-describing and machine and platform-independent¹¹. All of the computations for data generation were performed using MATLAB and output using MATLAB's native netCDF function suite.

The output data included both time-variate and time-invariate variables. The time-invariate data included latitude and longitude; CWP depth, which varies locationally; and plant spacing, the minimum distance between adjacent OTEC plants. Plant spacing values were based on densities derived from the annual mean current velocities. The remainder of the output data (the time-variable portion) were reported as mean annual, mean summer, and mean winter layers stacked into a single matrix per variable. These included:

- *Power* - in MW (net generating capacity) for a single plant
- *Vectorized current velocities* - at the depth of the cold water pipe intake (V_{in})
- *Warm water temperature (T_S)* - at the depth of the warm water pipe intake (20 m)
- *Temperature difference (ΔT)* - the difference between the warm and cold water sources. Given ΔT and T_S , temperature of the cold water, T_D may also be discerned.
- *Isotherms for seawater cooling* - the depths of the 8°, 14°, and 20°C cold water layers

The output gridding scheme for all the aforementioned variables was identical to that of the HYCOM+NCODA input data, with grid points separated by constant 0.08 degree longitudinal spacing, and latitudinal spacing varying between 0.08 ° at the equator and 0.0546 ° at the northern and southern extremes. Latitude was restricted to exclude waters too cold for OTEC power generation, ranging 46.9873° both north and south of the equator. This restriction results in a 1335 x 4500 point grid, with each variable or variable layer containing slightly more than 6 million data records each. For the full 12-variable data output, this amounted to more than 168 million data records produced. Isotherms for seawater air conditioning were output separately from the other variables, as these values may be considered separately from OTEC.

Land locations and waters too shallow for OTEC plant operation (<30 m) were given a flagged fill value for all variables except power, where these areas were assigned a power value of 0.

¹¹ Unidata | NetCDF, <http://www.unidata.ucar.edu/software/netcdf/>

6.2 Specific Areas of Interest

The annual mean power results generated in this study provide a useful tool for identifying locations of greatest interest for the implementation of OTEC and SWC. While seasonal power variability is significant in latitudes outside the tropics, the regions of highest possible OTEC power tend to cluster in tropical waters with little intra-annual temperature change, though this is not exclusively the case. For example, an annual average power value of 100 MW, the design power for the plant modeled in this study, can be met in latitudes as high as 26 degrees, and mean net power of 80 MW is achievable as far north as 36 degrees, offshore from North Carolina where the Gulf Stream breaks from the U.S. coast into the Atlantic Ocean. Seasonal variability is visualized in Figure 6-1, below, and may be explored in further detail using the NREL online atlas tool covered in Section 7.

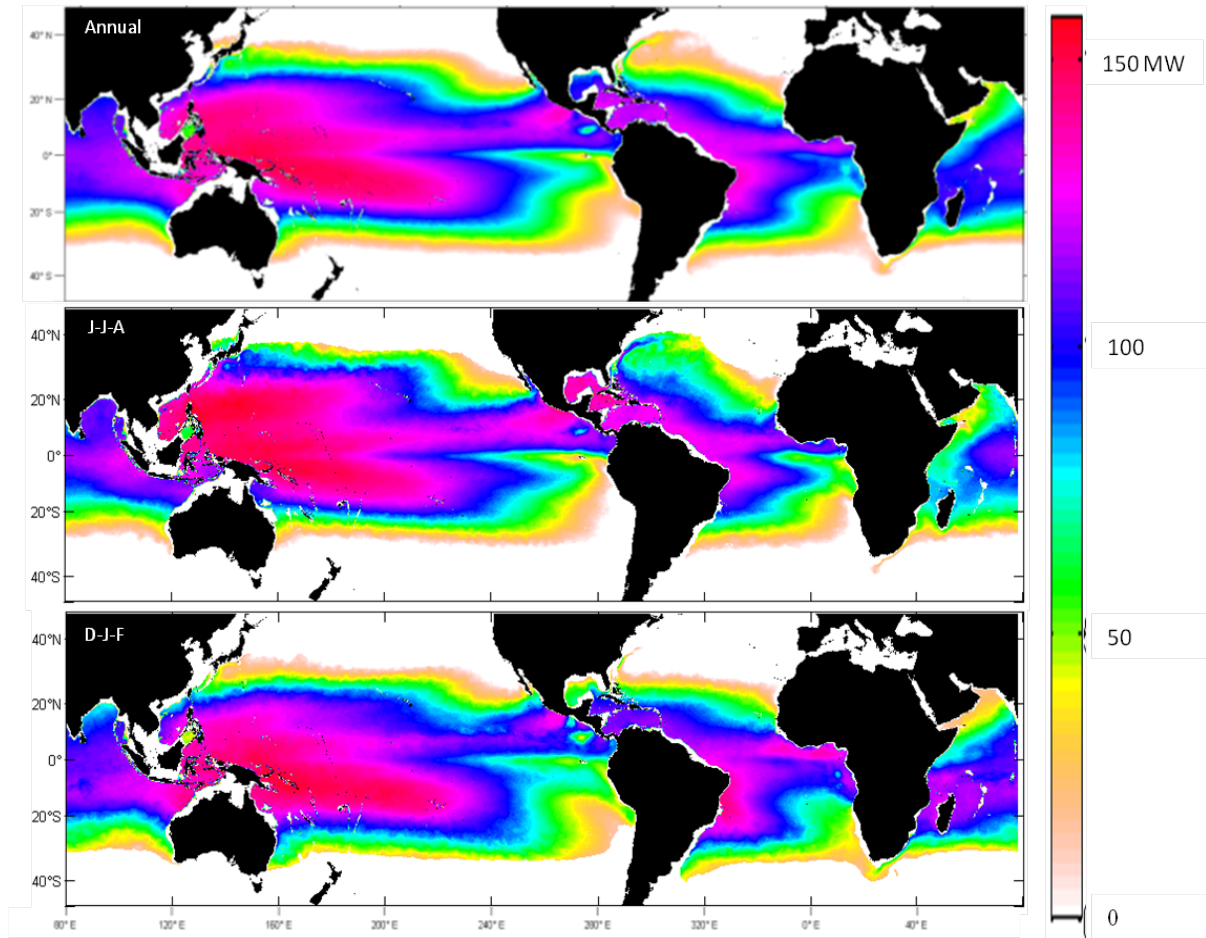


Figure 6-1 Annual and Seasonal (Jun-Jul-Aug and Dec-Jan-Feb) Mean Net Power Capacity

Results of the OTEC power model show a strong thermal energy resource throughout much of the tropical ocean. In the Indian Ocean, for example, a nominal 100 MW plant is capable of averaging its design power around most of the Indian subcontinent and islands in the Indian tropics. Likewise, extractable resources exist off the Atlantic coast of Africa, in the Pacific waters past the continental shelf of Southeastern China, and in many remote waters in the hearts of the Atlantic and Pacific Oceans.

However, a few regions present themselves as of particular interest for development, either because of their importance to U.S. interests, their proximity to islands limited by scant natural resources and high costs of energy, or as resources surrounding rapidly developing continental nations. These regions include the waters of Hawai‘i, almost the full coastline of Brazil, the islands in the South Pacific, the Gulf of Mexico, Caribbean and the Pacific coast of Mexico.

The following series of regional resource maps show the annual average values for net power capacity (A), optimized depth of cold water (B), and plant spacing (C) for a nominal 100 MW closed-cycle OTEC plant at several notable locations.

The Hawaiian Islands (Figure 6-2) are an area of keen interest for U.S. OTEC developers. The plant model used for this study was developed using input data from these islands and accurately achieves its design power in these waters. Potential power is distributed in a pronounced east-west division, with greater values on the leeward side of the island than on the windward side. A maximum power of 105 MW is achievable off the western side of the Big Island, near Kona. The steep bathymetry of the Hawaiian Islands allows long cold water pipes reaching 1000 m depth within only a few kilometers of the shoreline.

Since deep water current velocities are relatively low in this part of the Pacific, the average minimum plant spacing of 115 km in this region is roughly double the average of all OTEC valid grid point locations.

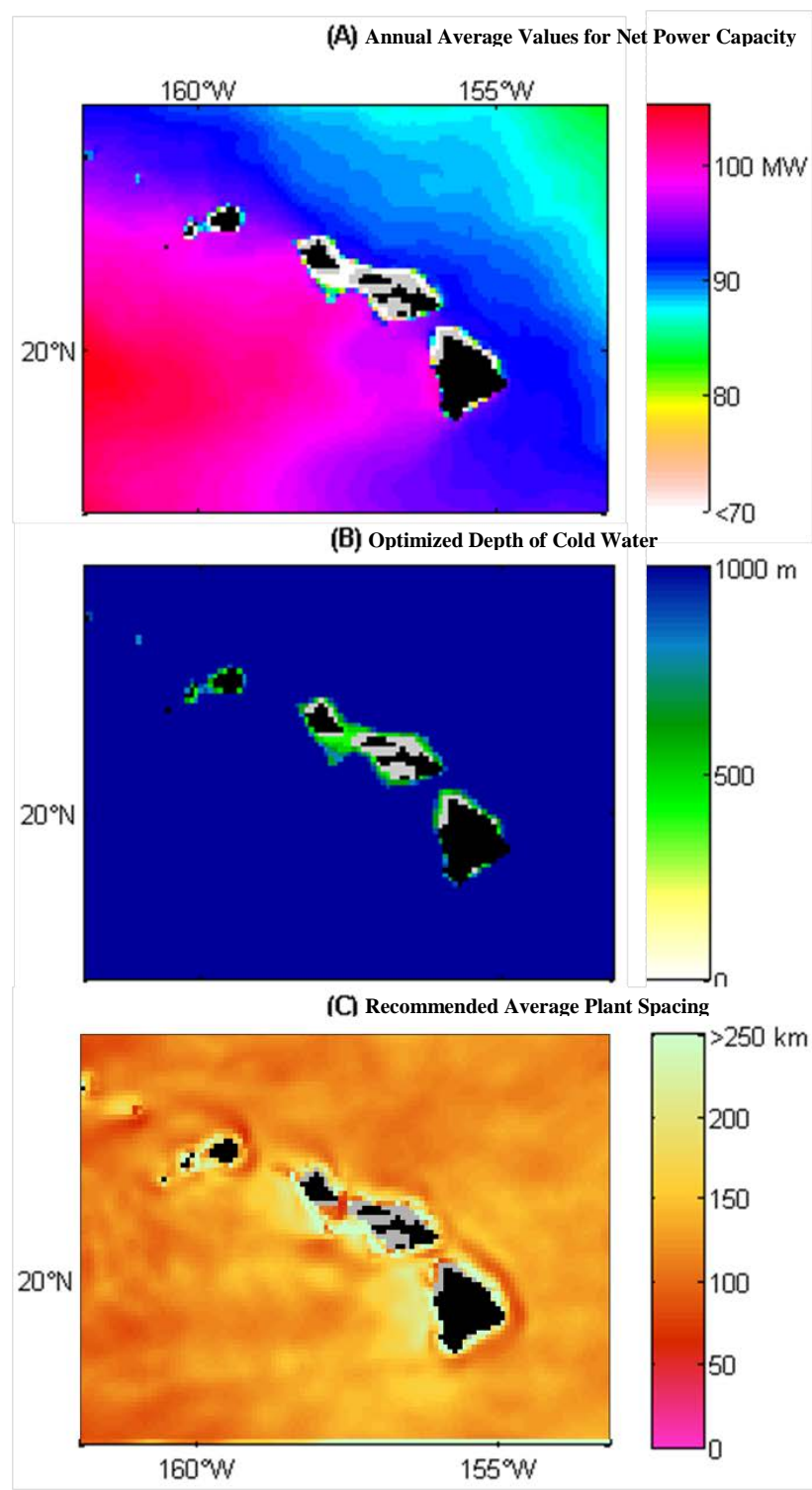


Figure 6-2 Hawaiian Islands

Multiple continental locations also represent attractive OTEC resources. Max power of 135 MW also exists off the easternmost point of Brazil (Figure 6-3). A high power resource, well above design value, hugs the shore closely along most of the coast of Brazil, French Guyana, Suriname, Venezuela, Colombia, and Panama, with many locations capable of producing greater than 100 MW from cold water at 600 m or less.

Around Brazil's coast, and among the Caribbean and Pacific islands, current velocities are relatively high, allowing plant spacing of frequently less than 10 km. This is an encouraging feature, suggesting scalability of OTEC technology in these regions.

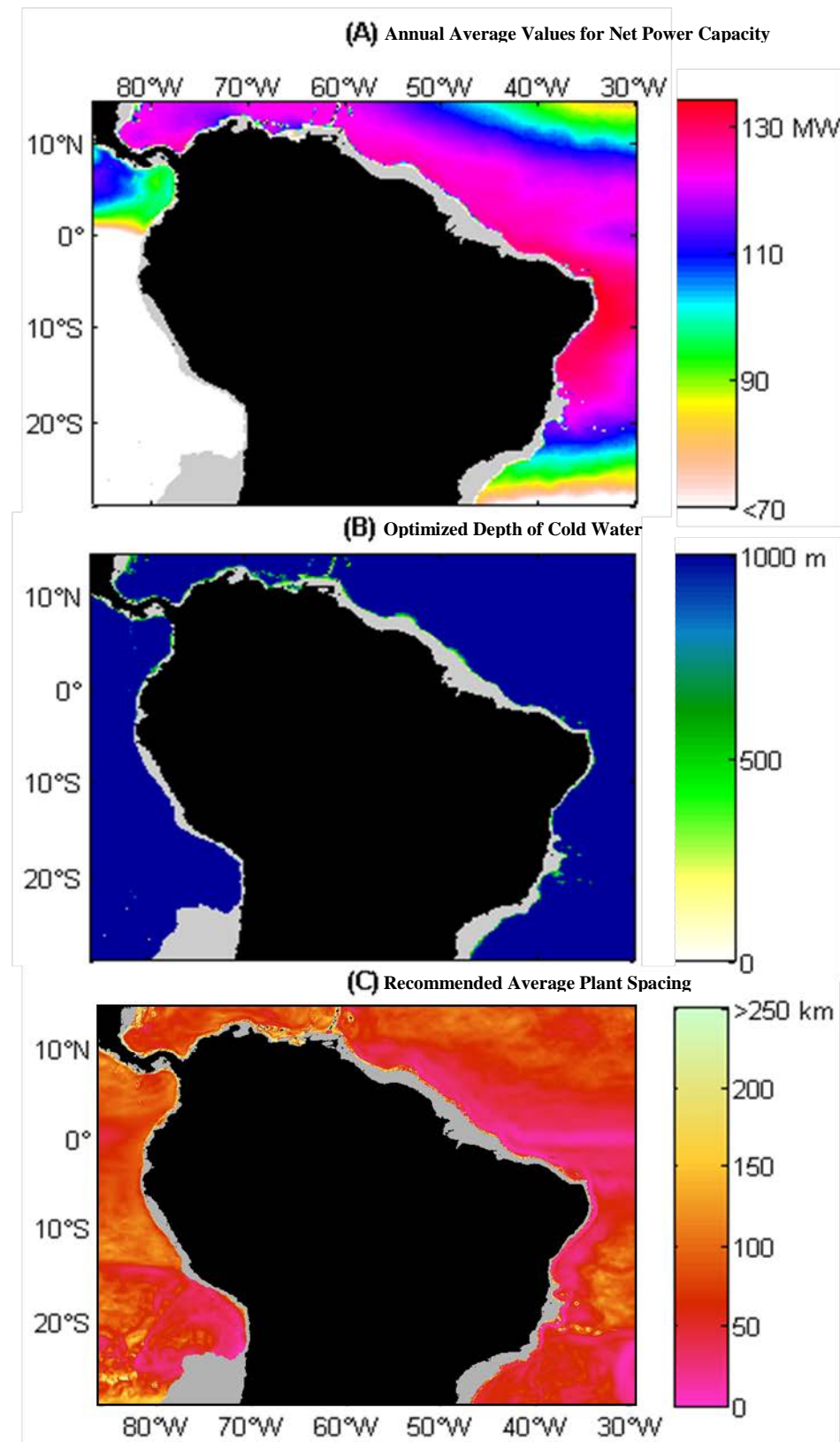


Figure 6-3 South America

The power achievable by an OTEC plant reaches its global maximum among the islands of the South Pacific (Figure 6-4). A plant sited in the Sea of Bismarck off the northern coast of Papua New Guinea may average as much as 157 MW over the year, more than 20 MW greater than a plant situated in any other region of the world.

The Pacific Islands also offer opportunities to produce power using some of the shortest cold water pipes, with power greater than 100 MW available off the east coast of Borneo, for example, in less than 400 meters of water. However, for all locations considered, greatest power in the region was always achieved by pushing offshore into waters approaching 1000 m, the limit of the cold water depths considered in this study.

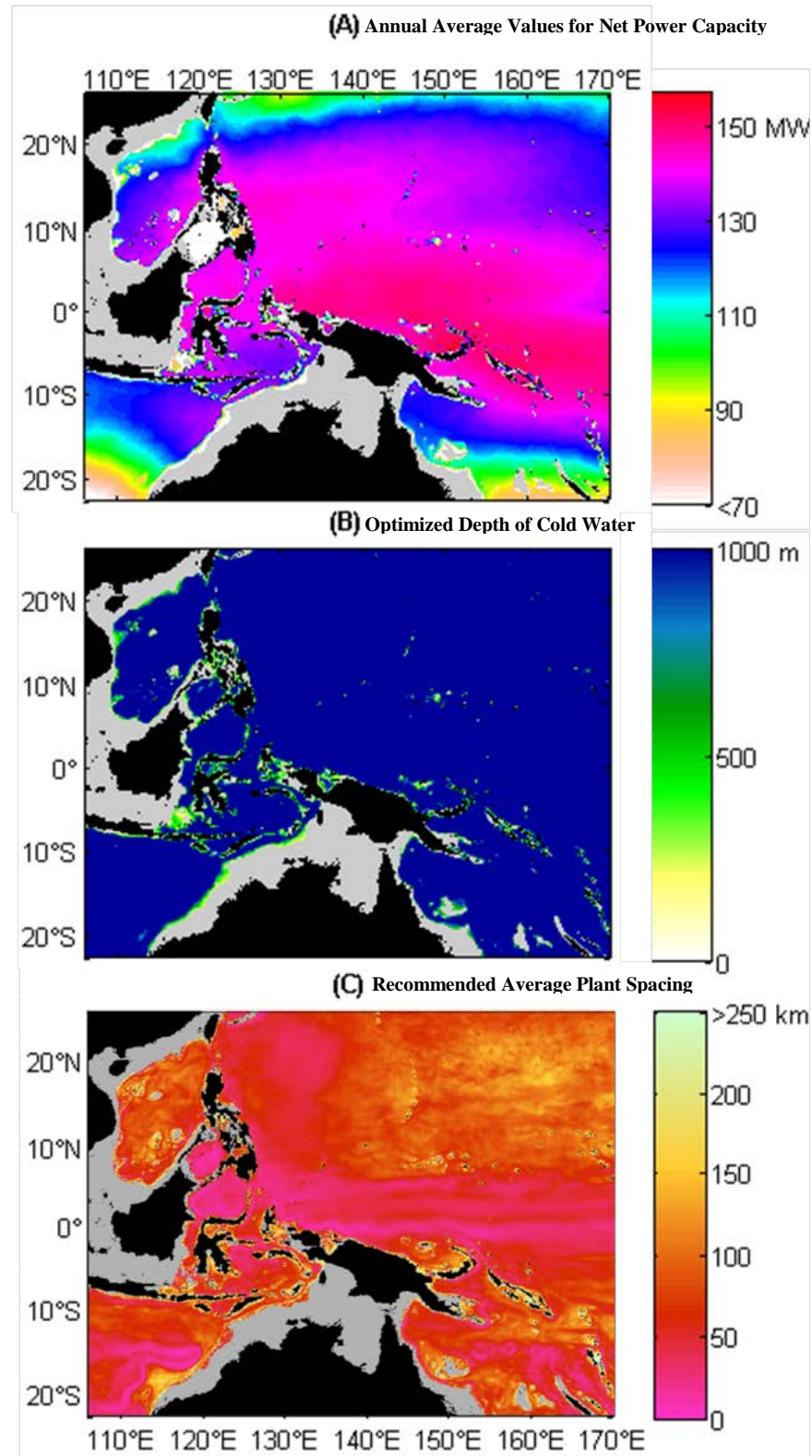


Figure 6-4 Australasia and South Pacific

In the Caribbean, as in the South Pacific, OTEC is possible nearly everywhere and is governed more by each island's bathymetry than by any other oceanic factor (Figure 6-5). A maximum value of 128 MW is possible in the waters near the southern crook of the Yucatán peninsula, in the waters between Belize, Honduras and Guatemala. In this location, power values greater than 100 MW can be generated using cold water drawn from 700 m or less. Very favorable power values ranging between 100 and 130 MW are also present year-round and near to shore off the southern coast of Cuba, the northern coast of Jamaica, and surrounding the islands of Hispaniola, and Puerto Rico. A seasonally variable resource is possible around the Tongue of the Ocean and eastern islands of the Bahamas, averaging 90-100 MW year-round but dipping to minima of around 65 MW during the northern winter.

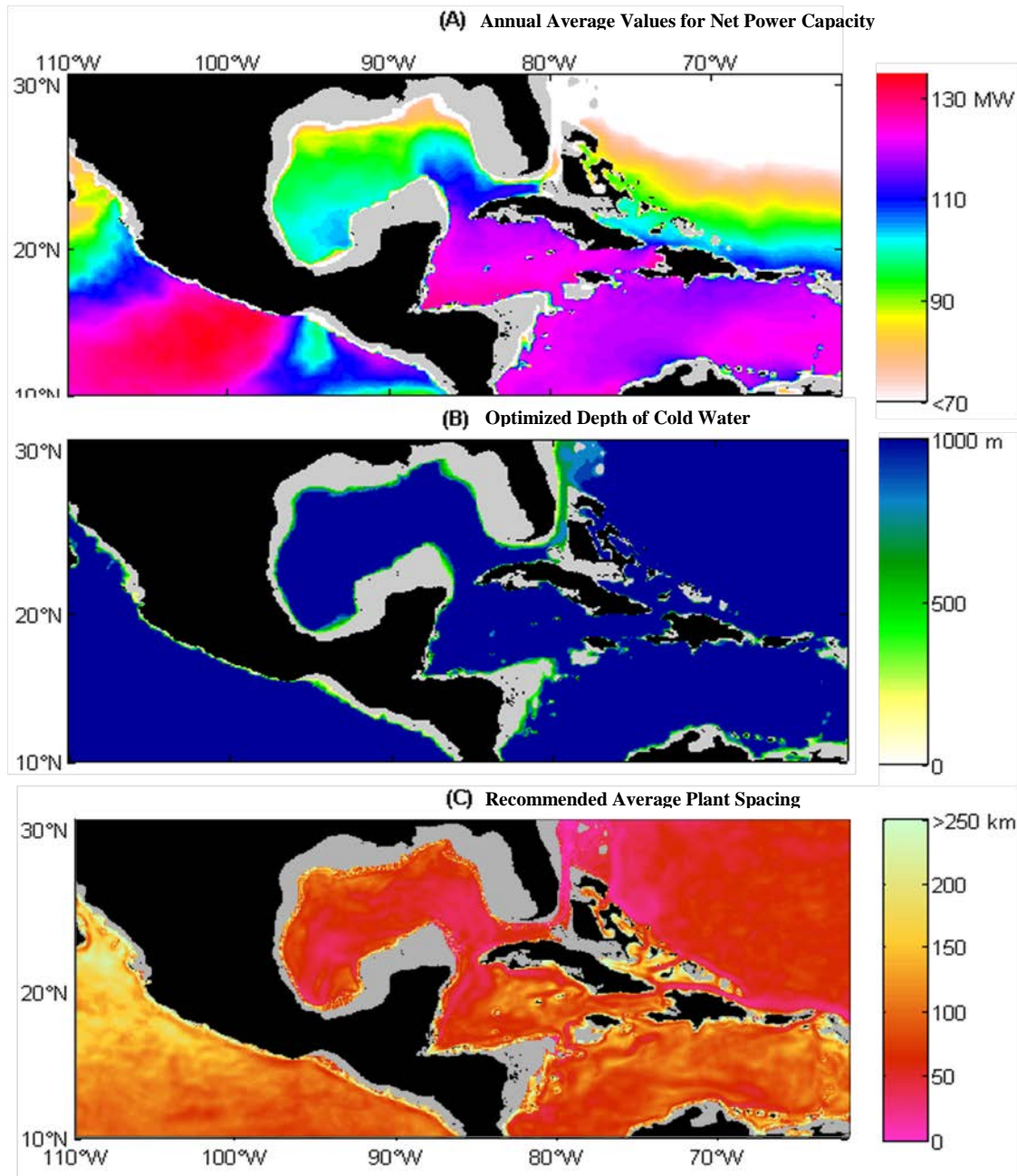


Figure 6-5 Gulf of Mexico, Florida Straits and the Caribbean

A seasonal resource is also available throughout the Gulf of Mexico, with summertime values ranging 130-140 MW throughout almost the entire gulf, but decreasing in winter to 60 MW and below through much of the region. Wintertime power values reach 90 MW along the south of the Gulf and 83 MW just southward from the Florida Keys. Still, the region can average year-round values of 90-110 MW (>110 in the Florida Keys, >90 in much of the northern Gulf and Straits of Florida). The northern and eastern resource is situated far from shore, however, as the continental shelf is wide in these waters. Power is generable much nearer to shore in the southern Gulf and Florida Keys. The western coast of Mexico, near the city of Acapulco, is also a hot spot for OTEC, with maximum projected power of 135 MW at a cold water depth of 1000 m (Figure 6-5).

Seawater cooling can be used for industrial or residential cooling needs where heat must be rejected. A typical resource for direct air-conditioning applications is no warmer than 8°C, (full SWC), which has been established as a minimum value of interest for this study. Water at temperatures between 8°C and 20°C can be used to supplement air conditioning processes, or to reject heat from many other low temperature industrial processes. Water temperatures above 20°C were not considered for this investigation as cost savings begin to break down as sea water temperature nears ambient temperatures. Depth profiles for three water temperatures of interest: 8°C, 12°C and 20°C were established to aid selection of optimal sites for SWC. A cool shallow resource just off the coast where a need may exist presents significant opportunity for energy and cost savings. Figure 6-6 shows locations where full SWC may be conducted using waters drawn from less than 300 meters depth (blue). This includes the vast majority of the coastline of any continent. Data are based on annual mean temperatures.

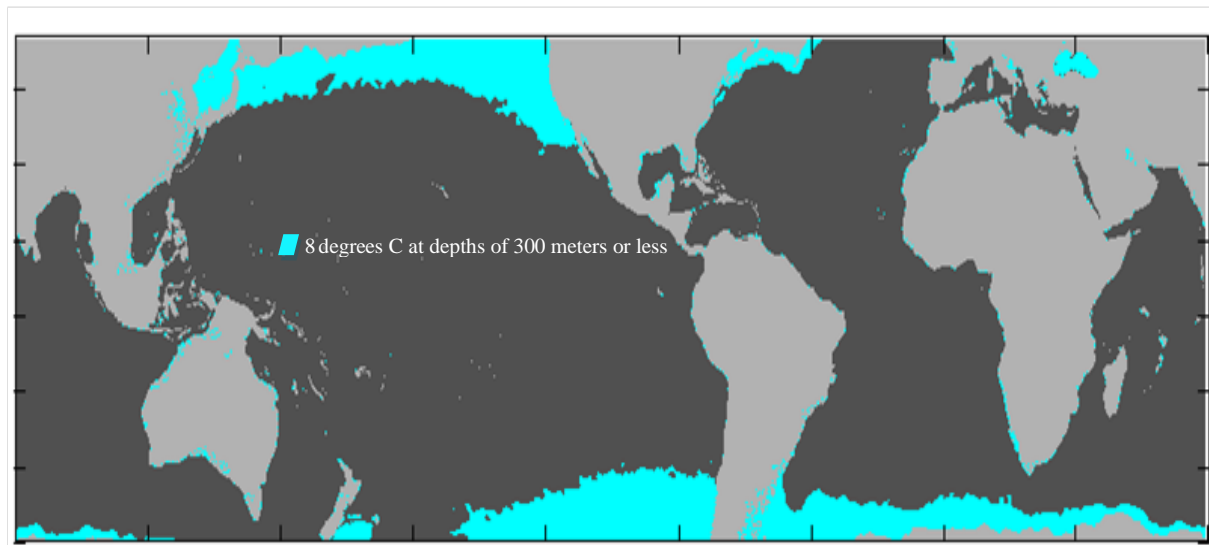


Figure 6-6 Prime Seawater Cooling resources (8° cold water found at depths less than 300 m)

SWC is also known by many other names such as Cold Seawater Based Air Conditioning (CSBAC) and Deep Ocean Water (DOW), suggesting that there are many specific applications for this resource. The shallower it can be found the more efficient the process becomes by reducing pumping losses. Studies have found that the efficiency of the energy intensive process to liquefy recovered natural gas deposits can be improved by approximately 7% by using 10 degree Celsius cold ocean water for cooling. This would be of great interest to the offshore oil and gas industry looking to transport their product back to shore.

6.3 Obtaining Regional Resource Calculations

As described in Section 5, the global power resource is limited by the bounds of sustainability imposed by global and local replenishment of cold water. An estimate of sustainable global power from OTEC can be generated by summing the power available per model grid point, with i and j representing the complete sets of OTEC feasible latitude and longitude coordinates respectively.

$$\text{Total Global Power} = \sum_{i=1}^{i_{max}} \sum_{j=1}^{j_{max}} \text{Net power for single plant}_{i,j} / \text{Plant Spacing}_{i,j}^2 * \text{Area}_{i,j}$$

Derivation of net power for a single plant was explained in Sections 2 and 3, and the equations for plant spacing were presented in Section 5.2. Since plant spacing is determined by incoming current velocities at depth, and power is based on temperature and depth input variables, the summation of power depends on all of the above: current velocities, temperatures, and depth.

The area of the i^{th}, j^{th} grid point was estimated by planar approximation of each rectangular grid block assuming a spherical earth of radius, R , equal to 6371 km¹². The length of the latitudinal and longitudinal sides of each grid block were determined by

$$\begin{aligned} \text{Length}_{i,j} &= d\text{Latitude}_{i,j} * \frac{\pi R}{180} \\ \text{Width}_{i,j} &= d\text{Longitude}_{i,j} * \frac{\pi R}{180} * \cos(d\text{Latitude}_{i,j}) \\ \text{Area}_{i,j} &= \text{Length}_{i,j} * \text{Width}_{i,j} \end{aligned}$$

where $d\text{Latitude}$ and $d\text{Longitude}$ represent the distance in degrees between adjacent HYCOM grid points.

Therefore the calculated Area of a HYCOM grid point at 0 degrees: 79.13 km², at 23 degrees: 66.99 km² and at 46 degrees: 38.10 km².

The following figures provide a preview of the OTEEV Projects visualization tool which is detailed further in Section 7. These screen shot images are utilized here to help demonstrate how the project has used the high resolution gridding of the input and output data to compute total net power within specific regions of interest comprising of multiple grid points.

¹² NASA Earth Fact Sheet, <http://nssdc.gsfc.nasa.gov/planetary/factsheet/earthfact.html>

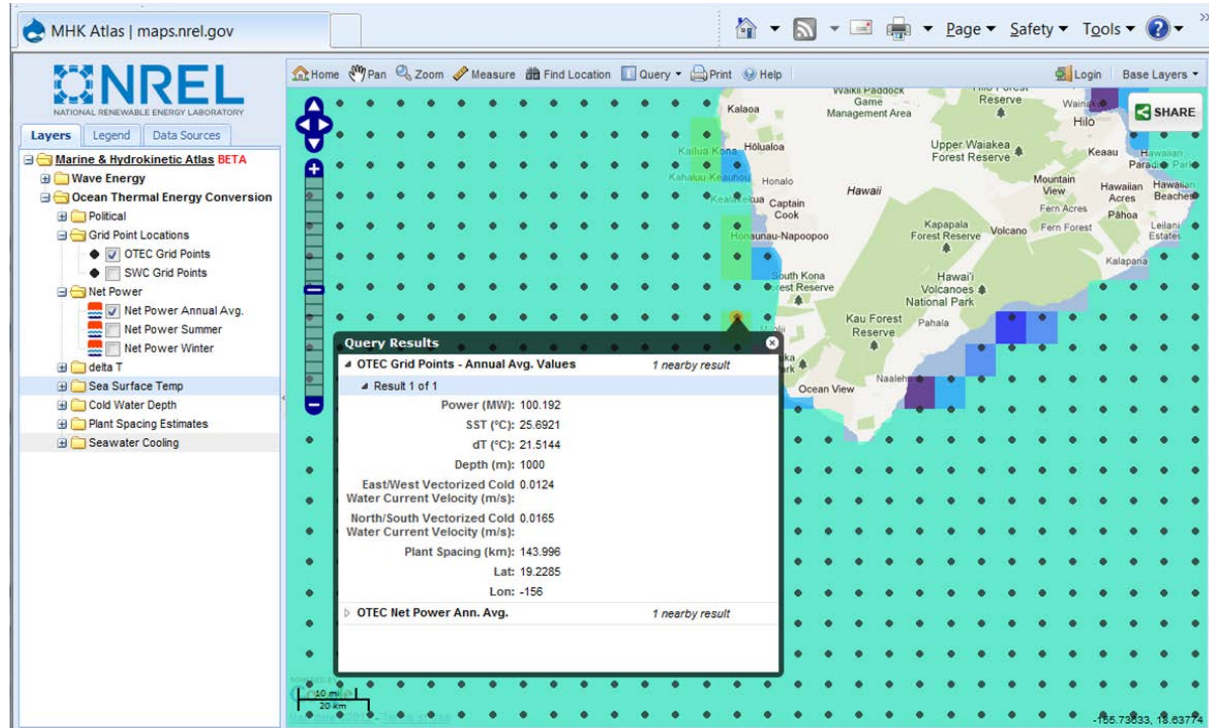


Figure 6-7 Resource Assessment by Grid Point: Hawai‘i¹³

As an example of a limited-area power calculation, consider a HYCOM+NCODA grid point near the big island of Hawai‘i (Figure 6-7). Here the HYCOM+NCODA deep-water velocity is 0.0206 m/s, which, per Section 5, implies a plant spacing of $\Delta x = 144$ km. The HYCOM+NCODA 1/12° grid has dimensions of 8.4 km × 8.9 km at this location. The average net power capacity available per plant here is 100.2 MW per the energy extraction model (Section 3). Then the total power available from this single grid point is

$$\text{Power per Grid Point} = 100.2 \text{ MW} \frac{8.40 \text{ km} \cdot 8.87 \text{ km}}{(144 \text{ km})^2} = 0.360 \text{ MW}$$

Table 6-1 Hawai‘i OTEC Characteristics

| Attribute | Value | Note |
|-----------------|----------------------|---|
| Latitude | 19.23 | Degrees North |
| Longitude | -156.00 | Degrees West |
| EEZ ID | 160 | United States – Hawaiian Islands |
| Net Power | 100.2 MW | Average Annual Net Power Capacity |
| Grid Point Area | 74.5 km ² | |
| V _{in} | 0.0206 m/s | Vectorized cold water current velocity magnitude = $\sqrt{EW^2 + NS^2}$ |
| Δx | 144 km | Plant Spacing |

¹³ http://maps.nrel.gov/mhk_atlas?visible=otec_power_ann&opacity=80&extent=-158,20,-154,18

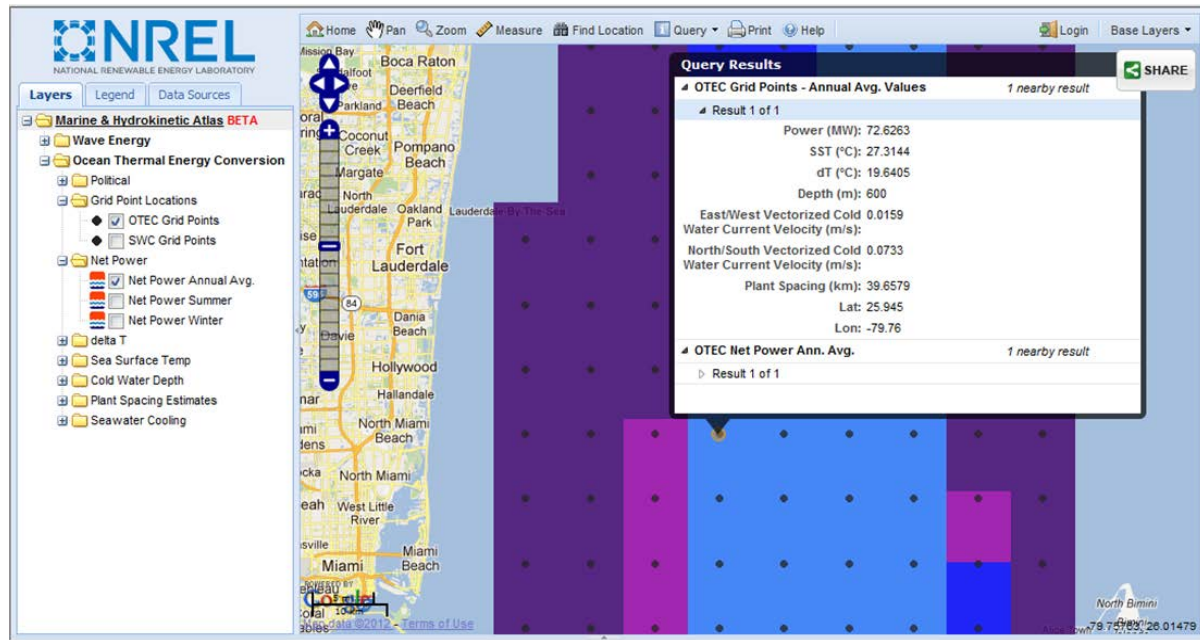


Figure 6-8 Ocean Data point off of Miami, Florida¹⁴

As an alternate example, a plant stationed off Miami, Florida is capable of averaging 72.6 MW annually. The length of the sides of a grid point here are 8.01 km x 8.87 km. By comparison, cold water current velocity at this location is 0.0750 m/s, implying a much smaller plant spacing value or Δx of 39.6 km. Then the total power capacity available ‘sustainably’ from this point is

$$\text{Power per Grid Point} = 72.6 \text{ MW} \frac{8.01 \text{ km} \cdot 8.87 \text{ km}}{(39.6 \text{ km})^2} = 3.289 \text{ MW}$$

Table 6-2 Miami, Florida OTEC Characteristics

| Attribute | Value | Note |
|-----------------|----------------------|---|
| Latitude | 25.95 | Degrees North |
| Longitude | -79.76 | Degrees West |
| EEZ ID | 163 | United States - East Coast of Florida |
| Net Power | 72.6 MW | Average Annual Net Power Capacity |
| Grid Point Area | 71.0 km ² | |
| V _{in} | 0.0750 m/s | Vectorized cold water current velocity magnitude = $\sqrt{EW^2 + NS^2}$ |
| Δx | 39.6km | Minimum Plant Spacing |

¹⁴ http://maps.nrel.gov/mhk_atlas?visible=otec_power_ann&opacity=80&extent=-80.5,26.5,-79,25

By taking the total power sum of all the grid points within a designated region, we can use the data's inherent resolution to produce localized estimates of total "sustainable" net power capacity and map out relative plant spacing in our visualization tools, further described in the following sections of this report.

Using this methodology consistently across the valid net power producing ocean area, the sustainable world OTEC resource as a sum of all grid point data is estimated to be

$$\text{Total Global Power Capacity} = 6.3 \text{ Terawatts}$$

This value does not include distance from shore or transmission losses, and offers no comment on relative economic feasibility, though it does provide base data which could be used for such an analysis. Integration of power over the exclusive economic zone can provide a first-order insight into the economic feasibility for various locations and is addressed in the following sections.

The 6.3 TWe global power capacity estimate is arbitrarily scaled by the selection of the Δz parameter (Section 5), which corresponds to the amount of cold water that can be safely diverted from the incoming flow for use by an OTEC plant. The parameter $\Delta z = 0.2$ meters was scaled here in homage to the 5 TWe global resource estimate by Nihous (2007), which was itself limited from an estimate several times larger. Thus Δz was scaled to reach the order of magnitude of the Nihous estimate, but can be readily adjusted to accommodate new research and insights into sustainable usage of the cold water resource at depth.

The values for OTEC maximum extractable capacity, in terms of net power produced, is what has been provided to this point on the report. The annual and seasonal averages, as modeled in the energy extraction model, suggest a realistic at-plant power output from the OTEC Cycle. Then by limiting the number of operational plants due to technical sustainability, we can provide useful total power capacities that can be assigned to regions of interest. However, one must consider several other factors that determine the total "delivered" power that reaches the users where and when they need it.

Delivered energy estimates are often calculated differently between the various ocean renewable resource categories. Seasonal ranges and daily intermittency of the resource along with transmission losses and system availability all factor into the total delivered power. OTEC and SWC systems can operate on a baseload level in that the thermal resource remains relatively constant throughout the day and night. However, seasonal temperature swings between summer and winter months have substantial impact on the available ΔT and thus the net power that an OTEC system can produce. For OTEC estimates the Annual Averages for net power have been used to determine the resource in terms of total units of electricity generated for the noted regions of interest.

By taking the annual average capacity and multiplying it by the number of hours in a year, we can determine the amount of electricity that a plant will deliver in terms of watt-hours per year, or, more appropriately for OTEC at the regional scale, Terawatt-hours per year (TWh/yr). With this in mind, every 114 Megawatts of average net power capacity is equivalent to approximately 1 TWh/yr of delivered OTEC electricity. (114 MW x 8760 Hours in a year = 1,000,000 MWh = 1 TWh)

6.4 Resource within the U.S. EEZ regions

Countries bordering marine areas have a defined exclusive economic zone (EEZ) which gives rights over the exploration and use of marine resource in their regions. Typically they extend to 200 nautical miles (370 kilometers) from the countries' coast, depending on the definition of neighboring countries EEZs. The oceanic territory within the U.S. EEZ is divided into a number of regions with different resource characteristics and energy needs. Table 6-4 lists these regions and the extractable net power.

Table 6-3 Power Within the Exclusive Economic Zones of US Interests

| Total Net Power under U.S. Sovereignty | | | | |
|---|---------------------------------------|---------------------------------------|---------------------------------------|--|
| Locations within the U.S. EEZ | Annual Average Net Power (GWe) | Net Power (GWe) Summer (J-J-A) | Net Power (GWe) Winter (D-J-F) | Yearly Electricity TWh/year (Based on Annual Average Net Power) |
| Continental U.S. (East Coast) | 39.0 | 92.3 | 11.5 | 342 |
| Continental U.S. (Gulf of Mexico) | 6.0 | 10.8 | 3.3 | 53 |
| Hawai‘i | 16.3 | 17.3 | 16.8 | 143 |
| Puerto Rico & U.S. VIs | 4.4 | 5.8 | 3.8 | 38 |
| Howland Island | 29.8 | 37.6 | 21.7 | 261 |
| Jarvis Island | 24.3 | 34.1 | 14.0 | 213 |
| Johnson Atoll | 4.1 | 4.0 | 5.2 | 36 |
| Mariana Islands | 15.6 | 17.4 | 15.8 | 137 |
| Marshall Islands | 43.2 | 43.0 | 46.0 | 378 |
| Micronesia | 129.3 | 179.8 | 125.9 | 1133 |
| Palau | 50.2 | 74.6 | 36.8 | 440 |
| Palmyra | 10.9 | 8.8 | 12.0 | 95 |
| Samoa | 151.7 | 151.9 | 184.0 | 1329 |
| Wake Island | 4.3 | 4.6 | 4.6 | 38 |
| Total US Interests | 529.2 | 682.1 | 501.5 | 4,636 TWh/yr |

In some of latter locations listed above the potential supply appears to exceed the current local demand for electricity. That excess electricity could be used to make other products such as potable water or pure hydrogen. With commercial scale OTEC systems, it is conceivable that a remote island nation with current limited industrial needs for imported fuel could eventually become a net power exporter. This also brings up the debate between developing near-shore grid-connected systems and constructing larger grazing facilities that float about the open oceans producing carbon free energy carriers that can be transported back to shore. Mobile OTEC plants would also allow for a greater extraction of available energy by migrating along with the seasonal shifts of the thermal resource depicted in Figure 6-1.

Ultimately the discussion begins to center in on the economics of each approach which takes us beyond the scope of this project and report. Lockheed Martin and partners are funded under DOE Award # EE0002663 to establish the Levelized Cost of Electricity (LCoE) as a function of the Life Cycle Cost Assessments of 100MW, 200MW and 400MW grid-connected power plants as well as a 400MW grazing

power plant. The LCoE, along with this resource assessment will allow criteria to compare to present cost of electricity at a potential OTEC site in determination of the applicability of the design on a site by site basis. The OTEEV tool covered in the next section makes envisioning these scenarios all the more possible.

6.5 Resource within the United Nations Recognized EEZs

“Ninety-eight nations and territories with access to the OTEC thermal resource with their 200 nautical mile EEZ were identified in the 1980’s.” (Vega, 2010) Table 6-3 provides a summary of the top nations with notable OTEC resources within their recognized EEZs.

Table 6-4 Top 10 Nations in Total OTEC Net Power

| Total Net Power within the EEZs of Several Top Nations | | | |
|---|---------------|--|--|
| Location | EEZ ID | Power-generating area within the EEZ (Annual Average) (km² × 10³) | Net Power (GWe) (Annual Average)¹⁵ |
| United States | Multiple | 12,335 | 529.20 |
| Brazil | 171 | 2,413 | 222.44 |
| Indonesia | 216 | 4,105 | 249.88 |
| Papua New Guinea | 17 | 2,213 | 129.89 |
| Japan | 210 | 3,194 | 126.14 |
| Philippines | 15 | 1,577 | 95.29 |
| Maldives | 39 | 885 | 75.26 |
| Madagascar | 42 | 1,070 | 63.09 |
| India | 26 | 1,888 | 31.64 |
| Mexico | 135 | 2,602 | 25.00 |

It is important to recognize that ocean thermal energy is a global resource as roughly a quarter of the estimated total world net power capacity can be technically extracted from within the EEZs of the nations listed above.

¹⁵ Multiplying the Net Power (GWe) values by 8.76 provides the Terawatt hours per year of the estimated electrical power generation from OTEC.

7 Visualization

The National Renewable Energy Laboratory (NREL) conducted the visualization of the data per objectives 4 and 5 of the SOPO (Section 1.4). The data were processed and included in the Marine & Hydrokinetic (MHK) Atlas. The MHK Atlas is an interactive web-based Geographic Information System (GIS) application that was deployed using NREL's OpenCarto framework. OpenCarto is an open architecture framework that uses open source libraries (e.g., MapServer, TileCache, Ext-JS and OpenLayers), and standards such as Styled Layer Descriptor (SLD), Web Mapping Service (WMS) and Web Feature Service (WFS). OpenCarto is designed to support analysis, visualization and data exploration, which is an ideal medium for the visual representation of the OTEEV data.

7.1 Data Processing

The data were converted from a net CDF file to a data point layer, and interpolated to a categorized polygon layer to allow effective visualization of the data at different spatial scales. There were two primary reasons to do this: 1) tightly clustered point data displayed at a small scale does not appropriately represent the data and visual aspects of the applied style or legend, but rather displays on the map as points overlaid on top of one another. At large scales the point data were not easy to visualize due to the points not being continuous. Polygon shapes display better for both small and large scale. 2) The data were quite extensive, with over 14 million records in the table. This large number of records introduced delays and server time-out issues when displayed as a styled point layer in the web application.

To satisfy the visual and technical requirements, a series of processing steps were performed on the data to address the visualization issues described above while maintaining data integrity. The spatially referenced point layer was used to interpolate raster grids representing each of the variables (net power, warm water temperature (T_S), delta T (ΔT), cold water depth, SWC) to be displayed as layers in the final application. The separated data were converted to raster grids and interpolated based on their spatial correlation. Each of the raster grids was individually reclassified by the value ranges determined for the visualization legend and converted to a polygon layer using the class ID. This process reduced the data detail to only what was necessary for visualization purposes. For example, SWC raster grids were reclassified so that all raster cells having a depth value greater than or equal to 1,000 m were changed to ID 1 (Table 7-1). Similarly, the net power annual average raster grid was reclassified so that all raster cells with net power values greater than or equal to 160 MW were changed to class ID 13 (Table 7-2).

Table 7-1 Grouping for Seawater Cooling (SWC) Variables

| Class ID | SWC 20° C (Depth – Meters) | SWC 14° C (Depth – Meters) | SWC 8° C (Depth – Meters) |
|----------|-------------------------------|-------------------------------|------------------------------|
| 1 | >= 1000 | >= 1000 | >= 1000 |
| 2 | 900 - 999.9 | 900 - 999.9 | 900 - 999.9 |
| 3 | 800 - 899.9 | 800 - 899.9 | 800 - 899.9 |
| 4 | 700 - 799.9 | 700 - 799.9 | 700 - 799.9 |
| 5 | 600 - 699.9 | 600 - 699.9 | 600 - 699.9 |
| 6 | 500 - 599.9 | 500 - 599.9 | 500 - 599.9 |
| 7 | 400 - 499.9 | 400 - 499.9 | 400 - 499.9 |

| Class ID | SWC 20° C (Depth – Meters) | SWC 14° C (Depth – Meters) | SWC 8° C (Depth – Meters) |
|----------|-------------------------------|-------------------------------|------------------------------|
| 8 | 300 - 399.9 | 300 - 399.9 | 300 - 399.9 |
| 9 | 200 - 299.9 | 200 - 299.9 | 200 - 299.9 |
| 10 | 100 - 199.9 | 100 - 199.9 | 100 - 199.9 |
| 11 | < 100 | < 100 | < 100 |

Table 7-2 Grouping for OTEC Variables

| Class ID | Net Power (MW) | SST (°Celsius) | Delta T (°Celsius) | Depth of Resource (Meters) |
|----------|-------------------|---------------------|-----------------------|-------------------------------|
| 1 | < 50 | < 20 | < 14 | > 1000 |
| 2 | 50 - 59.99 | 20 -20.99 | 14 -14.99 | 950 -1000 |
| 3 | 60 - 69.99 | 21 -21.99 | 15 -15.99 | 900 - 949.9 |
| 4 | 70 - 79.99 | 22 -22.99 | 16 -14.99 | 850 -899.9 |
| 5 | 80 - 89.99 | 23 -23.99 | 17 -17.99 | 800 - 849.9 |
| 6 | 90 - 99.99 | 24 -24.99 | 18 -18.99 | 750 - 799.9 |
| 7 | 100 - 109.99 | 25 -25.99 | 19 -18.99 | 700 - 749.9 |
| 8 | 110 - 119.99 | 26 -26.99 | 20 -20.99 | 650 - 699.9 |
| 9 | 120 - 129.99 | 27 -27.99 | 21 -21.99 | 600 - 649.9 |
| 10 | 130 - 139.99 | 28 -28.99 | 22 -22.99 | 550 - 599.9 |
| 11 | 140 - 149.99 | 29 -29.99 | 23 -23.99 | 500 - 549.9 |
| 12 | 150 - 159.99 | 30 -30.99 | 24 -24.99 | 450 - 499.9 |
| 13 | >= 160 | >= 31 | >= 25 | < 450 |
| | 10 MW increments | 1 degree increments | | 50m increments |

OpenCarto can access the data from the spatial database repository, and by creating unique layers for each data variable, the OTEEV data can be rendered in a map application. A unique layer was created for each data variable type. By default, the layers are generated as simple spatial geometries with no associated style. To apply cartographic styles to the map, Styled Layer Descriptor (SLD) rules were created for each class ID within the data layer. The OpenCarto framework retrieves the data from the data repository, applies the associated SLD based on the class ID attribute and then displays the styled image in an interactive mapping application. Once an area of interest has been identified by using the styled layers, users can access point specific data by enabling the point layers. These layers contain the original points that were used in the variable layer processing. These layers are best used at large scale and are not styled.

Each of the shapefiles that were processed for the application are available for download in the OpenEI datasets library and are linked within the metadata for each layer.

7.2 Tool Functionality

The MHK Atlas is a web-based application that was selected as the tool to visually display the OTEEV data; it is a specific application module that is hosted on the OpenCarto platform. The data are displayed by adding the layers, with applied SLDs, to the application module. The MHK Atlas application was assigned a URL (http://maps.nrel.gov/mhk_atlas) to allow users to access and interact with the data.

The basic components of the MHK Atlas are shown in Figure 7-1 and described thereafter.

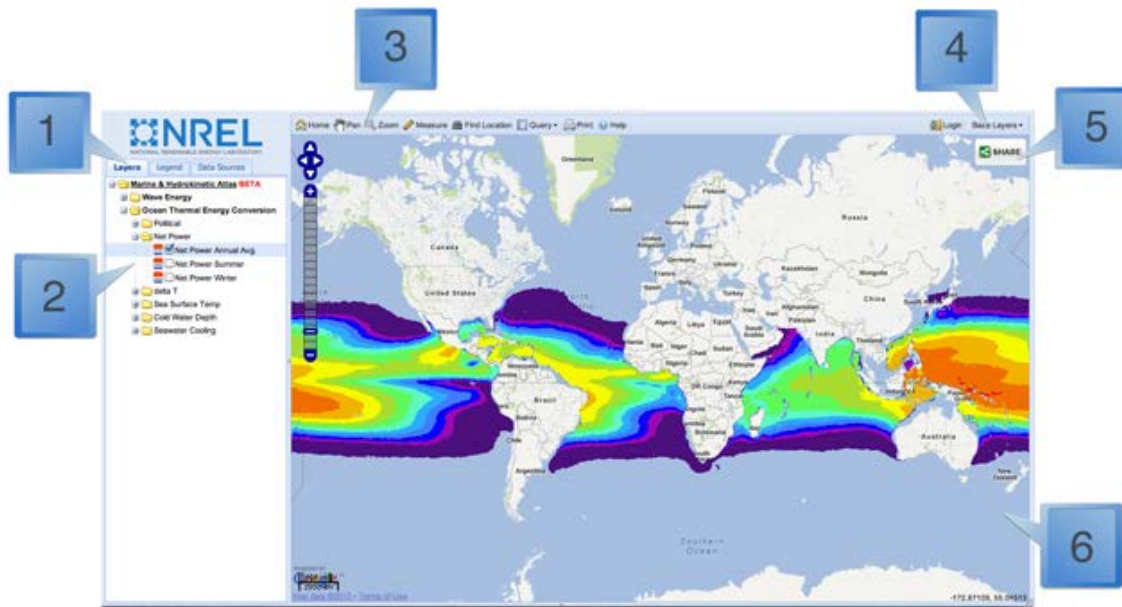


Figure 7-1 MHK_Atlas Tool Components

[1] Content Display Tabs

The tabs control the content displayed in the right application window. Options include: Layers, Legend and Data Sources.

[2] Content Display Window

Displays content of the active tab. The Layers tab displays the interactive layer tree, which allows the user to toggle data layers on and off for visualization. The Legend tab displays the legends of currently active layers. The Data Sources tab displays the metadata for each layer. Hovering over a layer in the layer tree produces a drop-down arrow that provides an alternative option to selecting the legend and metadata, as well as a transparency control.

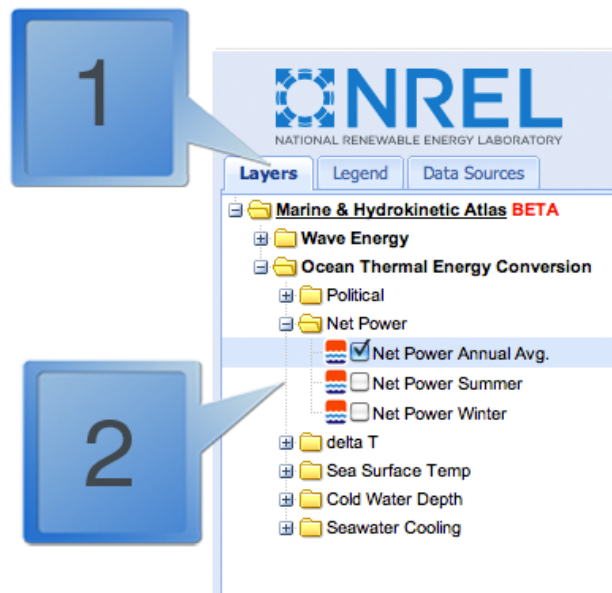


Figure 7-2 Selectable Layers

[3] Toolbar



Figure 7-3 MHK_Atlas Tool Bar Selections

The toolbar offers the most common features used in the mapping application conveniently above the data view window.

- The Home button sets the map to the default location and extent (the extent viewed when the application is first launched). The default location is centered on the U.S.
- The Pan and Zoom features allow movement around the map. These features can be used via the buttons in the toolbar or by using the tools in the upper left corner of the data view window.
- The Measure tool provides in-line measurement in units of miles or kilometers.
- Find Location is a georeference tool that will find and zoom to a location based on address, city, state, zip, or Lat/Long (decimal degrees).
- The Query tool will query the data by point, region or attribute. Results are highlighted on the map and graphically displayed. This is discussed in more detail in the Application Capabilities section.
- There are also Print and Help buttons.

[4] Base Layers Button

The base map layer can be changed. Options for this are the default Google Map, Google Satellite, Google Hybrid, Open Street Map or None. A slider control adjusts the base layer transparency (Figure 7-4).

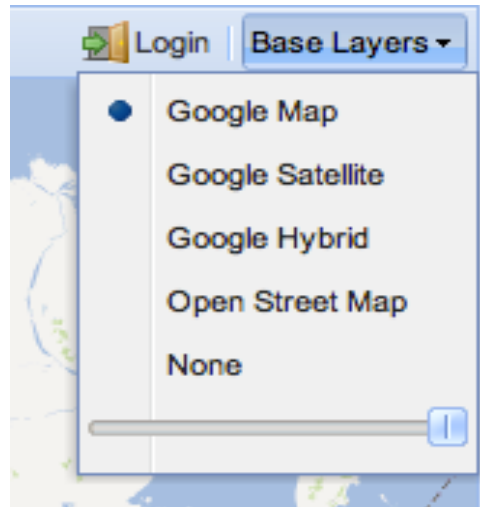


Figure 7-4 Base Map Layer Selections

[5] Share Button

The Share feature allows the user to share the application via several social media networks (Figure 7-5).



Figure 7-5 Sharing Through Social Media

[6] Map/Data View

The main application window dynamically displays the map and selected data.

Application Capabilities

The MHK Atlas has additional capabilities that allow the user to interact with the data and create customized visualizations and maps.

The query tool provides several options that return query results from the spatial database. Data can be queried by point, region, or attribute. The point query will return results from a single geometric feature and highlight that feature on the map. The query results populate in a new window that appears in the data view window. If several geometric features are near the queried point, multiple results will appear in the list (Figure 7-6).

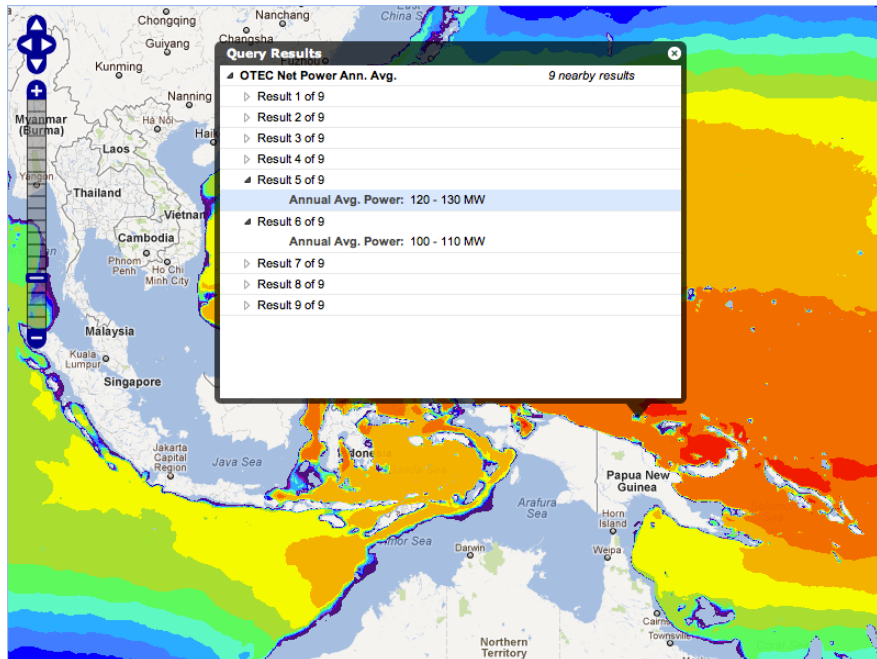


Figure 7-6 Point Query Result Display

With the region query active the cursor can be used to create a box over the area of interest. The results from the selected features are returned in a table that opens at the bottom of the application (Figure 7-7). The region query results can also be downloaded as a comma-separated value (CSV) file.

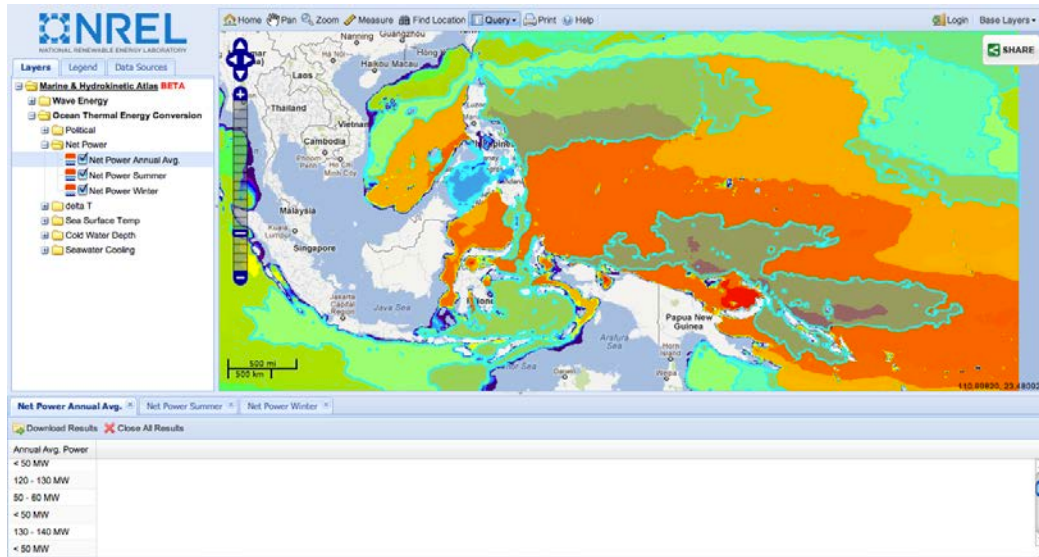


Figure 7-7 Query by Selected Region Feature

The query by attribute feature queries the available layers based on a selected attribute from the list and a user-selected value. The query results zoom to the feature(s) selected on the map returned in the query (Figure 7-8).

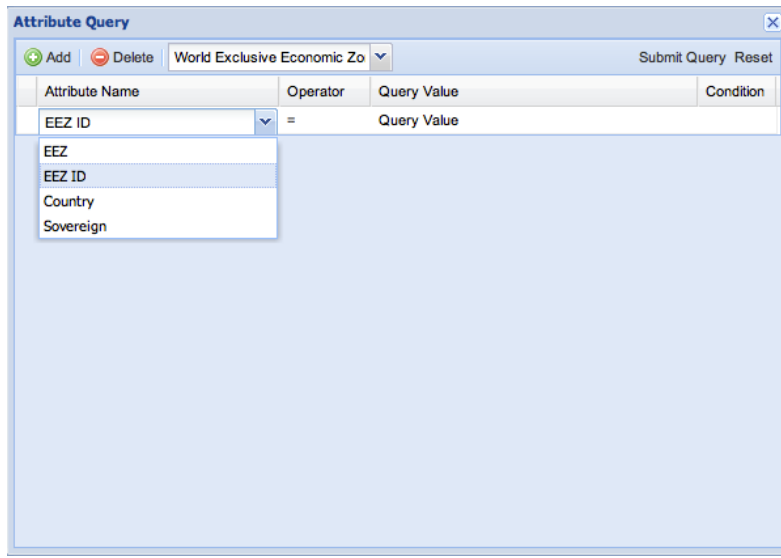


Figure 7-8 Attribute Query Feature List

The layer tree can also be customized to reorder the index of the layers. The layers can be moved using a drag and drop method to order them as desired. This provides flexibility for users to prioritize the data visualization based on their specific needs.

Layer thresholding is an option that excludes specific classes from each layer. This can be accomplished by accessing the layer legend and un-checking the boxes next to the desired classes, then clicking the Apply button (Figure 7-9)

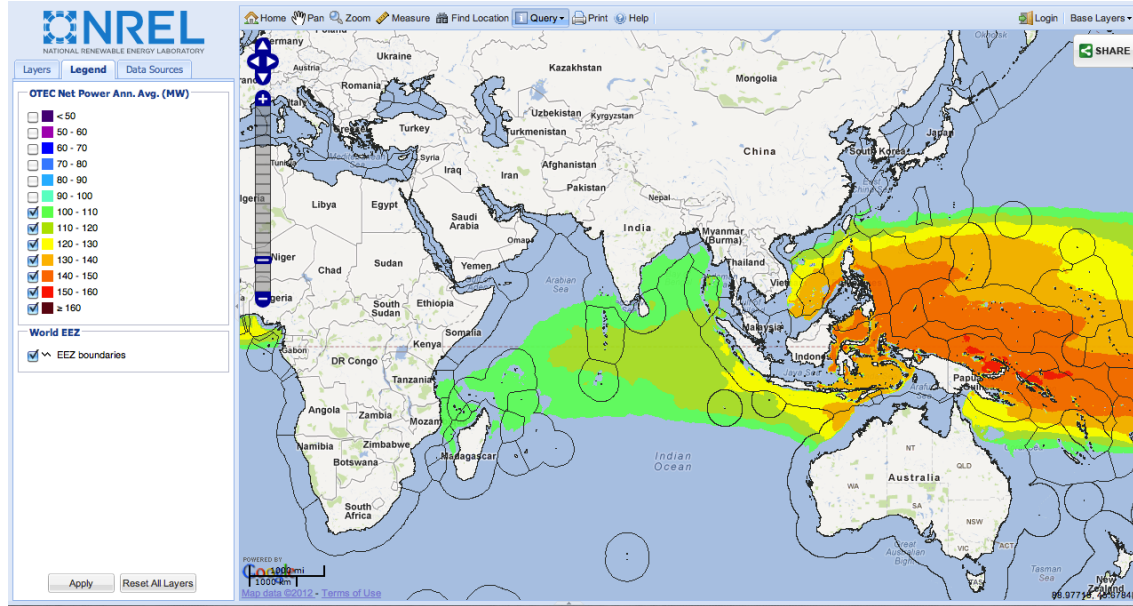


Figure 7-9 View Selection Capabilities

The color of the legend classes can also be changed. Clicking the swatches in the legend brings up a color palette; by clicking a different color the legend swatch will change to the selected color (Figure 7-10). The Apply button will become active and must be clicked to see the data change color on the map. Some web browsers may cache these changes and they may remain in place even if the application is closed and re-visited at another time. The layer can always be set to default by clicking the Reset button. The Apply and Reset buttons appear in both legend locations. They are at the bottom of the content display window when using the legend tab and at the bottom of the drop down window when hovering over a layer in the layer tree and selecting the drop-down arrow.

These capabilities allow users to generate their own thematic maps, download the data results and print them out if desired.

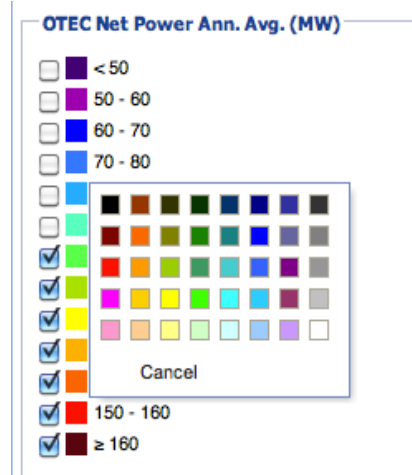


Figure 7-10 Customizable Color Palettes

Each layer contains metadata. The metadata are visible by either clicking the data sources content tab or hovering over a layer in the layer tree, selecting the drop-down arrow and then selecting metadata. The metadata discuss the source of the data in the layer and also provide links to other resources, including this report and the ability to download the data shapefiles (Figure 7-11).

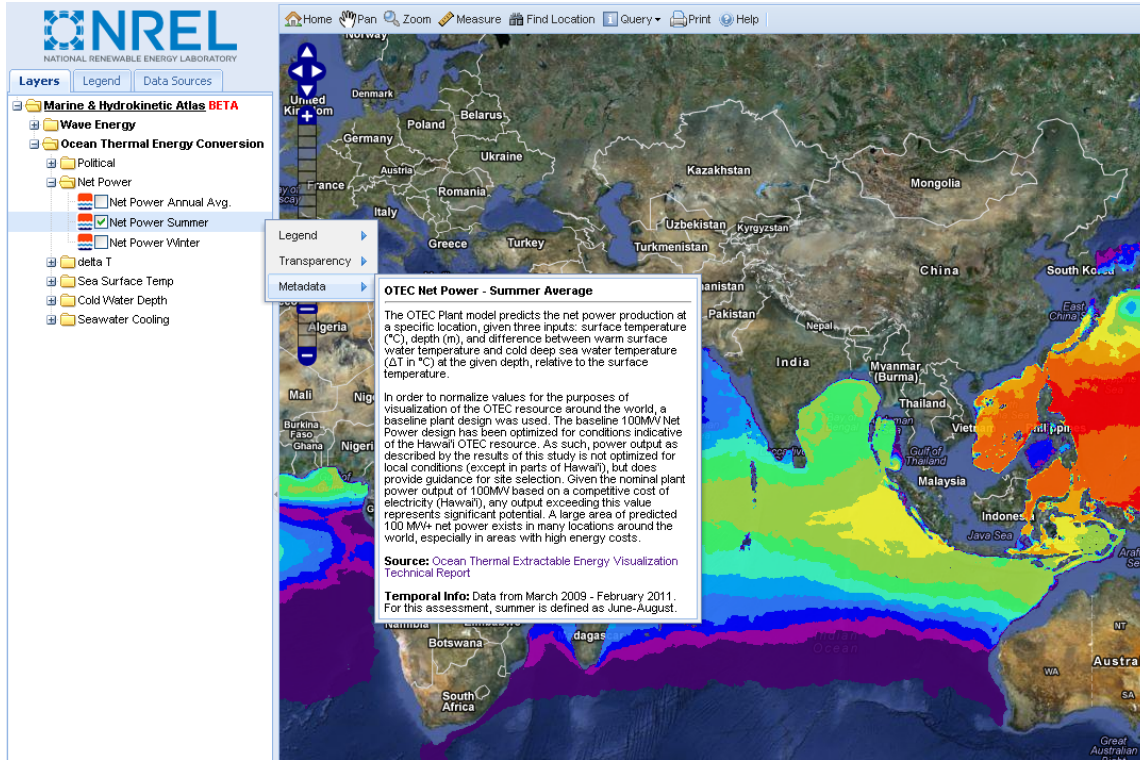


Figure 7-11 Example Selection Specific Metadata

Application Analysis

The interactive capabilities of the application can be used for basic data analysis on active layers. Specific results for selected geographic points or regions can be returned using the query tool as discussed above. The query results can be coupled with other layers to infer answers to questions such as determining net power potential in a selected EEZ. Another example of multiple layer analysis is the ability to display the point specific layer over the ΔT . This allows users to visualize the ΔT and provides the ability to query points for net power values at specific locations.

A combination of capabilities and tools can also be used to determine distance to a specified net power class. By using layer thresholding, a user can display only net power values that are greater than 100 MW. Then, using the measure tool, a distance from shore to the resource can be estimated.

The flexibility of the application and customization of the data will allow users to perform basic analysis, and with the capability of downloading the data, they can perform advanced analysis and further modeling.

7.3 Intended Audience

The mission of DoE's Water Power Program is to perform and sponsor the necessary research, development, test, evaluation and demonstration of innovative water power technologies to effectively generate renewable, environmentally responsible and cost-effective electricity from Marine and Hydrokinetic (MHK) resources.¹⁶

The MHK Atlas is a tool that helps move toward the achievement of this goal by providing an interactive visual interface that uses high quality, easy-to-use data. The shared OpenCarto framework allows thorough functionality testing and troubleshooting during the development process. Tool functionality can be cross-referenced with previously built applications. The data layers used in the application were tested in a development environment prior to inclusion and cross-referenced to the original point data to ensure accurate representation. This interactive visual interface is beneficial to audiences who may be familiar with MHK resources, and also to those who are exploring them for the first time.

The application can deliver insight and possibly uncover geographic regions that provide a high resource opportunity with regard to OTEC and SWC resources. This may help researchers determine ideal locations for more in-depth data collection and test sites. Developers may see opportunity to install plants at specific locations. The application will allow the professional and research communities to hone in on specific locations of interest.

In addition to identifying prime locations to extract these resources, the application also displays potential opportunity on a global scale. This may be of interest to stakeholders and investors who may have relations with organizations looking for funding to capture these resources. Also, politicians and lawmakers may be able to make future energy-related decisions and policies based on the overview of data made available via the application. Coastal and small island nations may find substantial resource potential located within their EEZ. Lastly, the application would be a great classroom tool to educate teachers and students alike on the OTEC and SWC resources.

7.4 Comparison to other Resource Assessments

Many other resource assessments are comprised of charts, graphs and static maps. What is unique about this application, and the way the data are displayed, is that the user can focus on the variables and locations they are interested in and interact with that data. The ability to download the data from this resource assessment is also unique and valuable.

The MHK Atlas joins the other suite of tools hosted on NREL's OpenCarto framework. Most of these applications work in the same fashion as that described in this section. This application benefits from the OpenCarto platform due to the continued development of the framework, regression testing and addition of projects. Framework evolution may introduce new application features in the future.

¹⁶ EERE Financial Opportunities by Audience
http://www1.eere.energy.gov/financing/solicitations_detail.html?sol_id=324

8 Conclusions and Recommendations

The OTEEV Project has concluded that the potential energy stored in the Earth's oceans is a significant renewable resource which, to this day, remains virtually untapped. With estimates of over 55,000 Terawatt hours per year of electrical power available sustainably, it can no longer be ignored. Both energy generation and energy conservation, in the form of seawater cooling, can be realized by exploiting the existing ocean thermocline using carefully designed, placed and operated systems with minimal impact to our environment. The technology to run these systems reliably and sustainably has been demonstrated over the past century, albeit on smaller and less-than-economical scales.

A key to building support for ocean thermal energy extraction commercialization is the ability to provide estimates of ocean thermal resources at a regional or local level. For example, if a regional utility in Florida understood that OTEC plants could provide Gigawatts of base load, renewable power directly cabled into high-load areas, interest in the technology would dramatically increase, resulting in market penetration and commercialization. Municipal leaders would be better able to make utility decisions if they understood the potential capacity of SWC. Support for mature OTEC technology would increase and greater numbers of industry members would take notice and determine how they might take advantage of the new markets. The OTEEV project focused on fulfilling this need for regional insight to facilitate commercialization and market penetration of the ocean thermal energy resource.

By reviewing the methods and steps followed in this project we can better grasp the overall promise of ocean thermal energy and the needs for continued research in this area.

8.1 Summary of the OTEEV Project

Data Gathering and Processing: The selection of the HYCOM+NCODA ocean data was based largely upon the quality and availability of temperature delta, current speeds and grid point resolution. HYCOM uses finite difference techniques to simulate the deep ocean's adiabatic flow field below the photic and mixed zones, and couples to the Navy Coupled Ocean Data Assimilation (NCODA) multivariate approach for regions close to the surface. Simulations are based on actual ocean measurements, where available, with a given day's simulation including both a 5-day forecast and a 4-day hindcast.

Develop and Energy Extraction Model: Characteristics for a nominal 100 MW net power OTEC plant operating on a single-stage ammonia Rankine cycle are core to the modeling approach. The nominal OTEC plant design corresponds to a location with 25.7 °C surface water (460,000 kg/s) and 4.1 °C deep ocean water from 1000m depth (366,000 kg/s). The size of the plant is feasible with current technology and large enough to be economical in the predictable future. Characteristics of significance are: heat exchanger sizing, cold water flow rate, cold water pipe sizing, discharge depth, pumping losses not associated with the cold water pipe, and transmission losses.

Independent Validation: NREL has provided an independent assessment of the OTEC power model using ASPEN to model the single-stage power process. NREL and LM Team results are within 3% for the baseline case (98 MW vs. 101 MW net power), and differ by no more than 12% at the extreme. The OTEC plant model yields the net power production, validity of location for OTEC, potential air conditioning cold water, and the corresponding latitude-longitude location. Net power predicted varies from -3 to +164MW over a range of selected locations and validity of location is positive for a net positive power production.

Plant Spacing and Resource Sustainability: In developing both global and regional estimates of power from the ocean thermal energy extraction the team took into consideration the localized sustainability. A plant spacing algorithm was developed as a function of the cold water circulation to establish limits on regional OTEC plant density. By applying this plant density factor to the net power results for each grid point within the data set, the team was able to produce regional and global capacity estimates of this resource.

Interactive Data Visualization for the public: To share the results of this assessment, NREL developed a web-based GIS application that takes OTEC power model output and displays the resource intensity for a particular area of interest. The visual display allows a more intuitive inspection of the resource database, from which users can zoom in to a particular area of interest, query the data to inspect the site's characteristics, and download the data to use in their own applications.

8.2 Suggestions for Future Research

Model Extractable Energy with Alternate Technologies - The OTEEV Project's OTEC plant model simulations, along with OTEC resource and district cooling visualizations, provide estimates of the renewable resource available in tropical ocean waters. While beyond the scope of the present effort, it is possible to produce significantly higher values for net power by going to a two-stage Rankine or hybrid cycle. In some cases the benefits of increasing net power may justify higher capital cost and complexity. Further increases are possible by cascading 3 or more stages. This implies that the resource estimate results presented here are quite conservative in estimating power potential. However, all multi-stage system net power gains must be traded off with costs associated with added system complexity and increased size of heat exchangers. Ultimately, cost becomes the limiting factor for multi-stage designs. Future models, visualizations and assessments could provide alternate cycles and designs to compare with the OTEEV results.

Enhanced Circulation Modeling - It is important to emphasize that these resource estimates are first developed in the context of single, isolated OTEC plants, and no inferences concerning actual sustainability of the ΔT resource at a particular location are possible from this analysis. Although solar heating will tend to replace the surface (warm) water used in the OTEC process, replacement of the deep (cold) water used depends on ocean currents at depth. Large-scale ocean circulation models will need to mature significantly, along with the monitoring data collected from MW-scale facilities before consensus can be built regarding the establishment of sustainable multi-plant designs and appropriate plant spacing.

Improved Data Accuracy and Integrity - As emphasized in the sensitivity analysis in Section 3.7, temperature difference or ΔT is clearly the driving factor in determining the power production from an ocean thermal energy system. However, the accuracy and age of the available ocean data set is significant to the results of our model and overall assessment. As newer and presumably more accurate data is collected we will have the ability to update and improve usefulness of these OTEEV models.

Locally specific socioeconomic and logistical Extraction filters as additional visualization layers -The advantage of presenting this information in an interactive format through a web based environment is that continual updates and improvements can be made to the tool as the application and its user group evolves. Development of additional functionality or layers as described in Section 7.2 could include the visual mapping of locally specific logistics or socioeconomic factors that pose issues with site approval.

8.3 Promise of Ocean Thermal Energy

Today, the urgency for renewable energy development and concerns for the environment are high, and resources such as ocean thermal energy are again being seriously considered for commercial application. OTEC provides the potential for electricity cabled directly to local grids wherever a plant can be located within an economically feasible distance from shore. At further distances, OTEC platforms can manufacture energy carriers such as ammonia or hydrogen that can be shipped to shore for subsequent utilization. Future applications include building plants of sufficient size to host energy-intensive manufacturing processes and the potential for synthetic fuel production. Shore access to cold seawater resources enables the benefit of seawater cooling to areas with significant air-conditioning loads.

From the resource assessment study alone we see that over 500 GWe of capacity can be harvested from within the U.S.'s Economic Exclusive Zones. This represents as much as 8% of the world's estimated resource of 6.3 Terawatts. What is more impressive is that the thermal energy stored in the ocean provides a steady and reliable baseload capacity that is extremely beneficial to remote island locations looking to reduce their dependency on imported sources of energy from the mainland. OTEC power extraction also appears to be strongest in locations where other renewable energy resources such as tidal, wave and wind are not, making it an excellent compliment to a broad national alternative energy portfolio.

Our global energy future will clarify over time as issues are better understood and technologies come and go. In the meantime, with OTEC technology developed and advanced based on the immediate needs of tropical coastal communities world-wide, this technology would be mature and poised for a tremendous expansion into grazing plants and energy carriers. Thus a potentially massive and clean energy technology would be available if and when needed to help solve a massive global problem. If other technologies can better provide all the firm power needed globally, then OTEC remains as a coastal community supplier. In either case, OTEC developed today is a winning strategy for the developer and a prudent risk-lowering strategy for the long-range global energy planner.

The OTEEV project focused on fulfilling a need for regional insight to facilitate commercialization and market penetration of the ocean thermal energy resource. The MHK_Atlas visualization tool provides a global perspective of the OTEC and SWC resources at a relatively high resolution, letting users identify areas of high ocean thermal energy potential. Its multiple layers, customization and query capabilities allow for some very powerful regional close-ups of the pertinent data. As does all the other currently available resource atlases it offers a first look for developers prior to actual design and siting of technology.

The OTEEV model, for the sake of consistency and site comparison, utilizes a single 100 MWe design the team considers to be the smallest economical and most efficient configuration available for the baseline conditions today. This approach provides a conservative yet defensible estimate upon which we can improve with customized systems designed for site specific conditions. By responsibly developing this technology over the next several decades through sustainable means, a significant percentage of the projected global energy needs can be met using only the stored thermal energy in the ocean.

9 Products, Presentations and Data Dissemination

During the OTEEV Project, several papers were produced to share details of the team's efforts and results with the technical and business communities per the final objective of the SOPO.

Conference Papers

Model-based Global Assessment of OTEC Resources with Data Validation off Southeast Florida

L. T. Rauchenstein, J. H. VanZwieten, Jr, and H. P. Hanson

Abstract: As part of an ongoing effort to create a publicly accessible GIS database that characterizes the global OTEC resource, more than two years of daily HYCOM (Hybrid Coordinate Ocean Model) temperature data were processed. This global dataset was used to estimate annual and seasonal averages of the temperature gradient between the sea surface and water at 1000 m depth, a parameter commonly used for quantifying OTEC potential. Periodic annual variation was also explored. At locations where the depth was less than 1000 m, the temperature difference was evaluated between the sea surface and near bottom water. These data show that the mean temperature difference can be as high as 26.5°C and commonly varies by less than 5°C annually. These HYCOM-based estimates were then compared against thermal profile measurements made during 58 sets of CTD casts performed off Southeast Florida.

Proceedings, IEEE OCEANS '11 Santander, No. 110115-112; DOI: 10.1109/Oceans-Spain.2011.6003534

Modeling Global Ocean Thermal Energy Resources

John Nagurny, Laura Martel, Eugene Jansen, Andrew Plumb, Pamela Gray-Hann, Donna Heimiller, Lynn T. Rauchenstein, and Howard P. Hanson

Abstract: The potential renewable energy stored in the ocean's thermocline at a given location can be estimated using a model of the ocean thermal energy conversion (OTEC) process. Combining such a model with a global climatology of oceanic stratification and a flexible visualization system, such as a Geographic Information System (GIS), provides a useful tool for estimating both global OTEC potential and locations with particularly rich resources.

We report here on the application of an OTEC Plant model developed at Lockheed Martin (LM) that includes critical assumptions and accounts for major contributing (and loss) factors to electrical power production. This model uses global climatology of the oceanic stratification based on open-source results from the Hybrid Coordinate Ocean Model (HYCOM) in data assimilation mode produced by the Naval Research Laboratory (NRL). Because the HYCOM results used here are gridded at approximately 1/12° in latitude and longitude, the resolution of the results is a significant improvement over previous ocean climate studies of this nature, notwithstanding the use of a computer model. In addition, a new algorithm that optimizes the depth of the cold water source (by balancing power production and power loss) is used, meaning that the previous condition of using a 1-km-deep cold source is relaxed.

Proceedings, IEEE OCEANS '11 Kona. No. 110422-055, ISBN: 978-1-4577-1427-6

Assessment of HYCOM as a Tool for Estimating Florida's OTEC Potential

James H. VanZwieten, Jr, Lynn T. Rauchenstein, Howard P. Hanson, and Manhar R. Dhanak

Abstract: Ocean thermal energy conversion (OTEC) uses the energy stored in the thermocline to evaporate and condense a fluid in a Rankine power cycle. A thermal energy resource assessment is conducted for waters surrounding Florida to help qualitatively assess the best locations for electrical power production by an OTEC plant in that state, using data modeled by the Hybrid Coordinate Ocean Model (HYCOM). The model's temperature predictions are then compared on a daily timescale against three years' worth of in situ temperature data collected by CTD and ADCP buoys spanning 160 km of the Atlantic coast of south Florida.

Proceedings, IEEE OCEANS '11 Kona. No. 110422-145, ISBN: 978-1-4577-1427-6

Ocean Temperature Estimates from Models and Observations with Applications to OTEC

James T. Potemra

Abstract: Large-scale estimates of ocean temperature, particularly at depth, are sparse. Accurate estimates of ocean thermal gradients are however important for proper and efficient placement of ocean thermal energy conversion (OTEC) plants. This study provides estimates from two data sets based on direct observation: the autonomous Argo profiling floats and the World Ocean Database (WOD), as well as from two large-scale, high resolution ocean models. These calculations can be used in geographic information system (GIS) models as a parameter for proper location of OTEC facilities.

Proceedings, IEEE OCEANS '11 Kona. No. 110422-139

Global OTEC Resource Assessment

Howard P. Hanson

Abstract: One of the five M&HK resource assessment projects funded from the DoE 2008 Funding Opportunity Announcement (FOA) was an assessment of OTEC resources; while other four assessments were for U.S. EEZ, the OTEC project was designed to examine the global resource. It was also designed to improve on previous work at the University of Hawai'i with improved resolution and better coastal coverage. The results are to be integrated into NREL's Renewable Energy Atlas GIS system. This talk describes the project and examines highlights of results.

Offshore Renewables – Getting the Green Light to Deploy and Produce, a By-invitation Workshop at Ecology & Environment, Inc. Eagles Nest Conference Center, Blue Mountain Lake, NY.

Observing Ocean Temperatures for Thermal Energy Resources

James T. Potemra

Summary: Editorial on the Ocean Thermal Extractable Energy Visualization project and benefits of the visualization tool. *Sea Technology Magazine*, March 2012, Vol. 53, No. 3, page 7.

2012 GMREC Presentation- Ocean Thermal Energy Resource Assessment

Matthew B. Ascari

Summary: Highlights of the Ocean Thermal Extractable Energy Visualization project presented as part of the 2012 Global Marine Renewable Energy Conference panel on resource assessments.

Websites/Visualization Tool

The Marine and Hydrokinetic Atlas is deemed to be the project's final product and official public dissemination of results, accessible online at http://maps.nrel.gov/mhk_atlas.

10 References Cited

- Avery, W.H., and C. Wu, 1994: Renewable Energy from the Ocean: A Guide to OTEC. Oxford University Press, Oxford, 446pp.
- Bleck, R., 1978: On the use of hybrid vertical coordinates in numerical weather prediction models. *Monthly Weather Review*, **115**, 3097–3114.
- Bleck, R., 2002: An oceanic general circulation model framed in hybrid isopycnic-Cartesian coordinates, *Ocean Modelling*, **37**, 55–88.
- Bleck, R., and D. Boudra, 1986: Wind-driven spin-up in eddy-resolving ocean models formulated in isopycnic and isobaric coordinates, *Journal of Geophysical Research*, **91**, 7611–7621, 1986.
- Bleck, R., and L. Smith, 1990: A wind-driven isopycnic coordinate model of the North and equatorial Atlantic Ocean, I, Model development and supporting experiments, *Journal of Geophysical Research*, **95**, 3273–3285.
- Bleck, R., H. Hanson, D. Hu, and E. Kraus, 1989: Mixed layer-thermocline interaction in a three-dimensional isopycnic coordinate model, *Journal of Physical Oceanography*, **19**, 1417–1439.
- Chassignet, E.P., Smith, L.T., Halliwell, G.R., Bleck, R., 2003. North Atlantic simulations with the HYbrid Coordinate Ocean Model (HYCOM): impact of the vertical coordinate choice, reference density, and thermobaricity, *Journal of Physical Oceanography*, **33**, 2504–2526.
- Chassignet, E.P., H.E. Hurlburt, E.J. Metzger, O.M Smedstad, J.A. Cummings, G.R. Halliwell, R. Bleck, R. Baraville, A.J. Wallcraft, C. Lozano, H.L. Tolman, A. Srinivasan, S. Hankin, P. Cornillon, R. Weisberg, A. Barth, R. He, F. Werner, and J. Wilkin, 2009:, US GODAE: Global ocean prediction with the HYbrid Coordinate Ocean Model (HYCOM). *Oceanography*, **22**, 64–75.
- Cummings, J.A., 2005: Operational multivariate ocean data assimilation. *Quarterly Journal of the Royal Meteorological Society*, **131**, 3583–3604.
- Eldred, Michael P ; Van Ryzin, Joseph C ; Rizea, Steven; Chen, In Chieh; Loudon, Robert; Nagurny, N. John; Maurer, Scott; Jansen, Eugen; Plumb, Andrew; Eller, Michael R.; and Brown, Victor R. R., 2011: Heat Exchanger Development for Ocean Thermal Energy Conversion. *Proceedings, OCEANS '11 Kona*, IEEE. In press. ISBN: 978-1-4577-1427-6
- Fox, D.N., W.J. Teague, C.N. Barron, M.R. Carnes, and C.M. Lee, 2002. The Modular Ocean Data Assimilation System (MODAS). *Journal of Atmospheric and Oceanic Technology*, **19**, 240–252.
- Hogan, T., and T. Rosemond, 1991: The description of the Navy Operational Global Atmospheric Prediction System's spectral forecast model. *Monthly Weather Review*, **119**, 1786–1815.
- IPCC (Intergovernmental Panel on Climate Change), 2007: Summary for Policymakers. In: Climate Change 2007: The Physical Science Basis. Contribution of Working Group I to the Fourth Assessment Report of the Intergovernmental Panel on Climate Change [Solomon, S., D. Qin, M. Manning, Z. Chen, M. Marquis, K.B. Averyt, M. Tignor and H.L. Miller (eds.)]. Cambridge University Press, Cambridge, United Kingdom and New York, NY, USA.

Naval Facilities Engineering Command, 2010: NAVFAC Ocean Thermal Energy Conversion (OTEC) Project - OTEC System Design Report Contract N62583-09-C-0083, CDRL A003,
<http://www.dtic.mil/cgi-bin/GetTRDoc?AD=ADA532389&Location=U2&doc=GetTRDoc.pdf>

NCEES (National Council of Examiners for Engineering and Surveying), 2005: Fundamentals of Engineering Supplied-Reference Handbook, 7th Ed. , Clemson, SC

Nihous, G.C., 2005: An order-of-magnitude estimate of ocean thermal energy conversion (OTEC) resources, *Journal of Energy Resources Technology*, **127**, 328–333.

Nihous, G.C., 2007: A preliminary estimate of ocean thermal energy conversion resources. *Journal of Energy Resources Technology*, **129**, 10-17.

Nihous, G.C., 2010: Mapping available Ocean Thermal Energy Conversion resources around the main Hawaiian Islands with state-of-the-art tools. *Journal of Renewable and Sustainable Energy*, **2**, 043104:1-9.

NOAA (National Atmospheric and Oceanic Administration) 2001: World Ocean Atlas 2001 National Oceanographic Data Center, NOAA, Washington, D.C.

Potemra, J.T., 2011: Ocean Temperature Estimates from Models and Observations with Applications to OTEC *Proceedings, OCEANS '11 Kona*, IEEE. In press.

Rauchenstein, L.T., J.H. VanZwieten, and H.P. Hanson, 2011: Model-based assessment of global OTEC resources with data validation off southeast Florida. *Proceedings, OCEANS '11 Santander*, IEEE. In press.

Rew, R.K. and G P. Davis, 1990: NetCDF: An Interface for Scientific Data Access. *IEEE Computer Graphics and Applications*, **10**, 76-82.

Teague, W.J., M.J. Carron, and P.J. Hogan, 1990: A comparison between the Generalized Digital Environmental Model and Levitus climatologies. *Journal of Geophysical Research*, **95**, 7167-7183.

VanZwieten, J.H., L.T. Rauchenstein, H.P. Hanson, and M.H. Dhanak, 2011: Assessment of HYCOM as a tool for estimating Florida's OTEC potential. *Proceedings, OCEANS '11 Kona*, IEEE. In press.

Vega, L.A., 2003: Ocean thermal energy conversion primer, *Marine Technology Society Journal*, **36**, 25-41.

Vega, L.A., 2010: Economics of Ocean Thermal Energy Conversion (OTEC): An Update. *Proceedings, 2010 Offshore Technology Conference held in Houston, Texas*. [OTC 21016]

Xue, Y., R.W. Reynolds, and V. Branzon, 2010: Sea surface temperatures [in “State of the Climate in 2009”]. *Bulletin of the American Meteorological Society*, **91**, S53-S56.

11 Abbreviations and Key Terminology

| Acronym/ Key Terminology | Description/Equations |
|-----------------------------|---|
| ADCP | Acoustic Doppler Current Profiler |
| ASPEN | Commercially Available Process Modeling Software |
| CSBAC | Cold Seawater Based Air Conditioning |
| CSV | Comma-separated value file |
| CTD | Conductivity Temperature Depth |
| CWP | Cold Water Pipe |
| D-J-F | December January February |
| DoE | Department of Energy |
| DOI | Department of the Interior |
| EEZ | Exclusive Economic Zone |
| FAU | Florida Atlantic University |
| FOA | Funding Opportunity Announcement |
| GIS | Geospatial Information System |
| GMT | Greenwich Mean Time |
| GODAE | Global Ocean Data Assimilation Experiment |
| GW | Gigawatt = 1,000,000,000 Watts |
| GWe | Gigawatts electric |
| HI | Hawai‘i |
| HX | Heat Exchanger |
| HYCOM | HYbrid Coordinate Ocean Model |
| HYCOM+NCODA | HYCOM using the Navy Coupled Ocean Data Assimilation |
| ID | Inner Diameter |
| IEEE | Institute of Electrical Electronics Engineers |
| IPCC | Intergovernmental Panel on Climate Change |
| ISBN | International Standard Book Number |
| J-J-A | June July August |
| kW | kilowatts = 1,000 Watts |
| LMTD | Log Mean Temperature Difference |
| M&HK | Marine & Hydrokinetic |
| MHK_Atlas | Marine and Hydrokinetic Atlas - http://maps.nrel.gov/mhk_atlas |
| MICOM | Miami Isopycnic Coordinate Model |
| MODAS | Modular Ocean Data Assimilation System |
| MPEE | Maximum Practically Extractable Energy |
| MRE | Marine Renewable Energy |
| MW | Megawatts = 1,000,000 Watts |
| MW/K | Megawatts per Kelvin |
| MWe | Megawatts electric |
| N-S | North-South |
| NCODA | Navy Coupled Ocean Data Assimilation |
| NODC | National Oceanographic Data Center |
| NDOC-WOA05 | National Oceanographic Data Center -World Ocean Atlas 2005 |
| netCDF | Network common data form |
| NOAA | National Oceanic and Atmospheric Administration |
| NREL | National Renewable Energy Laboratory |
| NRL | Naval Research Laboratory |

| Acronym/ Key Terminology | Description/Equations |
|-----------------------------|--|
| OTEC | Ocean Thermal Energy Conversion |
| OTEEV | Ocean Thermal Extractable Energy Visualization |
| PI | Principal Investigator |
| REFPROP | NIST supported database of Reference Fluid Thermodynamic and Transport Properties www.nist.gov/srd/upload/REFPROP9.pdf |
| SCOPE | Simple Communications Programming Environment |
| SLD | Styled Layer Descriptor |
| SOPO | Statement of Project Objectives |
| SST | Sound Sea Technology |
| SWC | Seawater Cooling |
| T_s | Temperature at Ocean Surface |
| T_d | Temperature at Ocean Depth |
| TOC | Total Ownership Cost |
| TW | Terawatt = 1,000,000,000,000 Watts |
| TWe | Terawatts electric. |
| UA | A measure of heat exchanger performance |
| UH | University of Hawai'i |
| WFS | Web Feature Service |
| WMS | Web Mapping Service |
| WOA | World Ocean Atlas |
| WOA05 | World Ocean Atlas 2005 |
| ΔT or Delta T | Temperature Difference as calculated by subtracting T_d from T_s |
| ΔX or Delta X | Represents the distance between floating OTEC plants. Listed as meters unless otherwise noted |
| ΔZ or Delta Z | Represents a nominal thickness layer volume of Cold Water that would be utilized by the OTEC process. |
| ΔT_{1000} | Temperature at 1000-meter ocean depth |

12 Appendices

Appendix A –Summary of Tasks from the Statement of Project Objectives

Appendix B –Static Head Loss Formulation

Appendix C –REFPROP Thermodynamic Values

Appendix D –Basis of Calculations

Appendix A – Summary of Tasks from the Statement of Project Objectives

Task 1.0 Resource Data Generation

This effort focuses on collecting existing quality-controlled datasets.

Subtask 1.1 Develop data requirements

Due to the complexity of the dynamic system characterizing the oceans, data sampling requirements are essential to maintain a controlled database reflecting the different scales of variability in physical parameters, such as spatial and temporal resolutions. The basic requirements for the data will be established under this task.

Subtask 1.2 Generate a database by gathering data from existing sources

No new ocean measurements or numerical simulations will be conducted in this project. Instead, this task will enable the team to collect and use existing data produced from direct measurements and validated through quality control procedures.

Subtask 1.3 Generate a database by gathering data from existing sources

When direct measurements are not available or are insufficient, data gaps will be filled with numerical model output.

Task 2.0 Energy Conversion Model Development

Subtask 2.1 Plant efficiency model

OTEC plant efficiency is a complex function of the cold-water temperature (T_D), warm water temperature (T_S), flow rates and plant design. OTEC performance prediction models will be used to reduce plant performance to an overall conversion efficiency matrix with T_D as one axis and T_S as the other for use in the energy conversion calculation.

Subtask 2.2 Develop model for sustainable and available heat flux

There are two components to sustainable energy resources. The first is the global sustainability. The second is regional sustainability. Under this project literature searches will be employed to select a validated, representative value of the thermohaline circulation as this is accepted as the limited factor for global sustainability. For regional sustainability, a discussion on cold water usage rate is presented which considers the draw-down rate vs. net influx of new cold water for multiple plants having a given spacing between them. A discussion of previous efforts dealing with resource sustainability is provided, along with recommendations for future work.

Subtask 2.3 Execute Energy Conversion Model

Execute the plant efficiency model and sustainable heat flux model with the data generated in Task 1.0 to generate extractable energy estimates for incorporation in the GIS database in Task 3.0.

Task 3.0 Incorporate Results into GIS Database

The overall objective of this task is to incorporate ocean thermal energy resource information generated in Task 1.0 along with consistent and reliable estimates of baseline, practical, recoverable and producible electrical energy as a result of Task 2.0 in a public GIS database, consistent in format with other renewable energy data at the NREL.

Task 4.0 Independent Validation and Verification

Under this project, NREL will provide independent validation and verification of the data and methodology used to generate the OTEEV tool.

*Subtask 4.1 Data Validation and Verification **

NREL will evaluate the data gathered in Task 1.0 for quality issues such as length of period of record, data completeness, bad data periods, etc.

Subtask 4.2 Methodology Validation and Verification

NREL will review a detailed description of the methodology used to compute the ocean thermal extractable energy from the input data, including details of all modeling software, examples of where this software has previously been used to compute ocean thermal resources, descriptions of new techniques or methods that are used in this study, etc. NREL will evaluate and approve the methodology, and includes a description as an adjunct to the GIS database.

Subtask 4.3 Final Validation and Verification

After the ocean thermal extractable energy data have been integrated into NREL's existing offshore renewable resource GIS, NREL will conduct an internal review of the system to be certain that all project requirements have been met. NREL will also seek input from all project partners and from outside users to evaluate the usefulness of the system. Based on discussions with the project partners, changes and refinements to the system may be made before the final publication of the OTEEV tool.

Task 5.0 Project Management and Reporting

Throughout the schedule, the LM team has included two efforts for Project Management.

- Overall Technical Direction will ensure completeness, correctness, continuity, and coordination of technical tasks.
- Technical Schedule and Cost Monitoring will ensure that programmatic schedule and cost targets are maintained.

Progress Briefings are scheduled quarterly to ensure that the entire team remains on task with aligned objectives, and the DoE customer is kept informed. Reports and other deliverables will be provided in accordance with the Federal Assistance Reporting Checklist following the instructions included therein.

As progress is made, publications and presentations summarizing the results of the OTEEV effort will be submitted to the following conferences, of which all team members are regular contributors:

EnergyOcean, IEEE Oceans, the Global Marine Renewable Energy Conference, and the Offshore Technology Conference.

NREL's public GIS web site (<http://www.nrel.gov/gis>) will be the primary repository for the ocean thermal energy estimates produced by this project. The resource estimates and associated data will become part of NREL's Global Marine and Hydrokinetic Energy Resource Atlas.

* The Specific task was considered unnecessary and removed as the HYCOM+NCODA dataset is self-documenting and complete.

Appendix B

Static Head Loss Formulation

Static Head Loss Formulation

Sea Water Density

$$\text{Freshwater Density} = -0.00584T^2 + 0.03T + 1000$$

$$\text{Sea Water Density} = 1.025 \times \text{Freshwater Density} = -0.00599T^2 + 0.031T + 1025$$

Sea Water Temperature (T) = Input in °C

Static Head (Simplified)

$$\text{Static Head} = \frac{\text{Cold Water Density} - \text{Warm Water Density}}{\text{Cold Water Density}} \times d$$

$$\text{Surface Water Density} = -0.00599T_s^2 + 0.031T_s + 1025$$

$$\text{Cold Water Density} = -0.00599(T_s - dT)^2 + 0.031(T_s - dT) + 1025$$

Cold Water Pipe Depth (d) = Input in meters

Static Head Correction Factor

Average ambient density on the outside of the cold water pipe can be determined as a function of pipe depth, cold water density and warm water density by use of a representative density vs. depth profile. The representative pycocline (density vs. depth profile) was determined by Florida Atlantic University using the NOAA CM2.1 model from the 1999 mean of roughly 2500 tropical locations between 20 degrees North and 20 degrees South. The pycocline data is provided below. Linear interpolation between the nearest two values was used to determine densities at 300m, 400m, 500m, 600m, 700m, 800m and 900m.

| <u>Depth (m)</u> | <u>Approx Density (kg/m³)</u> | <u>Depth (m)</u> | <u>Approx Density (kg/m³)</u> |
|------------------|--|------------------|--|
| 0 | 1022.437 | 215 | 1026.019 |
| 5 | 1022.45 | 225 | 1026.083 |
| 15 | 1022.477 | 236.123 | 1026.15 |
| 25 | 1022.64 | 250.6 | 1026.227 |
| 35 | 1022.894 | 270.621 | 1026.319 |
| 45 | 1023.175 | 298.305 | 1026.424 |
| 55 | 1023.434 | 300 | 1026.429 |
| 65 | 1023.685 | 335.676 | 1026.538 |
| 75 | 1023.918 | 384.634 | 1026.658 |
| 85 | 1024.148 | 400 | 1026.688 |
| 95 | 1024.373 | 446.937 | 1026.778 |
| 105 | 1024.588 | 500 | 1026.860 |
| 115 | 1024.792 | 524.171 | 1026.898 |
| 125 | 1024.983 | 600 | 1026.994 |
| 135 | 1025.156 | 617.736 | 1027.017 |
| 145 | 1025.312 | 700 | 1027.104 |
| 155 | 1025.452 | 728.828 | 1027.134 |
| 165 | 1025.577 | 800 | 1027.197 |
| 175 | 1025.687 | 858.422 | 1027.248 |
| 185 | 1025.784 | 900 | 1027.278 |
| 195 | 1025.871 | 1000 | 1027.350 |
| 205 | 1025.949 | 1007.257 | 1027.355 |

The approximate densities are used to establish average density up the outside of the cold water pipe for various cold water pipe depths. The static head equation is applied to each pipe section where the cold water density is the density at the cold water pipe depth, the average WW density is the average ambient density at the pipe section, and the depth is the length of that pipe section:

| <u>Depth (m)</u> | <u>1000m Static Head Contribution</u> | <u>Depth (m)</u> | <u>1000m Static Head Contribution</u> |
|------------------|---------------------------------------|--------------------------|---------------------------------------|
| 0 | - | 215 | 0.0133 |
| 5 | 0.0239 | 225 | 0.0126 |
| 15 | 0.0476 | 236.123 | 0.0134 |
| 25 | 0.0466 | 250.6 | 0.0164 |
| 35 | 0.0446 | 270.621 | 0.0210 |
| 45 | 0.0420 | 298.305 | 0.0264 |
| 55 | 0.0394 | 300 | 0.0015 |
| 65 | 0.0369 | 335.676 | 0.0301 |
| 75 | 0.0345 | 384.634 | 0.0358 |
| 85 | 0.0323 | 400 | 0.0101 |
| 95 | 0.0301 | 446.937 | 0.0282 |
| 105 | 0.0279 | 500 | 0.0274 |
| 115 | 0.0259 | 524.171 | 0.0111 |
| 125 | 0.0240 | 600 | 0.0298 |
| 135 | 0.0222 | 617.736 | 0.0059 |
| 145 | 0.0206 | 700 | 0.0232 |
| 155 | 0.0192 | 728.828 | 0.0065 |
| 165 | 0.0179 | 800 | 0.0128 |
| 175 | 0.0167 | 858.422 | 0.0072 |
| 185 | 0.0157 | 900 | 0.0035 |
| 195 | 0.0148 | 1000 | 0.0035 |
| 205 | 0.0140 | Total Static Head | 0.9364 |

For example, the calculation for the static head contribution of the pipe section between 0m and 5m for a 1000m cold water pipe is shown below:

$$\begin{aligned} \text{Static Head (1000m Cold Water Pipe)} &= \frac{\text{Cold Water Density} - \text{Warm Water Density}}{\text{Cold Water Density}} \times d \\ &= \frac{1027.350 \frac{\text{kg}}{\text{m}^3} - \frac{1022.437 \frac{\text{kg}}{\text{m}^3} + 1022.45 \frac{\text{kg}}{\text{m}^3}}{2}}{1027.350 \frac{\text{kg}}{\text{m}^3}} \times (5\text{m} - 0\text{m}) = 0.0239\text{m} \end{aligned}$$

The contributions of each section are then summed to determine total static head. Using the cold water pipe depth and cold water density in conjunction with the static head equation, it is possible to solve for the weighted Average WW Density as shown below. The calculation for the Average WW Density for a 1000m cold water pipe, given the density profile above is:

$$\begin{aligned} \text{Average WW Density} &= \text{Cold Water Density} - \frac{\text{Total Static Head} \times \text{Cold Water Density}}{d} \\ &= 1027.350 \frac{\text{kg}}{\text{m}^3} - \frac{0.9364\text{m} \times 1027.350 \frac{\text{kg}}{\text{m}^3}}{1000\text{m}} = 1026.388 \frac{\text{kg}}{\text{m}^3} \end{aligned}$$

It is not necessary to explore cold water pipe depths more shallow than 300m as no sites meeting these criteria are capable of producing net power.

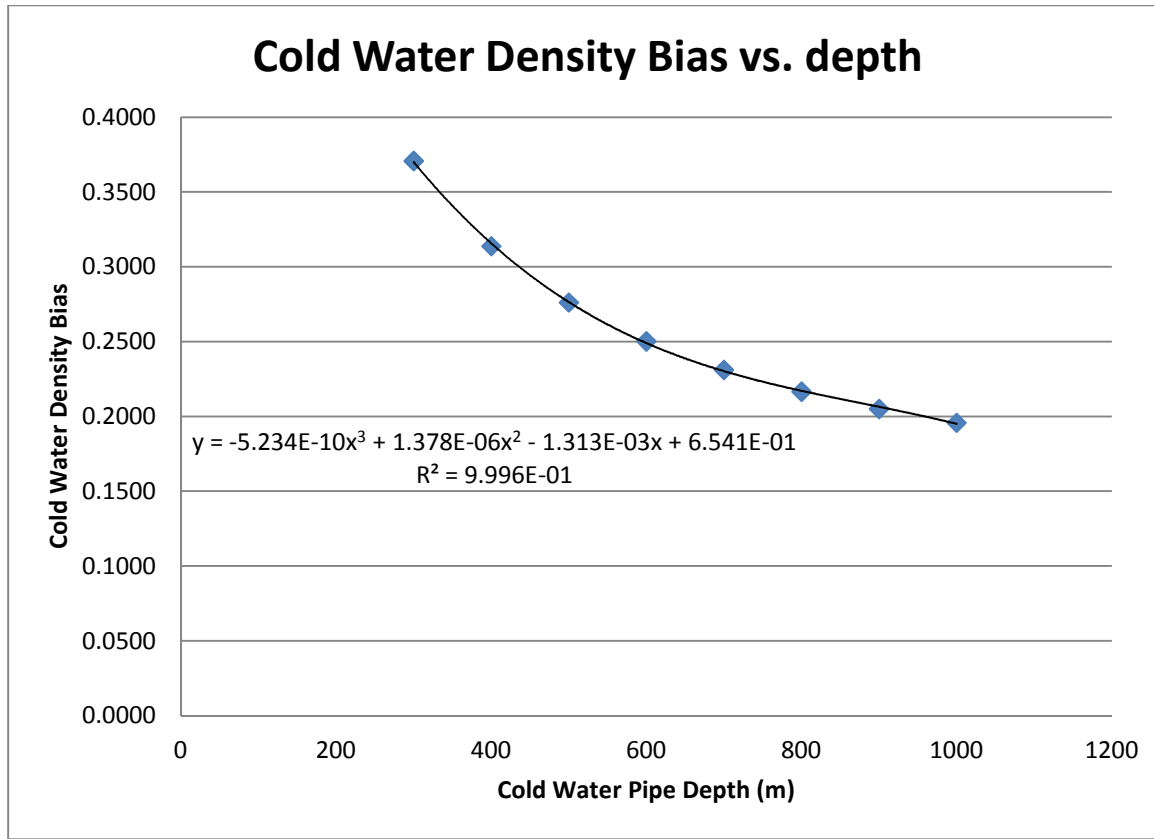
| Depth (m) | Average WW Density |
|------------------|---------------------------|
| 300 | 1024.948 |
| 400 | 1025.353 |
| 500 | 1025.639 |
| 600 | 1025.854 |
| 700 | 1026.025 |
| 800 | 1026.166 |
| 900 | 1026.285 |
| 1000 | 1026.388 |

From this average density, a factor can be used to determine bias towards the Warm Water Density using the following formula:

$$\text{Warm Water Density Bias} = \frac{\text{Cold Water Density} - \text{Average WW Density}}{\text{Cold Water Density} - \text{Surface Water Density}}$$

| Depth (m) | Bias |
|------------------|-------------|
| 300 | 0.3709 |
| 400 | 0.3138 |
| 500 | 0.2762 |
| 600 | 0.2503 |
| 700 | 0.2312 |
| 800 | 0.2166 |
| 900 | 0.2051 |
| 1000 | 0.1958 |

Plotting a function of Bias to Cold Water vs. depth and solving for the characteristic formula:



Solving the Cold Water Density Bias formula for Average WW Density:

$$\begin{aligned} \text{Average WW Density} \\ &= \text{Bias} \times (\text{Surface Water Density} - \text{Cold Water Density}) + \text{Cold Water Density} \end{aligned}$$

Substituting Average WW Density for Warm Water Density in the Static Head Formula:

$$\begin{aligned} \text{Static Head} &= \frac{\text{Cold Water Density} - \text{Average WW Density}}{\text{Cold Water Density}} \times d \\ &= -\text{Bias} \times \left(\frac{\text{Surface Water Density}}{\text{Cold Water Density}} - 1 \right) \times d \end{aligned}$$

Substituting for all terms:

$$\begin{aligned} \text{Static Head} &= (5.234 \times 10^{-10}d^3 - 1.378 \times 10^{-6}d^2 + 1.313 \times 10^{-3}d - 0.6541) \\ &\quad \times \left(\frac{-0.00599T_s^2 + 0.031T_s + 1025}{-0.00599(T_s - dT)^2 + 0.031(T_s - dT) + 1025} - 1 \right) \times d \end{aligned}$$

Appendix C

REFPROP Thermodynamic Values

NOTE: REFPROP – a refrigerant properties database published by the National Institute of Standards and Technology – is called directly to find all thermodynamic values in this exercise.

Assumptions

| | |
|-----------------------------|---------------|
| Warm Water Temperature | 25.7 °C |
| Warm Water Flow Rate | 460000 kg/sec |
| Cold Water Temperature | 4.1 °C |
| Cold Water Flow Rate | 366000 kg/sec |
| Cold Water Pipe Depth | 1000 m |
| Ammonia Mass Flow Rate | 4060 kg/sec |
| Turbine Expander Efficiency | 86 % |
| Ammonia Pump Efficiency | 75 % |
| Generator Efficiency | 97.5% |

In keeping with the thermodynamic model established for the system by Makai Ocean Engineering, the corresponding UA values are as follows:

| | |
|---------------|------------|
| Evaporator UA | 1410 MW/°C |
| Condenser UA | 1350 MW/°C |

Calculations

Ammonia boiling temperature and ammonia condensing temperature must be assigned and modified until the UA values for the evaporator and condenser converge on the values listed above.

For the base case, those values were found to be:

| | |
|--------------------------------|----------|
| Ammonia Boiling Temperature | 20.60 °C |
| Ammonia Condensing Temperature | 9.60 °C |

The Ammonia Boiling Temperature (saturation temperature) is then used to find the Saturated Vapor Enthalpy, Pressure and Entropy at the Evaporator Outlet.

| EVAPORATOR OUTLET | |
|--------------------------|----------------|
| Saturated Vapor Enthalpy | 1623.7 kJ/kg |
| Saturated Vapor Pressure | 8.7405 Bar |
| Saturated Vapor Entropy | 5.8406 kJ/kg-K |

The turbine inlet pressure is the Evaporator Outlet Saturated Vapor Pressure less a pressure loss of 0.1 Bar from evaporator to turbine inlet. That pressure loss of 0.1 Bar is assumed constant across all cases, because the ammonia mass flow rate will not fluctuate and volumetric flow rate will not change significantly.

| | |
|------------------------|------------|
| Turbine Inlet Pressure | 8.6405 Bar |
|------------------------|------------|

Turbine Inlet Temperature is determined using the Turbine Inlet Pressure and Evaporator Outlet Saturated Vapor Entropy (assumed isentropic):

| | |
|---------------------------|----------|
| Turbine Inlet Temperature | 20.24 °C |
|---------------------------|----------|

Turbine Inlet Enthalpy and Entropy is then determined using the Turbine Inlet Temperature as vapor temperature:

| | |
|------------------------|----------------|
| Turbine Inlet Enthalpy | 1623.5 kJ/kg |
| Turbine Inlet Entropy | 5.8447 kJ/kg-K |

Turbine Outlet Temperature is assumed equal to the Ammonia Condensing Temperature:

| | |
|----------------------------|--------|
| Turbine Outlet Temperature | 9.6 °C |
|----------------------------|--------|

Turbine Outlet Pressure and Saturated Vapor Enthalpy are determined from the Turbine Outlet Temperature (vapor temperature):

| | |
|---|-----------------|
| Turbine Outlet Pressure | 6.066 Bar |
| Turbine Outlet Saturated Vapor Enthalpy | 1614.91 kJ/kg-K |

The Adiabatic Turbine Outlet Entropy is determined using the Turbine Inlet Temperature (vapor temperature) :

| | |
|----------------------------------|----------------|
| Adiabatic Turbine Outlet Entropy | 5.8405 kJ/kg-K |
|----------------------------------|----------------|

The Adiabatic Turbine Outlet Enthalpy is determined using the Turbine Outlet Pressure and the Adiabatic Turbine Outlet Entropy:

| | |
|-----------------------------------|---------------|
| Adiabatic Turbine Outlet Enthalpy | 1579.16 kJ/kg |
|-----------------------------------|---------------|

Adiabatic Turbine Enthalpy Delta is the difference between the Turbine Inlet Enthalpy and the Adiabatic Turbine Outlet Enthalpy:

| | |
|----------------------------------|-------------|
| Adiabatic Turbine Enthalpy Delta | 44.32 kJ/kg |
|----------------------------------|-------------|

Turbine Outlet Enthalpy is determined as the Adiabatic Turbine Outlet Enthalpy plus the inefficiency of the turbine applied to the Adiabatic Turbine Enthalpy Delta:

| | |
|-------------------------|---------------|
| Turbine Outlet Enthalpy | 1585.37 kJ/kg |
|-------------------------|---------------|

Pump Inlet Liquid Enthalpy and Entropy are found using the Turbine Outlet Pressure (liquid pressure):

| | |
|----------------------------|----------------|
| Pump Inlet Liquid Enthalpy | 387.85 kJ/kg |
| Pump Inlet Liquid Entropy | 1.6314 kJ/kg-K |

Adiabatic Pump Outlet Liquid Enthalpy is determined using the Evaporator Outlet (inlet assumed same) Pressure and the Pump Inlet Liquid Entropy:

| | |
|---------------------------------------|--------------|
| Adiabatic Pump Outlet Liquid Enthalpy | 388.27 kJ/kg |
|---------------------------------------|--------------|

Evaporator Inlet Liquid Enthalpy is the Pump Inlet Liquid Enthalpy plus the inefficiency of the ammonia pump applied to the difference in enthalpy between the Pump Inlet Liquid Enthalpy and the Adiabatic Pump Outlet Liquid Enthalpy:

| | |
|----------------------------------|--------------|
| Evaporator Inlet Liquid Enthalpy | 388.42 kJ/kg |
|----------------------------------|--------------|

Evaporator/Condenser Thermal Load is a function of the ammonia mass flow rate applied to the enthalpy difference across each heat exchanger. Evaporator Inlet Liquid Enthalpy and Evaporator Outlet Saturated Vapor Enthalpy are used for the Evaporator. Turbine Outlet Enthalpy and Pump Inlet Liquid Enthalpy are used for the Condenser.

| | |
|-------------------------|-----------|
| Evaporator Thermal Load | 5015.4 MW |
| Condenser Thermal Load | 4861.9 MW |

Water discharge temperatures are calculated based on water inlet temperature and the temperature difference across the heat exchanger calculated by:

$$\frac{\text{Thermal Load}}{\dot{m}C_p}$$

where the mass flow rate of water is used and the constant pressure specific heat is assumed as 3993 J/kg.

| | |
|----------------------------------|----------|
| Warm Water Discharge Temperature | 22.97 °C |
| Cold Water Discharge Temperature | 7.43 °C |

The Minimum Delta Temperature is the difference between Discharge Temperature and the saturation temperature (Ammonia Boiling Temperature / Ammonia Condensing Temperature):

| | |
|----------------------------|---------|
| Evaporator Minimum Delta T | 2.37 °C |
| Condenser Minimum Delta T | 2.17 °C |

Saturation temperature is used for the ammonia side temperature at both ends of each heat exchanger for calculation of LMTD. UA is determined from the Thermal Load and LMTD.

| | |
|-----------------|-------------|
| Evaporator LMTD | 3.56 °C |
| Evaporator UA | 1410 MW/ °C |
| Condenser LMTD | 3.58 °C |
| Condenser UA | 1360 MW/ °C |

Applying the Generator Efficiency, Turbine Expander Efficiency and Adiabatic Turbine Enthalpy Delta to the Ammonia Mass Flow Rate yields Gross Power.

| | |
|-------------|----------|
| Gross Power | 150.9 MW |
|-------------|----------|

Appendix D

Basis of Calculations

| Basis of Calculations (Assumptions) | | | | | | | | | |
|-------------------------------------|--------------------------------|-------------------------------|--------------------------------|-------------------------------|---------------------------|----------------------------|---|-------------------------------------|--|
| Nominal NAVFAC Plant | Warm water temperature (Deg C) | Warm water flow rate (kg/sec) | Cold water temperature (Deg C) | Cold water flow rate (kg/sec) | Cold Water Pipe Depth (m) | Ammonia flow rate (kg/sec) | Delta T WW to CW (Deg C/K) - calculated | Ammonia boiling temperature (Deg C) | Ammonia condensing temperature (Deg C) |
| | 25.7 | 460000 | 4.1 | 366000 | 1000 | 4060 | 21.6 | 20.60 | 9.60 |
| 1 | 30.53 | 460000 | 4.19 | 366000 | 1000 | 4060 | 26.34 | 25.43 | 9.63 |
| 2 | 28.92 | 460000 | 4.60 | 366000 | 1000 | 4060 | 24.32 | 23.83 | 10.06 |
| 3 | 28.64 | 460000 | 4.37 | 366000 | 1000 | 4060 | 24.27 | 23.55 | 9.83 |
| 4 | 29.08 | 460000 | 3.98 | 366000 | 1000 | 4060 | 25.1 | 23.98 | 9.43 |
| 5 | 27.74 | 460000 | 3.98 | 366000 | 1000 | 4060 | 23.76 | 22.63 | 9.45 |
| 6 | 28.08 | 460000 | 4.32 | 366000 | 1000 | 4060 | 23.76 | 22.98 | 9.79 |
| 7 | 25.95 | 460000 | 3.96 | 366000 | 1000 | 4060 | 21.99 | 20.85 | 9.45 |
| 8 | 25.64 | 460000 | 5.81 | 366000 | 1000 | 4060 | 19.83 | 20.57 | 11.30 |
| 9 | 27.58 | 460000 | 6.62 | 366000 | 1000 | 4060 | 20.96 | 22.52 | 12.08 |
| 10 | 25.41 | 460000 | 4.39 | 366000 | 1000 | 4060 | 21.02 | 20.32 | 9.88 |
| 11 | 25.08 | 460000 | 5.48 | 366000 | 1000 | 4060 | 19.6 | 20.02 | 10.98 |
| 12 | 20.01 | 460000 | 3.62 | 366000 | 1000 | 4060 | 16.39 | 14.92 | 9.18 |
| 13 | 22.21 | 460000 | 4.39 | 366000 | 1000 | 4060 | 17.82 | 17.14 | 9.93 |
| 14 | 17.78 | 460000 | 3.64 | 366000 | 1000 | 4060 | 14.14 | 12.70 | 9.23 |
| 15 | 24.25 | 460000 | 5.45 | 366000 | 1000 | 4060 | 18.8 | 19.18 | 10.95 |
| 16 | 25.77 | 460000 | 8.11 | 366000 | 1000 | 4060 | 17.66 | 20.75 | 13.58 |
| 17 | 21.96 | 460000 | 5.59 | 366000 | 700 | 4060 | 16.37 | 16.90 | 11.13 |
| 18 | 27.4 | 460000 | 4.90 | 366000 | 700 | 4060 | 22.5 | 22.32 | 10.36 |
| 19 | 26.96 | 460000 | 4.70 | 366000 | 800 | 4060 | 22.26 | 21.88 | 10.18 |
| 20 | 23.55 | 460000 | 4.51 | 366000 | 800 | 4060 | 19.04 | 18.48 | 10.03 |
| 21 | 22.63 | 460000 | 3.98 | 366000 | 900 | 4060 | 18.65 | 17.54 | 9.52 |
| 22 | 26.12 | 460000 | 5.53 | 366000 | 900 | 4060 | 20.59 | 21.05 | 11.01 |
| 23 | 24.19 | 460000 | 8.31 | 366000 | 600 | 4060 | 15.88 | 19.18 | 13.80 |
| 24 | 27.93 | 460000 | 10.89 | 366000 | 600 | 4060 | 17.04 | 22.95 | 16.32 |
| 25 | 26.79 | 460000 | 9.03 | 366000 | 500 | 4060 | 17.76 | 21.78 | 14.48 |
| 26 | 28.89 | 460000 | 9.71 | 366000 | 500 | 4060 | 19.18 | 23.90 | 15.13 |
| 27 | 28.2 | 460000 | 9.29 | 366000 | 400 | 4060 | 18.91 | 23.20 | 14.72 |
| 28 | 28.94 | 460000 | 10.80 | 366000 | 400 | 4060 | 18.14 | 23.97 | 16.22 |

Basis of Calculations (Assumptions)

| Evaporator Outlet | | | |
|---|---|---|-----------------------------|
| Evaporator Outlet - saturated vapor h (kJ/kg) REFPROP | Evaporator Outlet - saturated vapor p (Bar) | Evaporator Outlet - saturated vapor s (kJ/kg K) | Turbine Inlet - quality (%) |
| 1623.7 | 8.7405 | 5.8406 | |
| 1626.8 | 10.1661 | 5.7857 | |
| 1625.9 | 9.6755 | 5.8038 | |
| 1625.7 | 9.5916 | 5.8069 | |
| 1626.0 | 9.7207 | 5.8021 | |
| 1625.1 | 9.3197 | 5.8174 | |
| 1625.3 | 9.4224 | 5.8134 | |
| 1623.9 | 8.8103 | 5.8378 | |
| 1623.7 | 8.7322 | 5.8410 | |
| 1625.0 | 9.2875 | 5.8186 | |
| 1623.5 | 8.6629 | 5.8439 | |
| 1623.3 | 8.5803 | 5.8473 | |
| 1619.5 | 7.2659 | 5.9070 | |
| 1621.2 | 7.8174 | 5.8808 | |
| 1617.6 | 6.7448 | 5.9336 | |
| 1622.7 | 8.3521 | 5.8570 | |
| 1623.8 | 8.7824 | 5.8389 | |
| 1621.0 | 7.7563 | 5.8837 | |
| 1624.9 | 9.2294 | 5.8209 | |
| 1624.6 | 9.1024 | 5.8260 | |
| 1622.2 | 8.1656 | 5.8652 | |
| 1621.5 | 7.9202 | 5.8762 | |
| 1624.0 | 8.8665 | 5.8355 | |
| 1622.7 | 8.3521 | 5.8570 | |
| 1625.3 | 9.4136 | 5.8137 | |
| 1624.5 | 9.0737 | 5.8271 | |
| 1625.9 | 9.6966 | 5.8030 | |
| 1625.5 | 9.4874 | 5.8109 | |
| 1626.0 | 9.7177 | 5.8022 | |

Evaporator Outlet

| Turbine Inlet | | | |
|--|-------------------------------------|--|---|
| Turbine Inlet - inlet pressure (bar) - REFPROP | Turbine Inlet - temperature (Deg C) | Turbine Inlet - enthalpy (kJ/kg) - REFPROP | Turbine Inlet - entropy (kJ/kg K) - REFPROP |
| 8.6405 | 20.24 | 1623.5 | 5.7892 |
| 10.0661 | 25.11 | 1626.7 | 5.7892 |
| 9.5755 | 23.50 | 1625.7 | 5.8074 |
| 9.4916 | 23.21 | 1625.5 | 5.8106 |
| 9.6207 | 23.65 | 1625.8 | 5.8057 |
| 9.2197 | 22.29 | 1624.9 | 5.8212 |
| 9.3224 | 22.64 | 1625.1 | 5.8172 |
| 8.7103 | 20.49 | 1623.7 | 5.8418 |
| 8.6322 | 20.21 | 1623.5 | 5.845 |
| 9.1875 | 22.18 | 1624.8 | 5.8225 |
| 8.5629 | 19.96 | 1623.3 | 5.848 |
| 8.4803 | 19.65 | 1623.1 | 5.8515 |
| 7.1659 | 14.50 | 1619.1 | 5.9119 |
| 7.7174 | 16.75 | 1620.9 | 5.8854 |
| 6.6448 | 12.26 | 1617.3 | 5.9388 |
| 8.2521 | 18.81 | 1622.5 | 5.8613 |
| 8.6824 | 20.39 | 1623.6 | 5.8429 |
| 7.6563 | 16.50 | 1620.7 | 5.8882 |
| 9.1294 | 21.97 | 1624.7 | 5.8248 |
| 9.0024 | 21.53 | 1624.4 | 5.8299 |
| 8.0656 | 18.10 | 1621.9 | 5.8695 |
| 7.8202 | 17.15 | 1621.2 | 5.8806 |
| 8.7665 | 20.69 | 1623.8 | 5.8395 |
| 8.2521 | 18.81 | 1622.5 | 5.8613 |
| 9.3136 | 22.61 | 1625.1 | 5.8175 |
| 8.9737 | 21.43 | 1624.3 | 5.831 |
| 9.5966 | 23.57 | 1625.7 | 5.8066 |
| 9.3874 | 22.86 | 1625.2 | 5.8147 |
| 9.6177 | 23.64 | 1625.7 | 5.8058 |

Turbine Inlet

| Turbine Outlet | | | |
|--------------------------------------|---|---|--|
| Turbine Outlet - temperature (Deg C) | Turbine Outlet - pressure (bar) - REFPROP | Turbine Outlet - Saturated vapor enthalpy (kJ/kg Deg C) - REFPROP | Turbine Outlet Adiabatic - entropy (kJ/kg K) - REFPROP |
| 9.6 | 6.066 | 1614.91 | 5.8447 |
| 9.6 | 6.0723 | 1614.93 | 5.7892 |
| 10.1 | 6.1632 | 1615.32 | 5.8074 |
| 9.8 | 6.1144 | 1615.12 | 5.8106 |
| 9.4 | 6.0303 | 1614.75 | 5.8057 |
| 9.5 | 6.0345 | 1614.77 | |

| Pump Inlet | Pump Outlet |
|--|--|
| Condenser Outlet, NH3 Pump Inlet h (kJ/kg) - REFPROP | Ammonia pump outlet adiabatic enthalpy (kJ/kg) - REFPROP |
| Condenser Outlet, NH3 Pump Inlet s (kJ/kg K) - REFPROP | Ammonia pump efficiency (%) |
| 387.85 | 1.6314 |
| | 388.27 75% |
| 387.99 | 1.6319 |
| 390.00 | 1.6389 |
| 388.92 | 1.6352 |
| 387.05 | 1.6286 |
| 387.14 | 1.6289 |
| 388.74 | 1.6345 |
| 387.14 | 1.6289 |
| 395.82 | 1.6593 |
| 399.49 | 1.6721 |
| 389.16 | 1.6360 |
| 394.32 | 1.6540 |
| 385.88 | 1.6245 |
| 389.39 | 1.6368 |
| 386.11 | 1.6253 |
| 394.18 | 1.6536 |
| 406.54 | 1.6966 |
| 395.02 | 1.6565 |
| 391.41 | 1.6439 |
| 390.56 | 1.6409 |
| 389.86 | 1.6385 |
| 387.47 | 1.6301 |
| 394.46 | 1.6545 |
| 407.58 | 1.7001 |
| 419.48 | 1.7411 |
| 410.79 | 1.7112 |
| 413.86 | 1.7218 |
| 411.92 | 1.7151 |
| 419.01 | 1.7395 |

| Pump Inlet | Pump Outlet |
|--|--|
| Condenser Outlet, NH3 Pump Inlet h (kJ/kg) - REFPROP | Ammonia pump outlet adiabatic enthalpy (kJ/kg) - REFPROP |
| Condenser Outlet, NH3 Pump Inlet s (kJ/kg K) - REFPROP | Ammonia pump efficiency (%) |
| | Evaporator Inlet subcooled enthalpy (kJ/kg) |
| | Ammonia pump efficiency (%) |

| Pump Inlet | Pump Outlet |
|--|--|
| Condenser Outlet, NH3 Pump Inlet h (kJ/kg) - REFPROP | Ammonia pump outlet adiabatic enthalpy (kJ/kg) - REFPROP |
| Condenser Outlet, NH3 Pump Inlet s (kJ/kg K) - REFPROP | Ammonia pump efficiency (%) |
| | Evaporator Inlet subcooled enthalpy (kJ/kg) |
| | Ammonia pump efficiency (%) |

| Evaporator Heat Transfer | | Condenser Heat Transfer | |
|--|---------------------------|--|--------------------------|
| Evaporator thermal load (MW) | Evaporator min DT (Deg C) | Condenser thermal load (MW) | Condenser min DT (Deg C) |
| Warm water discharge temperature (Deg C) | Evaporator LMTD (Deg C) | Cold water discharge temperature (Deg C) | Condenser LMTD (Deg C) |
| Evaporator min DT (Deg C) | Evaporator UA (MW/ Deg C) | Condenser min DT (Deg C) | Condenser UA (MW/ Deg C) |
| Evaporator LMTD (Deg C) | Evaporator UA (MW/ Deg C) | Condenser LMTD (Deg C) | Condenser UA (MW/ Deg C) |

| Gross to Net Power | |
|--------------------------|---|
| Generator efficiency (%) | Gross Power (MW) |
| | Total Fixed Losses (MW) - Intake, CW Pumping, WW Pumping, NH3 |
| | CWP Friction Head Loss (MW) |
| | Static Head Loss (MW) |
| | Net Power (MW) |
| | Original Net Power (MW) |

Nominal NAVFAC Plant